A NEW ANALYTICAL METHOD FOR METHYLMERCURY SPECIATION AND ITS APPLICATION FOR THE STUDY OF METHYLMERCURY-THIOL COMPLEXES

by

Marcos José de Lima Lemes

A thesis submitted to the Faculty of Graduate Studies of

The University of Manitoba

in partial fulfillment of the requirements of

DOCTOR OF PHILOSOPHY

Department of Chemistry

University of Manitoba

Winnipeg

Copyright © 2010 by Marcos José de Lima Lemes

"If you have built castles in the air, your work need
not be lost; that is where they should be.
Now put the foundations under them."

Henry David Throueau
(1817 - 1862)

Acknowledgement

Foremost, I would like to express my sincere gratitude to my supervisor Dr. Feiyue Wang for his continuous support of my Ph.D. study and research, for his patience, motivation, enthusiasm, ideas, resources and friendship. His guidance helped me in all the time of research and writing of this thesis. I could not have imagined having a better advisor and mentor for my Ph.D. study.

Besides my supervisor, I would like to thank my thesis committee, Drs. Gregg Tomy, Norm Hunter, and Mark Hanson, for their encouragement and insightful comments.

My sincere thanks also go to my fellow labmates: Debbie Armstrong, Dan Leitch, Bryan Page, Xioaxi Hu, Alex Hare, Jesse Carrie, Amanda Chaulk, Jeff Latonas, Alexis Burt, Mark Loewen, Lu Li, and Mohammad Khan for discussions over the years, for the hard but fun fieldworks, and for the insights into the Canadian and other cultures.

I would like to thank numerous professors and technical staff from the Department of Chemistry for their technical discussions, ideas, and encouragements, particularly Dr. F. Hruska, Dr. J. Stetefeld, Dr. L. Donald, M. Cooper, S. Mejia, K. Marat, T. Wolowiec, B. Careless, and W. Buchannon.

I would like to express my gratitude to my wife, Emy Komatsu, for her patience and love throughout these years, as well for her technical discussion on this thesis.

Last but not the least, I would like to thank my family: my parents Elzira and José Lemes, and my aunt Elza de Lima, for their care and support throughout my life.

ABSTRACT

Monomethylmercury (CH_3Hg^+ and its complexes; hereafter referred to as MeHg) in the intracellular environment is known to be predominantly bonded to thiol-containing biomolecules but the identities of these target biomolecules remain unknown. Some evidence suggests that binding with glutathione acts as a detoxification mechanism for MeHg, while binding with $_L$-cysteine permits MeHg transport across the blood–brain barrier resulting in neurotoxicity. However, the occurrence of these complexes in biological tissues has not been confirmed analytically, and little is known about their kinetic stability. In this thesis, methylmercury $_L$-cysteinate (CH_3HgCys) and methylmercury $_L$-glutathionate (CH_3HgGlu) were synthesized and structurally characterized by proton nuclear magnetic resonance (^1H NMR), electrospray ionization mass spectrometry (ESI-MS), and X-ray crystallography. A new analytical method was developed combining high performance liquid chromatography with inductively coupled plasma mass spectrometry (HPLC-ICPMS). The method was capable of separating and analyzing CH_3HgCys and CH_3HgGlu complexes, as well as CH_3HgX and inorganic HgX ($X = H_2O$, OH^-, or Cl^-), with detection limits at the sub-micromolar levels. Using a new enzymatic hydrolysis method to isolate MeHg species in biological tissues, the HPLC-ICPMS method was successfully applied for the determination of MeHg speciation in the muscle tissue of dogfish (*Squalus acanthius*). These results provide the first analytical evidence for the presence and dominance of CH_3HgCys in fish muscle. The analytical method was also used to study the kinetic stability of CH_3HgCys and CH_3HgGlu under a range of environmental and intracellular conditions. In general, CH_3HgGlu was more

stable than CH_3HgCys under light exposure or darkness. The stability of both compounds decreases dramatically with increasing ionic strength (I). Half-life of CH_3HgCys decreases from 34.1 h (I = 0.01 M) to 5.9 h (I = 0. 5 M) and the half-life of CH_3HgGlu decreases from 259 h (I = 0.01 M) to 35.9 h (I = 0. 5 M). Suggesting major differences in their cycling in freshwater ($I < 0.01M$), seawater ($I \approx 0.7M$) and body fluids ($I \approx 0.16$ M). The analytical technique and the findings from this thesis research provide a new analytical framework for the study of MeHg speciation in natural waters, and the metallomics of MeHg in biological systems.

TABLE OF CONTENTS

Acknowledgments……..... i

Abstract……..... ii

Table of Content……..... iv

List of Tables……..... vii

List of Figures……..... viii

List of Acronyms……..... xi

Chapter 1. Introduction…… 1

1.1 Objectives……..... 1

1.2 Mercury in the Environment…….. 1

1.3 Methylation of Mercury……..... 2

1.4 Methylmercury Speciation……..... 5

1.5 Methylmercury-Thiols in the Metallomics of Methylmercury….. 8

1.5.1 Metallomics……..... 8

1.5.2 Cysteine and Glutathione in the Metallomics of Methylmercury……. 10

1.5.3 Lability of MeHg Complexes with Thiols……..... 16

1.6 Kinetic Stability of Methylmercury-Thiol Complexes…….. 17

1.7 Analytical Techniques…… 19

1.7.1 Analytical Techniques for the Determination of Total Mercury Concentration……..... 19

1.7.2 Analytical Techniques for the Determination of Total Methylmercury Concentration……. 20

1.7.3 Analytical Techniques for the Determination of Methylmercury Speciation……... 28

1.8 Organization of this Thesis……..... 29

Chapter 2. Syntheses and Characterization of Methylmercury Cysteinate and Glutathionate…… 31
2.1 Syntheses of Methylmercury Cysteinate and Glutathionate……. 31
2.2 Elemental Analyses of the Compounds……. 32
2.3 Nuclear Magnetic Resonance (NMR) Characterization of the Compounds ……... 33
2.4 Refined Crystal Structure of CH_3HgCys ……..... 35
2.5 Mass Spectra and Fragmentation Patterns of the Compounds….. 39
2.5.1 CH_3HgCys and its Fragmentation Pattern……..... 41
2.5.2 CH_3HgGlu and its Fragmentation Pattern……..... 46
2.6 Conclusion…….. 50
Chapter 3. Development and Optimization of a HPLC-ICPMS Method for the Determination of Methylmercury Speciation in Aqueous Solution……. 51
3.1 Methodological Consideration……..... 51
3.2 Instrumentation……..... 52
3.3 Standard Solutions…… 53
3.4 Optimization of the Method……..... 53
3.4.1 Analytical Columns……..... 53
3.4.2 Mobile Phase……... 54
3.4.3 Other Parameters……..... 58
3.5 HPLC - Labile MeHg Species…….. 59
3.6 Optimized HPLC-ICPMS Method for MeHg Speciation in Aqueous Solution……..... 61
3.7 Conclusion…… 62
Chapter 4. Methylmercury Speciation in Fish by HPLC-ICPMS Following Enzymatic Hydrolysis…….. 63
4.1 Enzymatic Hydrolysis of the Fish Muscle Sample ……..... 63
4.2 Presence and Dominance of CH_3HgCys in Fish Muscle…..... 67
4.3 Molecular Weight Distribution of Methylmercury in the Fish Muscle Extractant …… 70
4.4 Conclusion…… 72

Chapter 5. Kinetic Stability and Decomposition Products of Methylmercury Cysteinate and Glutathionate……. …… 73
5.1 Kinetic Stability Study……..... 73
5.1.1 Influence of Light…… 74
5.1.2 Influence of Ionic Strength…….. 76
5.1.3 Influence of pH…… 77
5.2 Degradation Kinetics…… 78
5.3 Decomposition Products and Pathways……... 79
5.4 Conclusion…… 83
Chapter 6. Conclusions…… 85
6.1 Objectives Achieved……..... 85
6.2 Novelty and Significance of the Findings…… 87
6.3 Lessons Learned…….. 88
6.4 Future Perspectives……..... 89
References……..... 91
Appendices …… 115

LIST OF TABLES

Table 1.1 -	Formation constants of CH_3Hg^+ and its complexes…….	9
Table 1.2 -	Microscopic acid dissociation constants of CSH ……..…...	11
Table 1.3 -	Microscopic acid dissociation constants of GSH ……..…...	13
Table 1.4 -	Summary of the major analytical methods for the determination of total MeHg concentration in environmental and biological samples…	24
Table 2.1 -	Intramolecular and intermolecular bond distances and angles of CH_3HgCys…….	37
Table 4.1 -	Optimal conditions for MeHg-thiol speciation by HPLC-ICPMS…...	65
Table 4.2 -	Optimal conditions for MeHg-thiol identification by ESI-MS…….	65
Table 5.1 -	First-order degradation rate constants and half-lives of CH_3HgCys and CH_3HgGlu in the presence of white light…….....	79
Table A1 -	ESI-MS parameters for CH_3HgCys and CH_3HgGlu in both positive and negative modes..…….	118

LIST OF FIGURES

Figure 1.1 -	Biogeochemical cycle of Hg…….....	6
Figure 1.2 -	Microscopic ionization scheme for cysteine……..	11
Figure 1.3 -	Microscopic ionization scheme for glutathione…….	12
Figure 1.4 -	Molecular structures of **a)** CH_3HgCys and **b)** methionine…….	14
Figure 1.5 -	LAT1 carrying CH_3HgCys into the blood-brain barrier……	15
Figure. 2.1 -	Pictures showing **a)** Crystalline CH_3HgCys and **b)** Amorphous CH_3HgGlu…….....	32
Figure 2.2 -	^1H NMR spectra of **a)** CH_3HgCl, **b)** CH_3HgCys, and **c)** CH_3HgGlu…….....	34
Figure 2.3 -	Refined molecular structure of CH_3HgCys……	39
Figure 2.4a -	CH_3HgCys (m/z=336) and its fragment CH_3HgS (m/z=249) analyzed in the negative mode……...	40
Figure 2.4b -	CH_3HgGlu (m/z=522) and its fragments CH_3HgS (m/z=249), CH_3Hg+CysGly-OH (m/z=377), CH_3Hg+CysGly (m/z=393), CH_3HgGlu-NH_2 (m/z=508), and a cluster $CH_3Hg(Glu)_2$ (m/z=813) analyzed in the negative mode……...	41
Figure 2.5 -	CH_3HgCys and its fragmentation pattern using the negative-ion mode at varying cone voltages……...	42
Figure 2.6 -	CH_3HgCys and its fragmentation pattern using the positive-ion mode at varying cone voltages…….....	43
Figure 2.7 -	CH_3HgGlu and its fragmentation pattern using the negative-ion mode with varying cone voltages……...	47
Figure 2.8 -	CH_3HgGlu and its fragmentation pattern using the positive-ion mode at varying cone voltages…….....	48
Figure 3.1 -	Typical HPLC chromatogram of various MeHg compounds and inorganic Hg (500 mM) with mobile phase containing 8 mM MSA at pH 3.0……..	55

Figure 3.2 - Influence of salts in the mobile phase on the ICP-MS determination of **a)** CH_3HgCys and **b)** CH_3HgGlu……... 57
Figure 3.3 - Chromatograms of **a)** a mixed standard solution with 500 nM CH_3HgCys and 500 nM CH_3HgGlu; **b)** a 500 nM CH_3HgGlu solution, and **c)**, a 500 nM CH_3HgCys solution……. 60
Figure 3.4 - Typical chromatograms of calibration standards of various MeHg compounds and inorganic Hg……. 62
Figure 4.1 - Chromatograms of a mixed standard solution of 500 mM of CH_3HgCys and CH_3HgGlu **a)** before and **b)** after trypsin hydrolysis……... 67
Figure 4.2 - **a)** Chromatogram of the dogfish muscle after being extracted by the enzymatic hydrolysis with trypsin (after 10x dilution); **b)** ESI-MS spectrum confirming the CH_3HgCys peak in **a**; **c)** Same as **a** but the extractant was spiked with 30 nM of CH_3HgCys and 19 nM of CH_3HgGlu standard solution……. 69
Figure 4.3 - Elution profile of UV absorbance (280 nm) and total Hg in solubilized DORM-2 extractant after SEC……. 71
Figure 5.1 - Stability of CH_3HgCys (**a, c**) and CH_3HgGlu (**b, d**) under dark (**a, b**) and irradiated with white fluorescence light (**c, d**) of white light……..... 75
Figure 5.2 - Stability of CH_3HgCys (**a**) and CH_3HgGlu (**b**) at different ionic strengths in the presence of white light…….. 76
Figure 5.3 - Stability of CH_3HgCys (**a**) and CH_3HgGlu (**b**) at pH 5.5 ($I < 0.001$ M) and pH 7.5 ($I = 0.01$ M) in the presence of white light…... 77
Figure 5.4 - Chromatograms of the CH_3HgCys (**a**) and CH_3HgGlu (**b**) solution after various times of exposure to white light……..... 81
Figure A1 - Product ions setting for CH_3HgCys on positive mode……... 116
Figure A2 - Product ions setting for CH_3HgGlu on positive mode…….. 117
Figure A3 - Normalized signal obtained with different nebulizers for CH_3HgCys analysis by HPLC-ICPMS……. 119

Figure A4 - Influence of RF power on the intensity of Hg species by HPLC-ICP-MS……..... 120

Figure A5 - Chromatograms of the CH_3HgCys solution after various duration of exposure of exposure to white light at a) pH= 5.5, I= <0.001 M, and b) pH = 7.5, I= 0.10 M, T = 22 ^oC ……... 121

Figure A6 - Chromatogram of the CH_3HgGlu solution after various duration of exposure to white light at a) pH= 5.5, I= <0.001 M, and b) pH= 7.5, I= 0.10 M, T = 22 ^oC……..... 122

LIST OF ACRONYMS

ACN	Acetonitrile
ACS	American Chemical Society
a.m.u.	Atomic mass unit
Atm	Atmospheric pressure
API-MS	Atmospheric pressure ionization mass spectrometry
BBB	Blood-brain barrier
CH_3HgCys	Methylmercury cysteinate
CH_3HgGlu	Methylmercury glutathionate
CH_3HgX	Methylmercury bonded to a ligand X (X = H_2O, OH^-, or Cl^-)
CSH	$_L$-cysteine
CV-AAS	Cold vapor atomic absorption spectrometry
CV-AFS	Cold vapor atomic fluorescence spectrometry
DORM-2	Dogfish muscle certified reference material for trace metals
DRC	Dynamic reaction cell
EDTA	Ethylenediaminetetraacetic acid
ESI-MS	Electron spray ionization coupled with mass spectrometry
EtHg	Ethylmercury
GC-ECD	Gas chromatography with electron capture detection
GC-MS	Gas chromatography coupled with mass spectrometry
GSH	$_L$-glutathione
^{1}H NMR	Proton nuclear magnetic resonance
HPLC	High performance liquid chromatography
HPLC-ICPMS	High performance liquid chromatography coupled with inductively coupled plasma mass spectrometry
ICP-MS	Inductively coupled plasma mass spectrometry
K_f	Constant of formation
LAT	Large neutral amino acid transporter

ME	2-mercaptoethanol
MeHg	Methylmercury (CH_3Hg^+ and its complexes)
MeOH	Methanol
MSA	Methanosulfonic acid
NH_4Ac	Ammonium acetate
PB/EI-MS	Particle beam/electron ionization-mass spectrometry
PEEK	Polyetheretherketone
PFA	Perfluoroalkoxy
PhHg	Phenyl mercury
RF	Radio frequency
RSH	Thiols
SEC	Size exclusion chromatography
SPME	Solid phase microextraction
SRB	Sulfate reducing bacteria
TBABr	Tetrabutylammonium bromide
THF	Tetrahydrofuran acetic acid
TMS	Tetramethylsilane
UV	Ultra-violet
XANES	X-ray absorption near-edge structure

Chapter 1. Introduction

1.1 Objectives

At the time when this project started (2004), there was no analytical technique available for the determination of monomethylmercury (CH_3Hg^+ and its complexes; hereafter MeHg) speciation in environmental or biological samples. This thesis research aims to develop the first analytical method that is capable of determining MeHg speciation, particularly determining various MeHg-thiol complexes, and apply it for the study of MeHg-thiol complexes in natural waters and metallomics of MeHg in biological systems. The specific objectives are to:

(i) synthesize and characterize methylmercury cysteinate (CH_3HgCys) and methylmercury glutathionate (CH_3HgGlu) compounds;

(ii) develop an analytical method to speciate CH_3HgCys and CH_3HgGlu complexes with detection limits at the sub-micromolar levels;

(iii) apply this new method to speciate MeHg complexes in biological tissues; and,

(iv) study the kinetic stability of CH_3HgCys and CH_3HgGlu under various conditions.

1.2 Mercury in the Environment

Mercury, historically called quicksilver, is a chemical element with the symbol Hg. Hg is a peculiar element in that it is grouped as a transition metal (group 12 with 200.59 a.m.u.), but is liquid at 25 °C. Mercury itself has low vapor pressure (1.7×10^{-6}

atm; 25 ºC) and depending on which chemical form of Hg is present, it can demonstrate different properties; for example, volatility (e.g., elemental Hg, $(CH_3)_2Hg$), non-polar behavior (e.g., CH_3HgCl, CH_3CH_2HgCl), and polar behavior (e.g., $Hg(NO_3)_2$, CH_3HgOH, CH_3HgSR; SR = organic thiols). Hg exhibits valences of 0, +1 and +2. The mercurous ions (Hg_2^{2+}) are unstable under environmental conditions as they readily disproportionate into oxidation states Hg(0) and Hg(II) (Schuster, 1991). The formation of Hg(II)-complexes, which show thermodynamic stability up to four-coordinate species (Hoffmeyer et al., 2006), is of importance in natural systems due to their high stability (Gilmour and Riedel, 1995; Schuster, 1991).

Hg is a global contaminant (Clarkson, 1992), and its mobility, bioaccumulation and biomagnification are highly dependent on speciation and redox conditions in the environment (Stumm and Morgan, 1996). The ultimate concern of Hg in the environment is, however, its impact on human health. The impact of Hg on humans was lighted with the discovery of Minamata disease in Japan during the mid-1950s (Harada, 1995). Both inorganic Hg and MeHg have severe health effects in humans, but it is MeHg that is the main species involved in bioaccumulation and biomagnification in the food web with exposure caused primarily via dietary fish consumption (Bergquist and Blum, 2007).

1.3 Methylation of Mercury

Due to bioavailability and toxicity, MeHg is the most concerning Hg species as it is a known neurotoxin causing reproductive, immunosuppressive, and neurobehavioral risks to biota (NRC (National Research Council), 2000) and the Minamata Disease in humans (Harada, 1995). MeHg is indeed one of the most common contaminants in fish

and marine mammals due to its biomagnification along the food chain (Watras et al., 1998). Methylation of inorganic Hg in nature is thought to occur primarily via one of two microbial pathways: via sulfate reducing bacteria (SRB) (Compeau and Bartha, 1987; Compeau and Bartha, 1985; Ekstrom et al., 2003; Watras et al., 2005), and via reaction with methylcobalamin (Craig and Moreton, 1985; Craig and Morton, 1978).

Microbiological methylation of Hg by SRB occurs preferentially in oxic-anoxic transition zones, such as the deeper layer of a water column or surface layer of aquatic sediments where sulfate reduction takes place (Compeau and Bartha, 1984; Compeau and Bartha, 1985; Olson and Cooper, 1976; Stets et al., 2004). Other factors favoring the microbial Hg methylation process are higher temperature, lower pH, higher organic matter content and appropriate sulfate (200–500 μM) concentrations (Gilmour et al., 1992), while sulfide appears to limit the production of MeHg in saline sediments (Baeyens et al., 2003; Craig, 2003).

MeHg can also be formed readily by the reaction of inorganic Hg with methylcobalamin (CH_3B_{12}), a naturally occurring coenzyme of vitamin B_{12} (Eq. 1.1). The reaction involves the transfer of the methyl anion from Co^{3+} to Hg^{2+}, which is rendered catalytic by the enzymatic regeneration of CH_3B_{12} by microorganisms (Chemaly, 2002; Craig and Morton, 1978; Imura et al., 1971). Methylcobalamin has been identified in some acetogens (e.g., *Clostridium thermoaceticum*) (Chemaly, 2002) and methanogens (e.g., *Methanobacterium thermoautotrophicum*) (Stets et al., 2004).

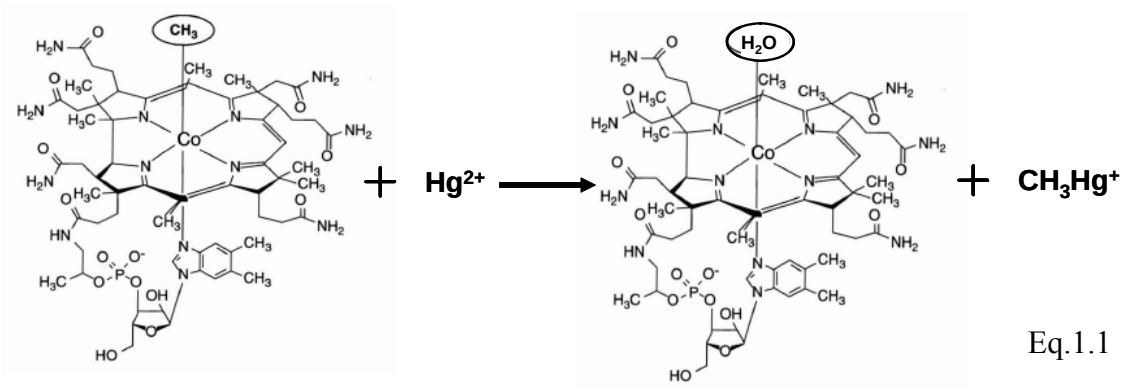

Eq.1.1

The formed CH_3Hg^+ can react further with CH_3B_{12} to produce dimethylmercury, $(CH_3)_2Hg$ (Eq. 1.2), but this reaction is much slower than the formation of CH_3Hg^+ (Chemaly, 2002; Craig and Morton, 1978; Imura et al., 1971):

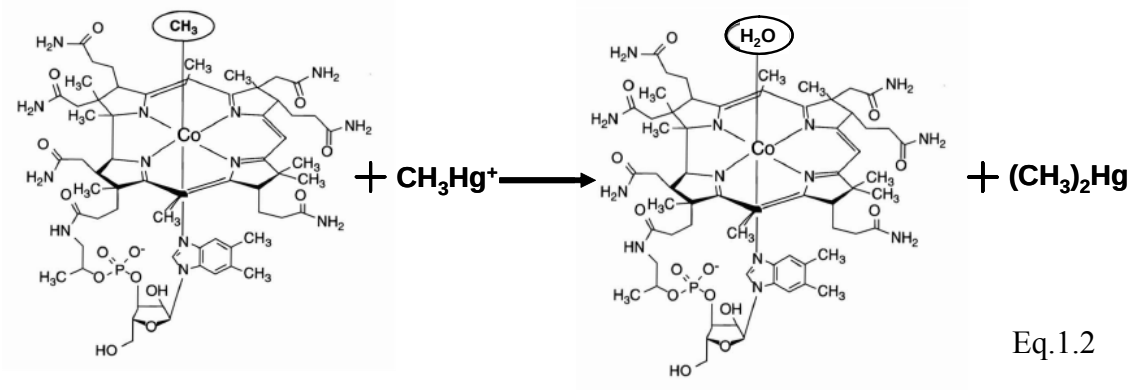

Eq.1.2

MeHg may also be formed from abiotic Hg methylation processes in the aquatic environment (Weber, 1993). Examples include Hg methylation in the presence of humic substances (Hintelmann et al., 1997; Lee et al., 1985; Nagase et al., 1984) and in some cases fulvic acid appears to be more effective (Nagase et al., 1984), though detailed mechanisms are not fully understood.

Figure 1.1 illustrates major processes and species involved in the cycling of inorganic Hg and MeHg in the aquatic environment. Hg is present in the atmosphere in various species such as elemental mercury (Hg^0) which is the dominant Hg species in the atmosphere, reactive and particulate Hg(II), together with small amount of $(CH_3)_2Hg$ and MeHg. Atmospheric deposition is often the major source of Hg to the aquatic environment, particularly in remote areas. In the aquatic environment, Hg is found to be mainly bound to aquatic particles, most of which eventually settles as bottom sediments. A small and highly variable proportion of the total Hg remains in the water column and is present as Hg^0, inorganic Hg(II) and MeHg. The partitioning of Hg between the solid and aqueous phases is subject to continuous change in response to dynamic environmental conditions and microbial activities. Aquatic organisms can take up Hg, particularly MeHg, and biomagnify it throughout the food web.

1.4 Methylmercury Speciation

Similarly, to inorganic Hg, MeHg is not one single chemical species but includes a variety of different CH_3Hg^+ complexes. Indeed, there are no free CH_3Hg^+ ions in aqueous solution; instead, they are present as aqua complexes $CH_3Hg(H_2O)_x^+$ with a

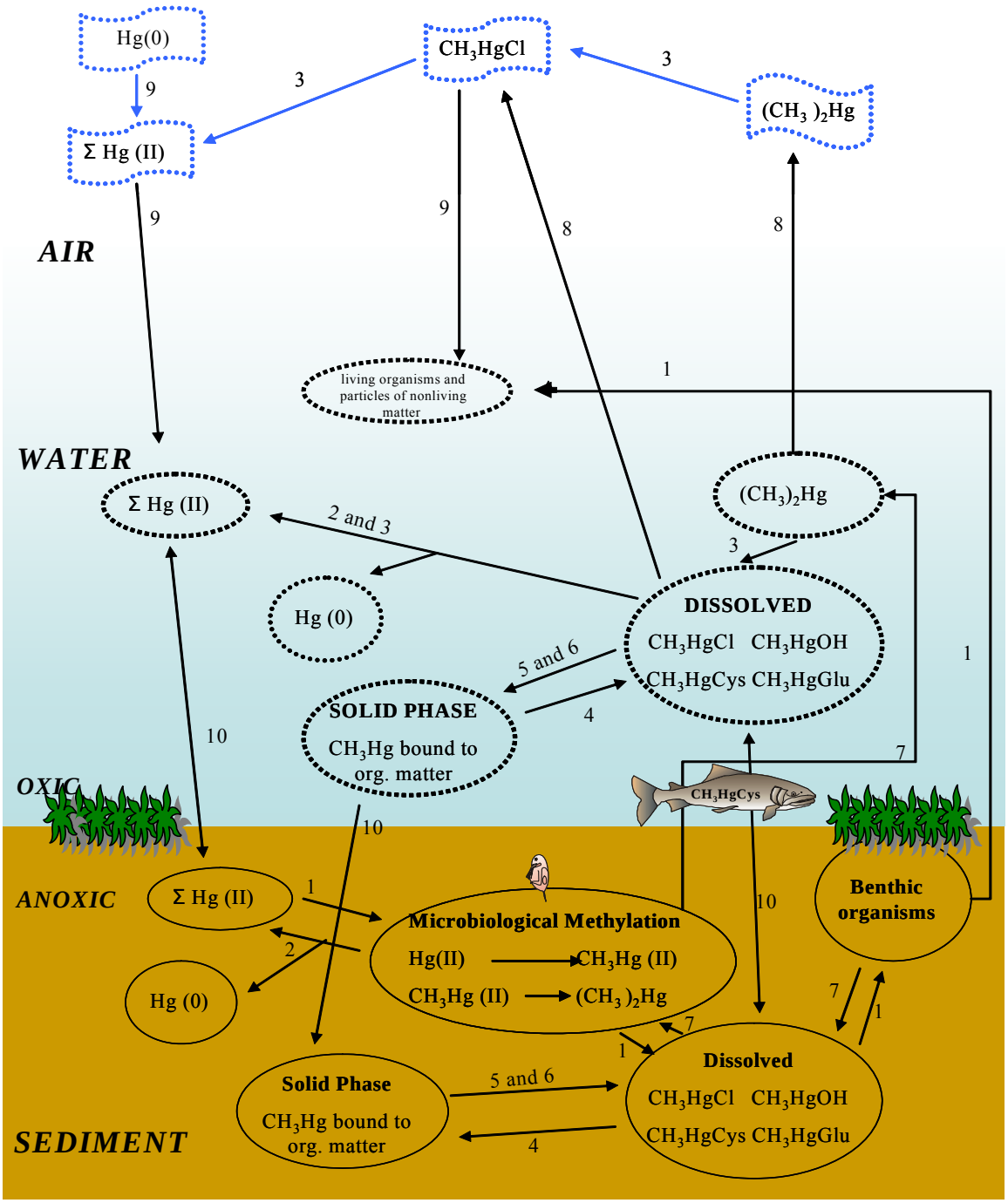

Figure 1.1 - Biogeochemical cycle of Hg. **1.** biological uptake; **2.** biotic demethylation; **3.** abiotic demethylation; **4.** absorption to the solid phase; **5.** . desorption; **6.** dissolution of solid phase; **7.** excretion from organisms; **8.** gas exchange; **9.** wet and dry deposition; **10.** physical processes. Modified from Craig (Craig, 2003)

covalent bond between Hg and O atoms (Stumm and Morgan, 1996). For simplicity, however, this aqua complex will be represented by CH_3Hg^+ throughout this thesis.

CH_3Hg^+ ions behave as a soft Lewis acid and have a strong preference for the addition of one ligand (Stumm and Morgan, 1996; Zhang et al., 2004). They can undergo rapid coordination reactions with S-, P-, O-, N-, and halogen-containing ligands; the rate of the formation of Cl^-, Br^-, and OH^- complexes is extremely fast (Raycheba and Geier, 1979; Schwarzenbach and Schellenberg, 1965). The general reaction takes the following form:

$$L^- + CH_3Hg^+ = CH_3HgL \qquad \text{(Eq. 1.3)}$$

where L^- is a complexing ligand.

Some of the common CH_3Hg^+ complexes are shown in Fig. 1.1. The stability constants for some CH_3Hg^+ complexes are listed in Table 1.1. It should be noted although Table 1.1 the best available dataset are far from definitive, as great uncertainties exist in their stoichiometries and formation constants due to the lack of appropriate analytical techniques for speciating various complexes under environmentally relevant conditions (Dyrssen and Wedborg, 1991; Zhang et al., 2004).

Dyrssen and Wedborg (1991) did a theoretical calculation for the sulfur-Hg(II) system in natural waters. Their calculations show that CH_3HgCl will dominate at low concentration of H_2S and/or thiols (RSH) in acidic, low salinity water, but an increase in sulfide or thiol concentration, or an increase of the pH to neutral or slightly alkaline conditions will result in a total dominance of CH_3HgSH and CH_3HgSRin the system.

Recently Zhang et al. (2004) reported the presence of 5-150 nmol thiols in sediment porewaters of three contrasting wetlands in Canada. Their thermodynamic

calculations using constants listed in Table 1.1 suggested that MeHg across the sediment-water interface was dominated by thiol and sulfide complexes; the concentrations of CH_3HgOH and CH_3HgCl complexes were negligible. Since previous studies on the cycling and bioavailability of CH_3Hg^+ were centered only on CH_3HgOH and CH_3HgCl complexes, they argued that there is a need to investigate the role of MeHg-thiol complexes.

1.5 Methylmercury-Thiols in the Metallomics of Methylmercury

1.5.1 Metallomics

Metal (including metalloid) ions have long been known to interact strongly with biomolecules, some are essential (e.g., Fe, Zn, Cu, Se, Ni) for the health of biota and others are non-essential. The absence of essential metals can result in deficiency syndrome, whereas elevated concentrations of both essential and non-essential metals may result in toxic effects, including carcinotoxicity (e.g., As, Cr, Pt), immunotoxicity (e.g., Au, Co, Cr, Ni, Pt), embryotoxicity (e.g., Hg), or neurotoxicity (e.g., Al, Hg, Mn) (Szpunar, 2004). The molecular basis of many of the metal-dependent biochemical processes remain elusive and the mechanisms by which the metal is stored or incorporated as a cofactor in a cell are often unknown (Szpunar, 2004). The function of a metal is determined by the complexation with a bioligand and its contribution to protein stability through its presence in the centre of large molecules, often with enzymatic activity. The activity of intracellular metal ions is controlled by several families of proteins, either detoxifying,

Table 1.1 - Formation constants of CH_3Hg^+ and its complexes (Dyrssen and Wedborg, 1991; Schwarzenbach and Schellenberg, 1965; Stumm and Morgan, 1996; Zhang et al., 2004): ($^{\blacklozenge}$) I = 0.1 M at 20 °C, (*) I = 1 M at 25 °C, and ($^{\nabla}$) I = 0 M at 25 °C

Reaction	Log K
$Hg^{2+} + CH_3^- = CH_3Hg^+$	~ 50*
$CH_{4(aq)} = CH_3^- + H^+$	~ -47*
$Hg^{2+} + CH_{4(aq)} = CH_3Hg^+ + H^+$	~3*
$CH_3Hg^+ + CH_3^- = (CH_3)_2Hg$	~37*
$CH_{4(aq)} + HgCl_2 = CH_3HgCl + H^+ + Cl^-$	- 5.2*
$CH_3Hg^+ + Cl^- = CH_3HgCl$	5.25*
$CH_3Hg^+ + H_2O = CH_3HgOH + H^+$	-4.63*
$2CH_3Hg^+ + H_2O = (CH_3Hg)_2OH^+ + H^+$	-2.11$^{\nabla}$
$CH_3Hg^+ + OH^- = CH_3HgOH$	9.37$^{\blacklozenge}$
$CH_3Hg^+ + CO_3^{2-} = CH_3HgCO_3^-$	6.1*
$CH_3Hg^+ + SO_4^{2-} = CH_3HgSO_4^-$	0.94*
$CH_3Hg^+ + S^{2-} = CH_3HgS^-$	21.04*
$CH_3Hg^+ + CH_3HgOH = (CH_3Hg)_2OH$	6.1*
$CH_3Hg^+ + CH_3HgS^- = (CH_3Hg)_2S$	16.34*
$HgS_{(S)} + CH_4 = CH_3HgS^- + H^+$	~ -26*
$CH_3Hg^+ + HS^- = CH_3HgS^- + H^+$	7.0$^{\nabla}$
$2CH_3Hg^+ + HS^- = (CH_3Hg)_2S + H^+$	23.52$^{\nabla}$
$3CH_3Hg^+ + HS^- = (CH_3Hg)_3S^+ + H^+$	30.52$^{\nabla}$
$CH_3Hg^+ + CSH^{2-} = CH_3HgCys^-$	16.90$^{\nabla}$
$CH_3Hg^+ + CSH^{2-} + H^+ = CH_3HgHCys$	26.07$^{\nabla}$
$CH_3Hg^+ + GSH^{3-} = CH_3HgCys^{2-}$	16.66$^{\nabla}$
$CH_3Hg^+ + GSH^{3-} + H^+ = CH_3HgHCys^-$	26.35$^{\nabla}$
$CH_3Hg^+ + GSH^{3-} + 2H^+ = CH_3HgH_2Cys$	30.01$^{\nabla}$

protecting or simply involving in cell cycle (Finney and O'Halloran, 2003).

To highlight the importance of metal ions in biochemistry, a new term "metallomics" was proposed in 2004 and considered to be at the same level of scientific significance as genomics and proteomics (Haraguchi, 2004). The metallomic information consists of the identities of the individual metal species (*qualitative metallomics*), their concentrations (*quantitative metallomics*) (Szpunar, 2004) and their interactions with biomolecules. Chemical speciation of metal ions (e.g., their oxidation state and molecular environment) is crucial in metallomics research, because the bio-availabilities, essentialities and toxicities of metal ions depend on their chemical forms (Hasegawa et al., 2005).

1.5.2 Cysteine and Glutathione in Metallomics of Methylmercury

Sulfhydryl amino acids, thiol-containing proteins and enzymes are abundant in biological systems and play important roles in intracellular activities by controlling or detoxifiying metal ions. From a MeHg metallomics point of view, the most important thiols are cysteine (CSH) and glutathione (GSH). CSH availability is the rate-limiting factor in GSH synthesis (Bannai and Tateishi, 1986). GSH is a major antioxidant in mammalian cell systems, constituting approximately 90% of the intracellular non-protein thiols (Shanker and Aschner, 2001). In human blood, the sulfhydryl (mainly GSH and CSH) concentration is about 0.5mM in the plasma and 12-20 mM in the red blood cell (Rabenstein, 1978).

In aqueous solution, both CSH and GSH undergo acid dissociation reactions as illustrated in Fig. 1.2 and 1.3, respectively. The acid dissociation constants are shown in Tables 1.2 and 1.3.

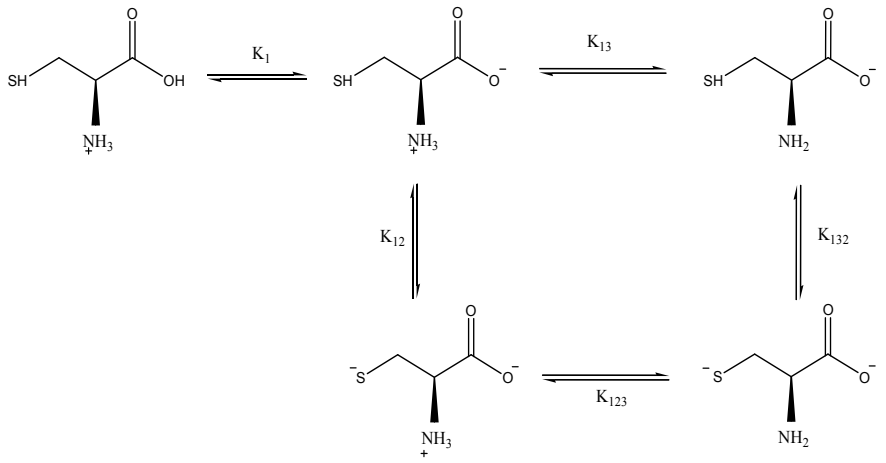

Figure 1.2 - Microscopic ionization scheme for cysteine. Modified from Canle (Canle et al., 2006)

Table 1.2 – Microscopic acid dissociation constants of CSH (I= ~0.01 M, T= 25 ºC) (Clement and Hartz, 1971; Reid and Rabenstein, 1981)

pK_1	1.92 ± 0.14
pK_{12}	8.45 ± 0.05
pK_{13}	8.68 ± 0.15
pK_{123}	10.2 ± 0.11
pK_{132}	9.99 ± 0.17

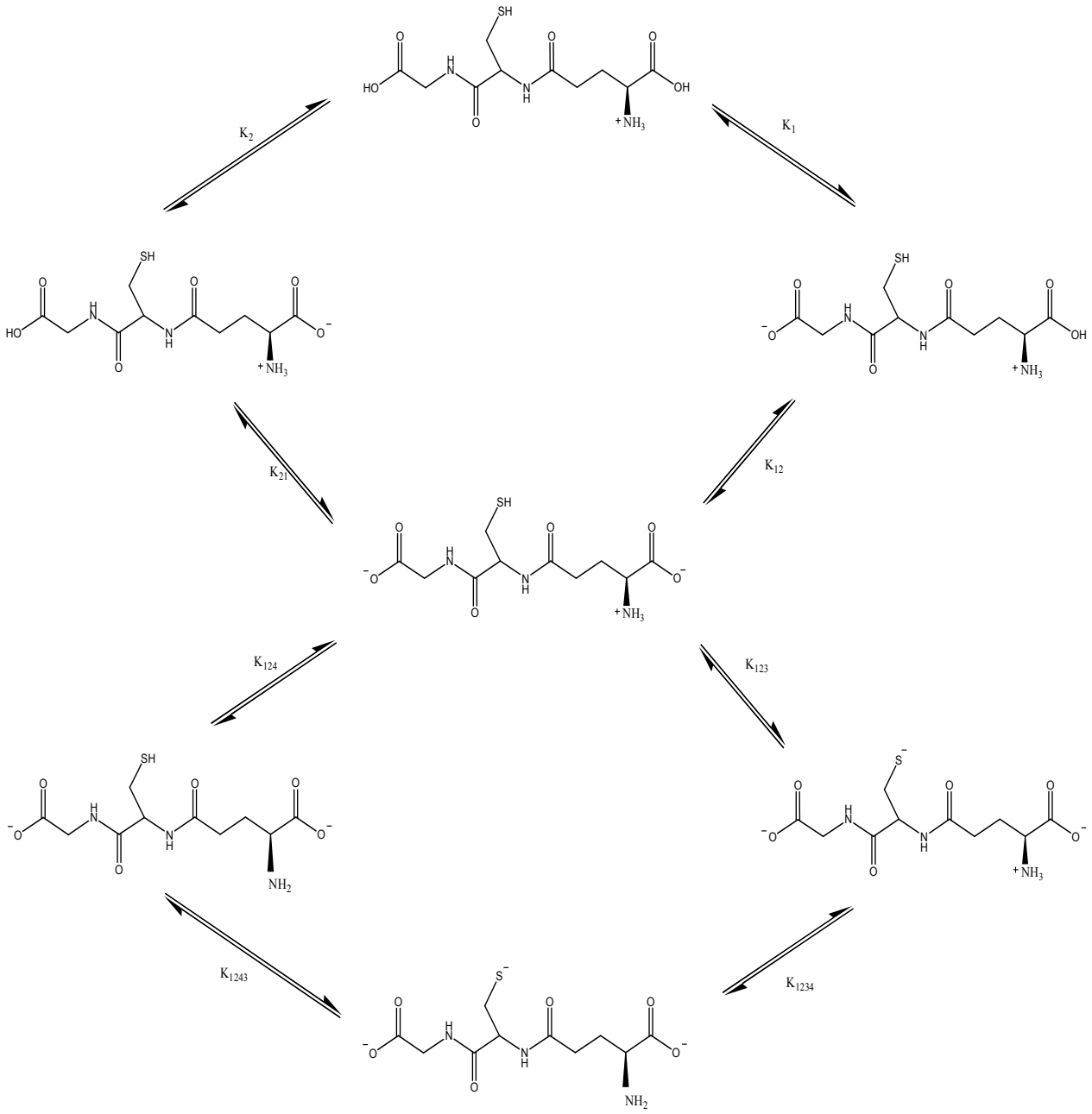

Figure 1.3 - Microscopic ionization scheme for glutathione. Modified from (Rabenstein, 1973)

Table 1.3 – Microscopic acid dissociation constants of GSH (I= 0.3-0.4 M, T= 25 ºC) (Rabenstein, 1973).

pK_1	2.09 ± 0.05
pK_2	3.12 ± 0.05
pK_{12}	3.36 ± 0.10
pK_{21}	2.33 ± 0.01
pK_{123}	8.93 ± 0.04
pK_{124}	9.13 ± 0.04
pK_{234}	9.28 ± 0.10
pK_{1243}	9.08 ± 0.02

It has been generally established that CH_3HgCys is the complex that is responsible for MeHg transport across the placenta and the blood-brain barrier (BBB) (Aschner et al., 1994; Clarkson, 1992). CH_3HgCys is thought to be transported across BBB by the L-type large neutral amino acid transporters (LAT1 and 2) (Aschner et al., 1994; Bridges and Zalups, 2006; Simmons-Willis et al., 2002). The uptake of CH_3HgCys by LAT1 and 2 is likely due to molecular mimicry of CH_3HgCys with the amino acid methionine (Bridges and Zalups, 2006; Clarkson, 1993; Simmons-Willis et al., 2002), although recent studies suggest that such mimicry occurs only in the Lα region of the molecules (Fig. 1.4) (Hoffmeyer et al., 2006). Kinetic analysis of transport indicated that the apparent affinities, Michaelis constant (K_m), of CH_3HgCys uptake by LAT1 and 2 (98 ± 8 and 64 ± 8 μM respectively) were comparable with those for methionine (99 ± 9 and 161 ± 11 μM), whereas the maximal velocities (V_{max}) were higher for CH_3HgCys (286 ±

12 and 75 ± 11 pmol/oocyte per 15 min) than for methionine (97 ± 16 and 54 ± 12 pmol/oocyte per 15 min), indicating that CH_3HgCys may be a better substrate than the endogenous amino acid (Simmons-Willis et al., 2002).

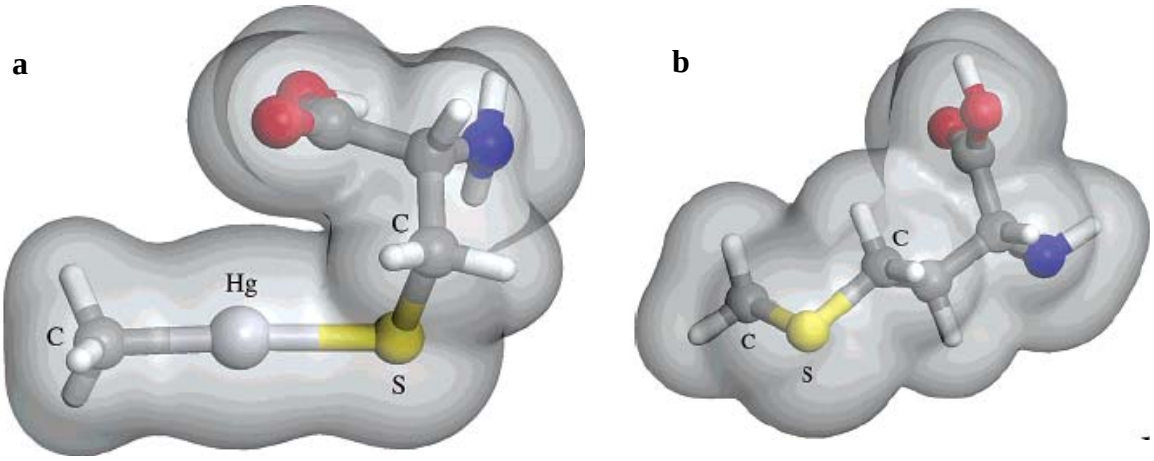

Figure 1.4 – Molecular structures of **a)** CH_3HgCys and **b)** methionine (Hoffmeyer et al., 2006)

The L system of carries is the major route of entry of large neutral amino acids into brain endothelial cells from blood (Keper et al., 1992). Since the carrier proteins are polar, the diffusion of neutral MeHg complexes such as CH_3HgCl is not favored. Figure 1.5 illustrates the speciation change between MeHg complexes and their transport across BBB.

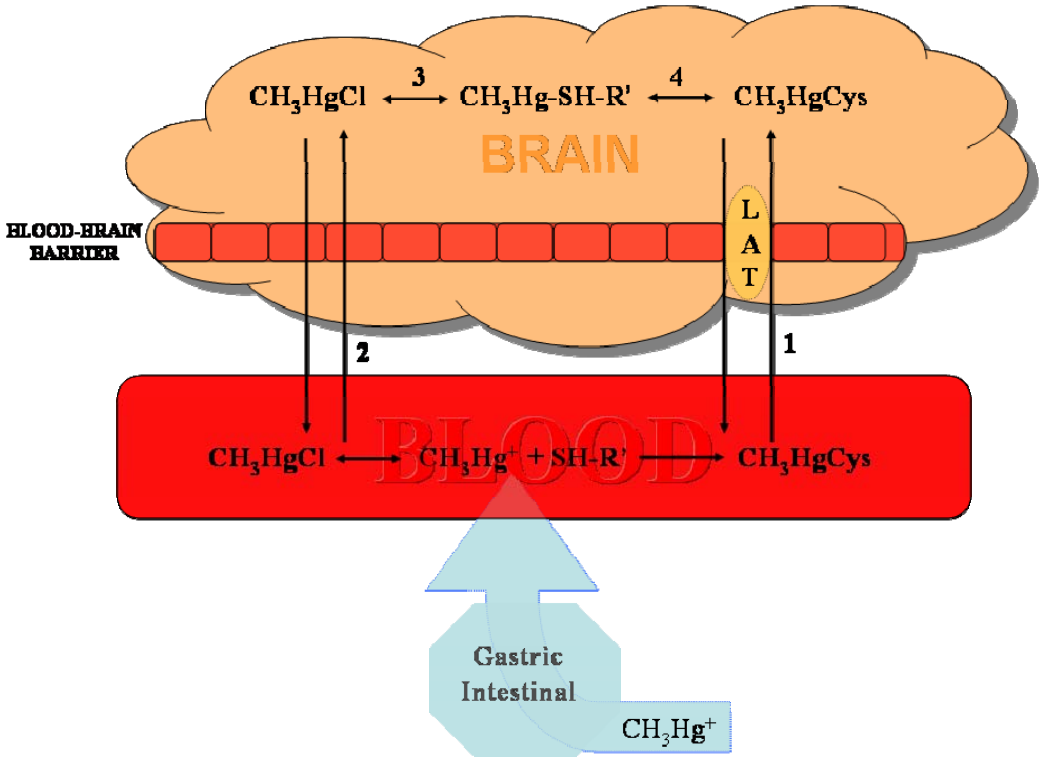

Figure 1.5 – LAT1 carrying CH_3HgCys into the blood-brain barrier: **1)** CH_3HgCys is transported via system L; **2)** small amount of CH_3HgCl may also be transported via diffusion; **3)** and **4)** rapid exchange of CH_3Hg^+ between chlorides and –SH groups. Modified from (Aschner and Aschner, 1990)

On the other hand, other thiols such as GSH could potentially be used to detoxify MeHg (Arnold et al., 1983; Rabenstein, 1978). A number of reports have implicated a crucial role for GSH in modulating MeHg neurotoxicity (Dringen et al., 2000). A significant correlation between GSH levels and MeHg toxicity has been established in a MeHg-resistant cell line (Gachhui et al., 1991; Shanker and Aschner, 2001).

Despite all the experimental and theoretical work, there has been no analytical tool for identifying and quantifying CH_3HgCys and CH_3HgGlu in biological materials, which is one of the major focuses of this thesis (Chapters 2-4).

1.5.3 Lability of MeHg Complexes with Thiols

CH_3Hg-SR complexes are extremely stable thermodynamically with formation constants in the 10^{15}-10^{30} range (Stumm and Morgan, 1996; Zhang et al., 2004). CH_3Hg^+ demonstrates thermodynamic stability up to three-coordinate species (Hoffmeyer et al., 2006); yet NMR studies have shown the cation in these complexes is labile in the presence of free thiols (Rabenstein and Reid, 1984)**.** The average lifetime of the CH_3Hg^+ complexed by intramolecular GSH is estimated to be less than 0.01s in intact erythrocytes**,** which indicates exchange of CH_3Hg^+ between thiol ligands to be rapid in the cell (Rabenstein et al., 1982). Its lability is indicated as well by the observations on nuclear magnetic resonance (NMR) spectra in biological systems such as human erythrocytes and hemoglobin (Arnold et al., 1985; Rabenstein et al., 1982).

The rapid displacement of a complexed thiol ligand by a free thiol ligand was suggested to occur via an associative mechanism . In the case of CH_3HgCys and CH_3HgGlu (charge is neglected for simplicity):

$$CH_3Hg\text{-}S\text{-}R + S\text{-}R' \longrightarrow H_3C\text{-}Hg\begin{matrix} S\text{-}R \\ \diagdown\, S\text{-}R' \end{matrix} \longrightarrow CH_3Hg\text{-}S\text{-}R' + S\text{-}R \qquad (1.4)$$

S-R and S-R’ refer to the sulfur atom in GSH and CSH, respectively.

It has been proposed by Geier (Geier and Erni, 1973) and then confirmed by Rabenstein and Reid (1984) that, when the formation constant (K_f) of CH_3HgX is larger

than that of CH_3HgY, the forward reaction rate constant k of the following reaction is slower than that of the backward reaction rate constant (k_{-1}), and that k_{-1} increases with increasing in K_f of CH_3HgY (Eq. 1.5):

$$CH_3HgX + Y \underset{k_{-1}}{\overset{k}{\rightleftharpoons}} CH_3HgY + X \qquad \text{(Eq. 1.5)}$$

For example, when X= $^-SCH_2CH(\overset{+}{N}H_3)CO_2^-$ and Y= $^-SCH_2CO_2^-$, $K_{f,\ CH3HgX}$ = 15.99 < $K_{f,\ CH3HgY}$ = 16.93 (Arnold and Canty, 1983), and it has been shown that k = 1.6×10^8 L/ mol s > k_{-1}=4.6×10^6 L/ mol s (Rabenstein and Reid, 1984),

A second reaction pathway involves "direct exchange":

$$CH_3HgX + CH_3Hg^*Y \rightleftharpoons CH_3HgY + CH_3Hg^*X \qquad \text{(Eq. 1.6)}$$

It is unlikely that the pathway described in (eq. 1.6) is important in the toxicology of MeHg since it does not result in the transfer to free ligands. Considering the abundance of sulfhydryl groups, the associative pathway as shown in Eq. 1.4 is probably the predominant exchange pathway in biological systems (Rabenstein and Evans, 1978).

1.6 Kinetic Stability of Methylmercury-Thiol Complexes

Although the thermodynamic stabilities, as measured by the formation constants, of some MeHg-thiol complexes have been determined experimentally or based on theoretical calculations (see Table 1.1), the kinetic stability of MeHg-thiols in intra- and

extra-cellular environments is unknown. Existing studies are almost exclusively focused on photolytic or microbial demethylation of MeHg in the form of CH_3HgCl and/or CH_3HgOH (Ahmed and Stoeppler, 1986; Ahmed and Stoeppler, 1987; Fitzgerald et al., 2007; Hammerschmidt and Filtzgerald, 2006; Sellers et al., 1996; Yu and Yan, 2003). These studies have shown that both CH_3HgOH and CH_3HgCl are generally stable at circumneutral pH (6-8) (Ahmed and Stoeppler, 1987; Leermakers et al., 1990; Yu and Yan, 2003), low temperature 4 ^oC (Lanses et al., 1990), low concentration (0.4 – 0.6 nM) (Leermakers et al., 1990; Yu and Yan, 2003), high ionic strength (sea water) (Compeau and Bartha, 1983), and under the dark (Ahmed and Stoeppler, 1987; Yu and Yan, 2003). The decomposition products may include inorganic Hg^{2+} and elemental Hg(0), probably via a Hg(I) intermediate which undergoes disproportionation (Eqs. 1.7 and 1.8) (Ahmed and Stoeppler, 1987; Christmann and Ingle, 1976; Inoko, 1981; Lo and Wai, 1975; Olson, 1977; Tossell, 1998; Yu and Yan, 2003):

$$CH_3HgCl + h\nu + H^+ = CH_4 + HgCl^+ \qquad \text{(Eq. 1.7)}$$

$$2HgCl = HgCl_2 + Hg^0 \qquad \text{(Eq. 1.8)}$$

It remains unknown whether the same decomposition reaction can be applied to MeHg-thiol complexes, which will be the focus of Chapter 5 of this thesis.

1.7 Analytical Techniques

1.7.1 Analytical Techniques for the Determination of Total Mercury Concentration

Major developments have been made in recent decades for the determination of total Hg concentration in natural waters and biological tissues; detection limits at picomolar levels can now been performed in many laboratories based on cold vapor atomic absorption spectrometry (CV-AAS) (Ahmed and Stoeppler, 1986; Park and Do, 2008; Shabani et al., 2004), cold vapor atomic fluorescence spectrometry (CV-AFS) (Bloom et al., 1995; EPA Method 1631, 2002; Logar et al., 2000), and inductively coupled plasma mass spectrometry (ICP-MS) (Allibone et al., 1999; Brown et al., 1995; Fatemian et al., 1999).

The CV-AFS is probably the most sensitive technique for the determination of total Hg at ultra-trace levels; detection limit as low as 0.2 pM can be commonly achieved. In brief, the cold Hg vapor is generated by the addition of an excess amount of BrCl which oxidizes all the Hg in the sample to Hg(II), followed by titration of the remaining BrCl by hydroxylamine, and reduction of Hg(II) to Hg(0) by $SnCl_2$ or $NaBH_4$ (Chen et al., 2002; EPA Method 1631, 2002). Essentially 100% of Hg in the form of Hg^0 gas reaches the spectrophotometer and the fluorescence can be readily measured after excitation; scattering of light from water vapor and oxygen can be completely eliminated (EPA Method 1631, 2002).

Although ICP-MS generally has lower sensitivity than CV-AFS, it has the capability of determining various stable isotopes of Hg, which renders it particularly useful when studying Hg methylation and transformation pathways using Hg enriched

isotopes (Christopher et al., 2001; Heumann, 2004; Martin-Doimeadios et al., 2002; Smith, 1993). Recently, multicollector ICP-MS (MC-ICP-MS) has been shown to be capable of determining isotopic fractionation of Hg in nature (Bergquist and Blum, 2007; Evans et al., 2001; Foucher and Hintelmann, 2006).

1.7.2 Analytical Techniques for the Determination of Total Methylmercury Concentration

Since MeHg is the major exposure pathway for Hg in higher trophic animals and humans, it has long been recognized that knowing the total Hg concentration is not sufficient to infer the toxicity of Hg; there is a need to differentiate the concentration of MeHg from the total Hg concentration. The first analytical method for determining the MeHg concentration was reported by Westoo (Westoo, 1966) and was based on gas chromatography (GC) following benzene extraction. Since then, a variety of analytical methods have become available, some of them are summarized in Table 1.4.

These methods in general consist of a separation step to isolate MeHg from other Hg species (i.e., inorganic Hg, other organomercuric species) followed by analysis using various detectors. Common separation techniques include GC (e.g., Cela-Torrijos (1996); Forsyth and Marshal (1983); Xu et al. (2005)), HPLC (e.g., Harrington (2000); Percy et al. (2007); Rai et al. (2002)(Harrington, 2000; Percy et al., 2007; Rai et al., 2002), and capillary electrophoresis (CE) (e.g., Li et al. (2007); Schramel et al. (1998). The detectors can be electron capture detection (ECD), atomic absorption spectrometry (AAS), atomic fluorescence spectrometry (AFS), or mass spectrometry (MS).

GC-ECD was the first analytical method for total MeHg analysis (Westoo, 1966); however, one of the drawbacks of this technique is that the halogen-bearing compounds co-extracted with MeHg interfere with the determination because of the non-specificity of the ECD (Cai et al., 1996). An improvement was to volatize MeHg by aqueous ethylation with sodium tetraethylborate ($NaBEt_4$), followed by purge and trapping and separation by GC, and then detection by either AAS (Fischer et al., 1993) or AFS (Bloom, 1989; Cai et al., 2000; Logar et al., 2002). Several variations of this procedure have been applied for the determination of total MeHg in fish (Cappon and Smith, 1978; Davis et al., 2007; Forsyth et al., 2004; Logar et al., 2000; Velez et al., 2007; Wagemann et al., 1998), sediment (Cappon and Smith, 1978; Leermakers et al., 2005), human urine (Cappon and Smith, 1978), hair and blood (Gibièar et al., 2007) samples.

HPLC coupled with different detection methods has been recently considered as the most promising technique for speciating MeHg from other forms of Hg. The majority of HPLC methods reported in the literature are based on reversed phase separations (e.g., with C8 and C18 columns) (Blanco et al., 2000; Harrington, 2000; Harrington and Catterick, 1997; Percy et al., 2007; Rai et al., 2002), though cation-exchange columns have also been used (Vallant et al., 2007). When using reversed phase HPLC, the mobile phase usually contains an organic modifier (e.g., CSH, 2-mercaptoethanol), a chelating or ion pair reagent in order to improve chromatographic separation and/or to avoid adsorption of mercurial species to the stationary phase, and in some cases, a pH buffer. A number of protocols described in Table 1.4 are not sensitive enough to detect MeHg in uncontaminated samples.

Pre- or post-column derivatization is commonly involved in the analysis of MeHg by HPLC or GC. Solid phase micro-extraction (SPME) has been employed as a derivatization process to increase the volatility of Hg species prior to GC separation (Davis et al., 2007; Leermakers et al., 2005; Parkinson et al., 2004). Pre-column ethylation derivatization, as mentioned above, is the most common process currently practiced in GC separation of MeHg (Bloom, 1989; Ebdon et al., 2002; Gibièar et al., 2007; Horvat et al., 1993; Shade and Hudson, 2005). Cold vapor (CV) post-column derivatization on GC has significant use for MeHg determination (Fischer et al., 1993; Gardfeldt et al., 2003; Logar et al., 2002) when it is used as the separation device and AAS or AFS is used as detector.

Post-column online derivatization is the most common technique used in HPLC to produce Hg cold vapor after column separation (Foltin et al., 1996; Rio-Segade and Bendicho, 1999); CV pre-column derivatization using thiol compounds has been reported (Sarzanini et al., 1992) for MeHg analysis using HPLC.

Capillary electrophoresis (CE) is a relatively new and still developing technique for the determination of MeHg; CE typically involves complexation with various thiols and other chelating agents (e.g., CSH), though direct analysis without complexation has also been reported (Kubán et al., 2007; Li et al., 2005b).

When comparing various separation techniques for MeHg analysis, HPLC has the advantage of not requiring conversion of Hg to volatile derivatives prior to separation, as is necessary in GC. However, HPLC techniques have the disadvantage of having higher detection limits compared to GC (see Table 1.4) (Boszke, 2005). Compared with GC or HPLC methods, CE shows several advantages, including high resolving power, rapid and

efficient separations, minimal reagent consumption and the possibility of separations with only minor disturbances of the existing equilibrium between the different species (Silva da Rocha et al., 2001).

Table 1.4 - Summary of the major analytical methods for the determination of total MeHg concentration in environmental and biological samples.

Separation Technique	Detector	Analyte	Stationary Phase	Mobile Phase	Derivatization	Detection Limit	References
GC	AAS	MeHg; Hg	Cryogenic, OV-3	He	Ethylation	4 - 167 pg	(Fischer et al., 1993; Logar et al., 2000; Sanchez-Urıa and Sanz-Medel, 1998)
	AFS	MeHg; Hg; EtHg	DB-1; OV-3, Cryogenic	He	Ethylation	0.6 - 1.3 pg	(Bloom, 1989; Cai et al., 1996; Devai et al., 2001; Ebdon et al., 2002; Gardfeldt et al., 2003; Gibièar et al., 2007; Hintelmann and Evans, 1997; Logar et al., 2002; Ortiz et al., 2002; Sanchez-Urıa and Sanz-Medel, 1998; Shade and Hudson, 2005)
	MS	MeHg	OV-3, HP-1; MXT silcosteel	He, Ar	SPME; Ethylation	0.1 - 58 pg	(Davis et al., 2007; Hintelmann and Nguyen, 2005; Karlsson and Skyllber, 2003; Martin-Doimeadios et al., 2002; Sanchez-Urıa and Sanz-Medel, 1998)
	ECD	MeHg	AT-5 and HP-1	He, Ar		10 - 80 ng mL^{-1}	(Cela-Torrijos et al., 1996; Westoo, 1966; Westoo, 1967)
	MIP-AES	MeHg; Hg	Multicapillary	He	Ethylation	Hg=0.5 pg MeHg=0.6 pg	(Botana et al., 2002)

Table 1.4 - (*continued*)

Separation Technique	Detector	Analyte	Stationary Phase	Mobile Phase	Derivatization	Detection Limit	References
HPLC	ICP-MS	MeHg; Hg	Kromasil 100-5C_{18} Spherisorb S5 ODS2	10 mM TBABr and 60% methanol		16 - 400 ng L^{-1}	(Boszke, 2005; Harrington, 2000; Harrington and Catterick, 1997)
	CV-AAS	MeHg; Hg	Novapak C18	60% methanol 0.01 M TBABr 0.025 M NaCl	CV	20 x $l0^{-3}$ - 1.0 ng	(Boszke, 2005; Harrington, 2000; Rio-Segade and Bendicho, 1999; Sanchez-Urıa and Sanz-Medel, 1998)
	ICP-MS	MeHg, Hg(II), EtHg, PhHg	Spherisorb ODS-2; α-chrom $C_{18;}$ SphereClone 5 µm ODS2	5% methanol/water 0.06 M NH_4Ac and 0.1% w/v CSH, pH 6.8		Hg=3-5 pg MeHg= 1pg-11ng EtHg= 4pg-8ng PhHg=1.8pg	(Boszke, 2005; Castillo et al., 2006; Harrington, 2000; Qvarnstrom and Frech, 2002; Rai et al., 2002; Wan et al., 1997; Wilken and Falter, 1998)
	ICP-MS	MeHg; Hg	Hamilton PRP-X200	50 M pyridine,0.5% CSH and 5% methanol, at pH 2		MeHg=1.0 pg Hg(II)=1.6 pg	(Vallant et al., 2007)
	ICP-MS	MeHg; Hg	Novapak C18	0.06 M^{1} NH_4Ac, 5% v/v methanol, 0.1% v/v ME			(Boszke, 2005; Harrington, 2000; Morton et al., 2002)
	ICP-AES	MeHg; Hg	Gemini RP, Hamilton PRP-1	50 mM phosphate-buffer; 10 mM CSH at pH 7.5		MeHg=30ng Hg(II)=24ng	(Boszke, 2005; Harrington, 2000; Percy et al., 2007)

Table 1.4 - (*continued*)

Separation Technique	Detector	Analyte	Stationary Phase	Mobile Phase	Derivatization	Detection Limit	References
HPLC	API-MS	MeHg, Hg(II), Ethyl-Hg, PhHg	Kromasil 100-5C_{18}	0.01% v/v ME in methanol: water (1:1 v/v)		Not determined	(Harrington et al., 1998)
	PB/EI-MS	MeHg, Hg(II) and PhHg	C_{18}	60% methanol and 0.01% ME; pH 5.5		MeHg=0.75ng Hg(II)=0.077ng, PhHg=0.051ng	(Krishna et al., 2007)
	UV	MeHg	chromspher RP-18	30% methanol 0.1mM ME, pH5.2 (NH4Ac)		0.10 - 25ng	(Boszke, 2005; Hintelmann et al., 1993)
	UV	MeHg, Hg, PhHg	Separon SIX,	5% MeOH, 95% water (5mM H_2SO_4) 5mM NaBr, pH2	dithizone solution	MeHg= 1.1 ng MeHg=2.2 ng PhHg= 6.2 ng	(Foltin et al., 1996)
	UV	MeHg, Hg, PhHg	Xterra C18 column	(35+35+30, v/v/v) Methanol/THF/0.1 M sodium acetate buffer + 166µM EDTA	dithizone solution	MeHg=0.12ng Hg=0.14ng PhHg=0.16ng	(Hashemi-Moghaddam and Saber-Tehrani, 2008)
	AFS	MeHg	Nucleosil ODS C_{18}	5% MeOH 95% water (0.01% ME pH5	Post-UV	0.015 - 0.1 ug	(Boszke, 2005; Harrington, 2000; Ramalhosa et al., 2001; Sanchez-Urıa and Sanz-Medel, 1998)
CE	UV	Hg, MeHg, EtHg, PhHg	HP 3D	100 mM sodium borate, pH 8.35		10 - 88 ng	(Gaspar and Pager, 2002; Pager and Gaspar, 2002)

Table 1.4 - (*continued*)

Separation Technique	Detector	Analyte	Stationary Phase	Mobile Phase	Derivatization	Detection Limit	References
CE	ICP-MS	Hg, MeHg, EtHg		25 mM sodium tetraborate, pH 9.3		2×10^{-3} - 20 ng	(Boszke, 2005; Silva da Rocha et al., 2000a; Silva da Rocha et al., 2000b; Silva da Rocha et al., 2001)
	AFS	Hg, MeHg		30 mM boric acid, 8% methanol, pH 9.4		3 - 9.5 ng	(Li et al., 2005a)
	AAS	Hg, MeHg, PhHg		100 mM boric acid, 10% methanol, pH 8.3		3 ng	

Abbreviations: SPME, solid phase microextraction; PB/EI-MS, particle beam/electron ionization-mass spectrometry; API-MS. Atmospheric Pressure Ionization Mass Spectrometry; UV, ultra violet; TBABr, tetrabutylammonium bromide; NH_4Ac, ammonium acetate; ME, 2-mercaptoethanol; THF, tetrahydrofuran acetic acid; EDTA, ethylenediaminetetraacetic acid, EtHg, ethylmercury; PhHg, phenyl mercury

1.7.3 Analytical Techniques for the Determination of Methylmercury Speciation

All the methods described in Table 1.4 are aimed at separating MeHg from inorganic Hg or other organomercuric species (e.g., dimethylmercury). In other words, they measure total MeHg concentration, but are not capable of determining individual MeHg species. As discussed earlier, it is unlikely that MeHg occur as free $CHHg^+$ cations, be it in biota or in the environment, and be present as complexes with various inorganic (e.g., OH^-, Cl^-, HS^-) and organic (e.g., thiols, humic and fulvic acids) ligands (Zhang et al., 2004). These different groups of MeHg complexes have different chemical reactivities, bioavailabilities, and toxicities. Therefore, analysis of total MeHg may not be sufficient to infer the cycling and toxicity of MeHg in the environment or in biological systems. Analytical techniques that are capable of separating and analyzing individual MeHg species are thus needed.

By comparing the Hg L_{III} X-ray absorption near-edge structure (XANES) of swordfish muscle (*Xiphias gladiu*) spectrum to several standards, including Hg, CH_3HgCl and MeHg complexed with thiols spectra, Harris et al.(Harris et al., 2003) concluded that the MeHg in the fish muscle was predominantly in the form of MeHg-thiol complexes; it remains, however, unknown to which thiols the MeHg ions are bonded, as XANES can only identify the local Hg-S environment. Hintelmann and Simmons (Hintelmann and Simmons, 2003) were the first to use electrospray ionization (ESI-MS) to study MeHg speciation in aqueous solutions. They were able to differentiate polynuclear complexes of CH_3Hg^+ such as $[(CH_3Hg)_2OH]^+$ and $[(CH_3Hg)_3O]^+$, but with limited applicability due to higher detection limits comparing to HPLC. (Krupp et al., 2008) were successful in

hyphenating HPLC with ICP-MS and ESI-MS to determine several MeHg species (CH_3HgCys and CH_3HgGlu) in aqueous solutions spiked with laboratory standards, but were not able to determine MeHg speciation in real-world plant samples due to the inability to extract the mentioned compounds from the samples.

1.8 Organization of this Thesis

To address the objectives of the research, this thesis is organized in six chapters. Chapter 1, the present chapter, provides a general introduction on MeHg and issues relevant to the research. Since no MeHg-thiol complexes are commercially available, they have to be first synthesized in the laboratory. Chapter 2 reports the synthesis and characterization of CH_3HgCys and CH_3HgGlu. The synthesized compounds were then used as the standards, along with commercially available CH_3HgCl and inorganic Hg, in the development of a HPLC-ICPMS method for MeHg speciation which is described in Chapter 3. Chapter 4 describes the application of the new speciation method for the study of MeHg speciation in a fish muscle sample after enzymatic hydrolysis, which provided the first analytical evidence of the presence and dominance of CH_3HgCys in biological samples. Chapter 5 describes the application of the speciation method for the study of the kinetic stability of CH_3HgCys and CH_3HgGlu in aqueous solutions under various conditions. Chapter 6 summarizes the conclusions from the thesis, as well as the lessons learned and future perspectives. Additional information is included in the appendices.

Chapters 3 and 4 formed the basis of the following article, which was recently published: Lemes M. and Wang F. 2009. Methylmercury speciation in fish muscle by HPLC-ICP-MS following enzymatic hydrolysis. Journal of Analytical Atomic

Spectrometry 24: 663–668. Manuscripts are being prepared from other chapters of the thesis.

Chapter 2. Syntheses and Characterization of Methylmercury Cysteinate and Glutathionate

This chapter describes the synthesis of methylmercury cysteinate (CH_3HgCys) and methylmercury glutathione (CH_3HgGlu) and their characterization by elemental analysis, ^1H NMR, X-ray crystallography, and ESI-MS.

2.1 Syntheses of Methylmercury Cysteinate and Glutathionate

CH_3HgCys was synthesized by mixing equimolar concentrations of CH_3HgOH (Alfa Aesar, 95%) with CSH (Sigma, ≥98%) in ultra-pure deionized water (MilliQ-Element; "ultra-pure water" hereafter) following a procedure similar to Taylor et al. (Taylor et al., 1975) under an ultra pure Ar (99.999%) atmosphere. In brief, CH_3HgOH (2 mmol) and CSH (2 mmol) were mixed in 150 mL of H_2O in a 250-mL round bottom flask and stirred for 3 hr at pH = 6.5 at room temperature. The volume of the solution was then reduced to ~20 mL in a rotary evaporator (Büchi Rotavapor) and the mixture was left to crystallize under an Ar atmosphere. The crystalline product was then filtered through a 0.2-μm pore-size hydrophilic polypropylene membrane (Pall). The yield was ~96%. The crystallization process was rapid (within 24 hr). Fig. 2.1a shows a picture of the CH_3HgCys crystals obtained after crystallization.

CH_3HgGlu was synthesized following a similar procedure as that of CH_3HgCys as described above, with the exception that GSH was used instead of CSH; see Fig. 1.3, in Chapter 1 (Rabenstein, 1973). The initial product was gel-like at 4 °C that became liquid at room temperature. Following a similar procedure and after adding acetone to the

product, Neville and Drakenberg (Neville and Drakenberg, 1974) obtained a "syrupy residue". By adding benzene instead of acetone and letting it evaporating at room temperature under Ar, we were able to obtain a white, amorphous powder after two weeks with a yield of 89% (Fig. 2.1b).

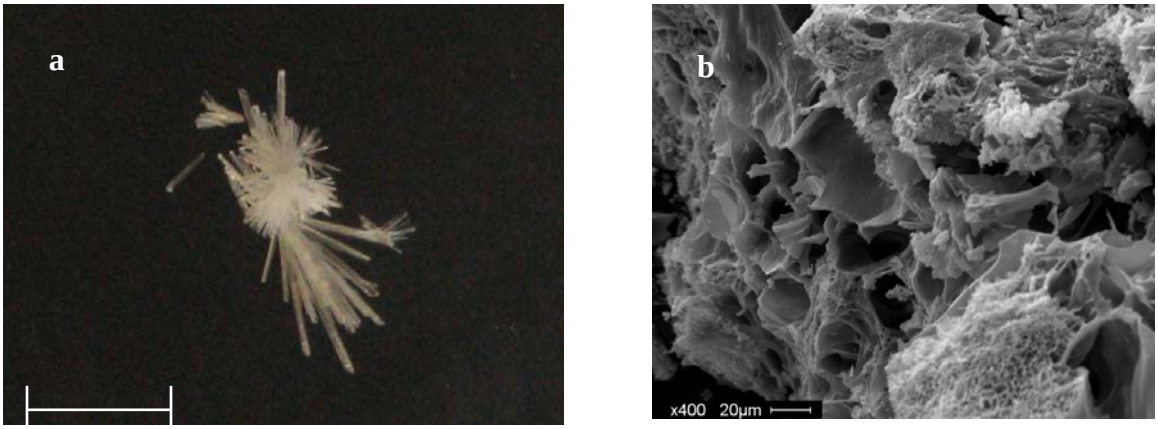

Figure 2.1 – Pictures showing **a)** Crystalline CH_3HgCys (after being aged for two month), and **b)** Amorphous CH_3HgGlu. Picture **a** was taken by a regular camera, whereas picture **a** was taken by scanning electron microscopy at the Department of Geological Sciences, University of Manitoba.

2.2 Elemental Analyses of the Compounds

Elemental analysis was done at Guelph Chemical Laboratories Ltd., Ontario, Canada. For the CH_3HgCys, the theoretical values are: C, 14.25; H, 2.67; N, 4.15; O, 9.49; S, 9.51; Hg, 59.92%, and the found values were: C, 13.94; H, 2.92; N, 4.14; O, 9.78; S, 9.30; Hg, 60.02%. For the CH_3HgGlu, the theoretical values are: C, 25.30; H, 3.67; N, 8.05; O, 18.39; S, 6.14; Hg, 38.43%, and the found values were: C, 24.90; H, 3.69; N, 7.88; O, 18.90; S, 5.88; Hg, 38.25%.

2.3 Nuclear Magnetic Resonance (NMR) Characterization of the Compounds

^{1}H NMR spectra were recorded on an AMX 500 NMR spectrometer (Bruker) at a probe temperature of 298 K. The synthesized CH_3HgCys and CH_3HgGlu were dissolved in D_2O (~ 5 μM) for the measurement. Spectra were recorded at a pulse width of 90°, relaxation delay of 3 s, scan number of 128, and a spectral width 8620.69 Hz (17 ppm). The proton chemical shifts were reported in ppm (δ) relative to the internal tetramethylsilane (TMS, δ=0.0) standard. The data were collected by Dr. K. Marat and Mr. T. Wolowiec at the Department of Chemistry, University of Manitoba.

Figure 2.2 shows the ^{1}H NMR spectra of CH_3HgCys and CH_3HgGlu. For comparison, that of CH_3HgCl is also shown. In both cases, a sharp central resonance line (δ = 0.62 ppm for CH_3HgCys, and 0.64 ppm for CH_3HgGlu) was flanked symmetrically by two less intense satellite lines (δ = 0.79 ppm and 0.45 ppm for CH_3HgCys, and δ = 0.82 and 0.47 for CH_3HgGlu). The satellites lines are due to the methyl groups bonded to ^{199}Hg which has a nuclear spin of ½ and a natural abundance 16.87%, whereas the central resonance is due to methyl groups bonded to all other isotopes of Hg. When compared with CH_3HgCl (Fig. 2.2a), binding between MeHg and CSH or GSH resulted in the central resonance of the methyl group protons that are directly attached to Hg being shifted to a higher field (Fig. 2.2b and c). The coupling constant $J(^{199}Hg\text{-}^{1}H)$ was calculated to be 213.7 Hz for CH_3HgCl, 172.5 Hz for CH_3HgCys, and 172.6 Hz for CH_3HgGlu, comparing very well with those reported for the aqueous solution of CH_3HgOH (260-203 Hz for pH = 1.0 - 13.0), and mixed aqueous solutions of CH_3HgOH

with CSH (178 – 173 Hz for pH = 1.0 – 13.0) and with GSH (175 – 170 Hz for pH = 1.0 – 13.0) (Rabenstein and Fairhurst, 1975).

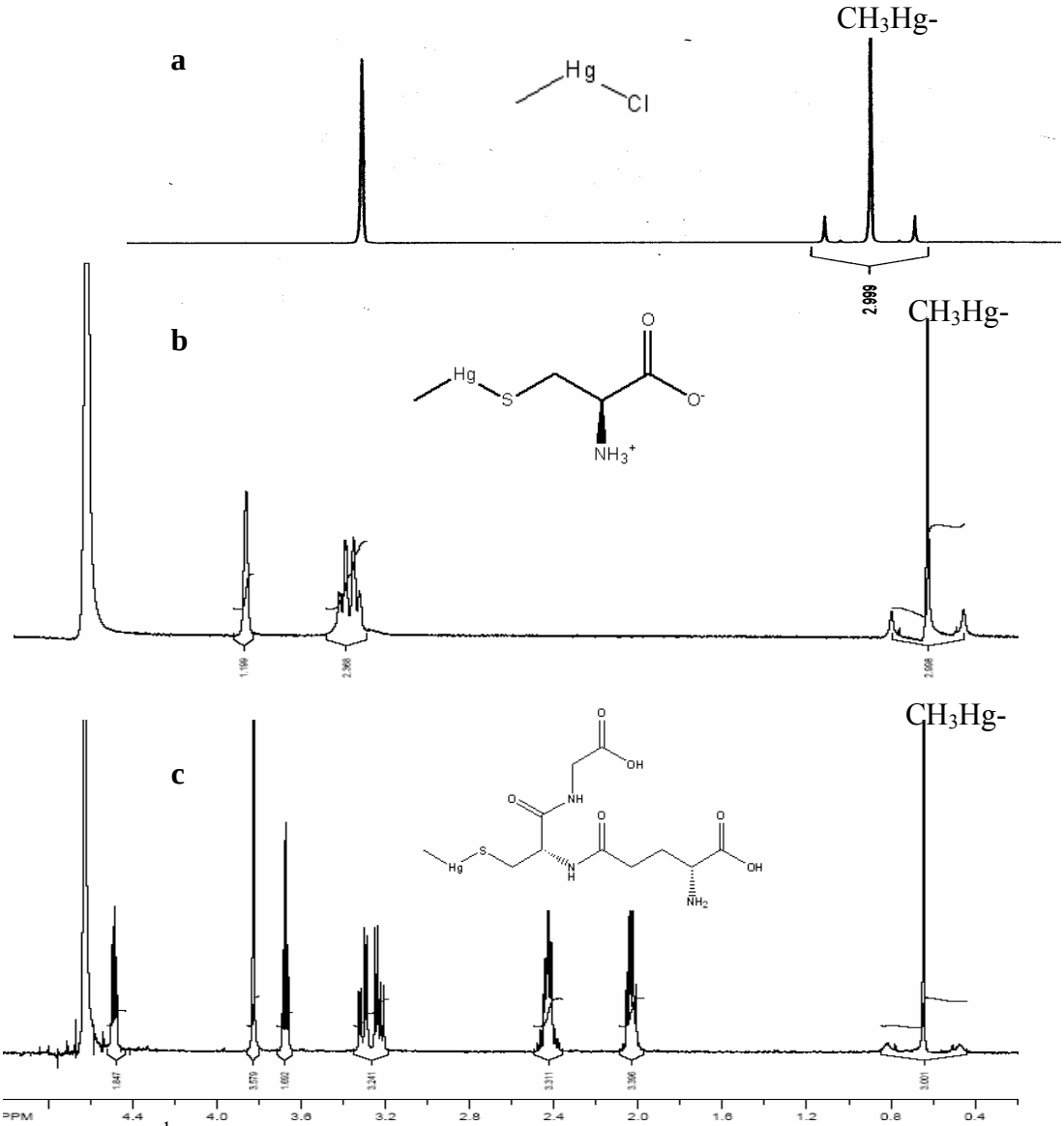

Figure 2.2 - ^{1}H NMR spectra of **a)** CH_3HgCl (in CD_3OD), **b)** CH_3HgCys (in D_2O), and **c)** CH_3HgGlu (in D_2O). The resonance lines at 3.3 ppm in (**a)** and 4.65 ppm in (**b)** and (**c)** were due to the residual protons present in the solvent CD_3OD and D_2O, respectively

2.4 Refined Crystal Structure of CH_3HgCys

Since the CH_3HgGlu synthesized was amorphous, X-ray crystallography was done only for CH_3HgCys. A prismatic CH_3HgCys crystal (0.06 x 0.06 x 0.24 mm) was mounted on a Bruker 4-circle single-crystal diffractometer equipped with an APEX CCD area detector using graphite-monochromated Mo Kα (λ = 0.71073 Å) radiation. The crystal-glass-fiber end was dipped in epoxy and the crystal coated prior to data collection. In excess of a hemisphere of data intensity, was collected (293 K) to 60° 2θ using a frame width of 0.2° and a frame time of 15 seconds, at a crystal-to-detector distance of 5 cm. Integration of the intensity data was carried out using the SAINT program, along with standard corrections (for Lorentz, polarization and background effects). A total of 17091 reflections were integrated, corrected for absorption effects using the SADABS program, and identical reflections (at different Ψ angles) combined using the XPREP program, to give a total of 8685 reflections in the Ewald sphere. The rapid data collection (<24 hr) and the epoxy coating on the crystal prevented any measurable deterioration, and a time-decay correction was not employed. This contrasts with 12% intensity loss experienced by Taylor et al. (Taylor et al., 1975) for the standard reflections measured during their data collection. Systematically absent reflections are consistent with space group P212121, with 2573 unique data with a Laue (mm) merging of 3.4% (Friedel pairs were not merged). Scattering curves for neutral atoms, together with anomalous dispersion corrections, were taken from International Tables for X-ray Crystallography (Wilson, 1992). The Bruker SHELXTL program was used for the refinement of the crystal structure with initial coordinates of all non-hydrogen atoms taken from Taylor et al.

(1975). Least-squares refinement (based on Fo2 and all 2573 data) for a model involving anisotropic displacement of all non-hydrogen atoms converged to an R1 index of 3.4% (2308 observed unique reflections |Fo| > 4σF) and wR2 index of 8.3% for all data. The absolute structural configuration was clearly established [Flack parameter = 0.004(14)]. Residual peaks in the difference-Fourier map conforming to sensible H positions were inserted into the model and allowed to refine with the following constraints for chemically equivalent H atoms: (1) the donor-atom — H distances were restrained to equal the observed electron density maxima (as opposed to the internuclear distance) as suggested by the software, and (2) the isotropic displacement parameters were restrained to be equal. The program PLATON was used for molecular geometry and drawing (Spek, 2005). The analysis was done by Mr. M Cooper at Department of Geological Sciences, University of Manitoba. The crystal structure of CH_3HgCys was first established by Taylor (1975) and is refined here. An ORTEP plot of the molecular structure is shown in Fig. 2.3. Selected bond distances and angles are collected in Table 2.1.

The unit cell parameters obtained by least-squares refinement of 5983 reflections ($I > 10\sigma I$; to 55° 2θ) are a = 6.3857(4), b = 26.0567(14), and c = 5.2863(3) Å and agree well with those reported by Taylor (1975). Taylor et al. (1975) were not able to resolve the hydrogen locations in the molecule, however with our refined model, we can clearly depict the locations of all the protons in the molecule (Fig. 2.3). The amine group is found to be protonated ($-NH_3^+$), whereas the carboxyl group is deprotonated ($-COO^-$), which is in agreement with the I.R. results of Taylor et al. (1975). The angle of C-Hg-S was also found to be 178.8º, which is more linear than that previously reported by Taylor (1975).

Table 2.1 - Intramolecular and intermolecular bond distances and angles of CH_3HgCys

	Distance (Å)			**Angle (º)**	
	This study	Taylor et al. (1975)		This study	Taylor et al. (1975).
Hg - C(4)a	2.084(10)	2.10(4)	C(4)a - Hg - S	178.8(3)	177.6 (0.9)
Hg - S	2.358(2)	2.362 (12)	Hg - S - C(1)	100.8(2)	100.4 (0.9)
S - C(1)	1.823(9)	1.81 (3)	S – C(1) - C(2)	114.8(5)	113.7 (1.1)
C(1) - C(2)	1.506(9)	1.48 (4)	C(1) - C(2) - C(3)	114.2(5)	116.1 (1.3)
C(2) - C(3)	1.539(8)	1.53 (3)	C(1) - C(2) - N	110.7(5)	115.0 (1.3)
C(2) - N	1.489(8)	1.53 (4)	C(3) - C(2) - N	109.5(5)	105.7 (1.1)
C(3) - O(1)	1.242(7)	1.24 (3)	C(2) - C(3) - O(1)	117.6(5)	123.0 (1.3)
C(3) - O(2)	1.256(7)	1.33 (3)	C(2) - C(3) - O(2)	115.8(5)	112.7 (1.3)
Hg - O(2)	2.860(5)	2.85 (2)	O(1) - C(3) - O(2)	126.5(5)	124.0 (1.3)
			S - Hg - O(2)	84.5(1)	84.9 (0.4)
			C(4)a - Hg - O(2)	95.5(3)	95.7 (0.9)
O(3) - O(1)b	2.759(7)	2.73(3)	O(3) - H(10) - O(1)b	145(9)	
O(3) - O(2)c	2.738(6)	2.73(3)	O(3) - H(11) - O(2)c	164(9)	
N - O(3)	2.713(7)	3.42 (3)	N - H(1) - O(3)	162(8)	
H(10)...O(1)b	1.90(6)				
H(11)...O(2)c	1.78(3)				
H(1)...O(3)	1.85(3)				

The most significant difference between the structure reported here and that of Taylor et al. (1975) is in the geometry of the carboxylate group. It was postulated by Taylor et al. that the difference in the [C(3)—O(2) = 1.33(3) and C(3)—O(1) = 1.24(3) Å] distances associated with the carboxyl C(3) position may be related to a possible weak intramolecular bonding interaction between the Hg atom and the O(2) oxygen atom of the carboxylate group [Hg….O(2) = 2.85(2) Å]. We saw similar observations (within 1 standard error) distances within our carboxylate group [C(3)—O(2) = 1.256(7) and C(3)—O(1) = 1.242(7) Å], and a similar Hg….O(2) separation of 2.860(5) Å. A comparison of the hydrogen bonding supplied by the solvent water molecule [H(10)—O(3)—H(11)], to the O(1) and O(2) sites, reveals a slightly "linear" and shorter hydrogen bond to the O(2) anion of the nearby carboxylate group (Table 2.1). For our structure, the slightly longer C(3)—O(2) distance in combination with the slightly stronger H(11)…O(2) hydrogen bond, would serve to maintain the overall bonding requirements at the O(2) oxygen relative to a similar converse argument made for the O(1) oxygen. As such, for our structure there is no need for any additional bonding to O(2) *via* the Hg atom in order to satisfy the bonding requirements of the O(2) anion.

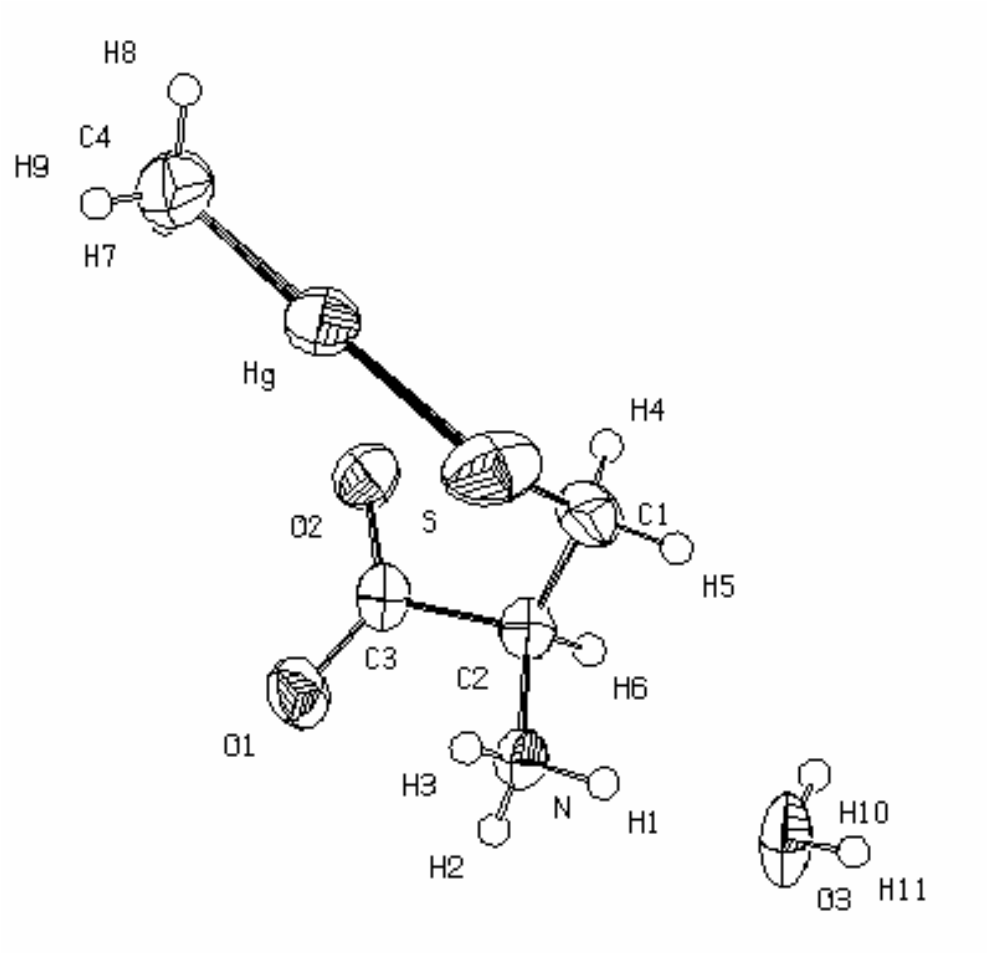

Figure 2.3 - Refined molecular structure of CH_3HgCys

2.5 Mass Spectra and Fragmentation Patterns of the Compounds

The mass spectra of the compounds were recorded on an API 2000 (Applied Biosystems), a Quattro-LC (Micromass), and a G6140A QQQ LC-MS (Agilent) electrospray ionization mass spectrometer. All three systems gave similar fragmentation patterns of CH_3HgCys and CH_3HgGlu under both positive and negative scan modes using an infusion pump. Only the spectra obtained from the Agilent system are shown below.

For the analysis, the synthesized CH_3HgCys and CH_3HgGlu standards were dissolved in a small amount of ultra-pure water and diluted to 5 µM with CH_3OH before

being injected into ESI source with a micro-syringe. Infusion experiments of CH_3HgCys and CH_3HgGlu utilized the built-in Harvard syringe pump operating at a flow rate of 30 $\mu L\ min^{-1}$. Typical spectra of CH_3HgCys and CH_3HgGlu under the scan mode showed a stable $[M-H]^-$ parent ion and some of their fragments (Fig 2.4a and 2.4b), respectively. The number of fragments and/or cluster depends on the operating parameters (e.g., cone voltage).

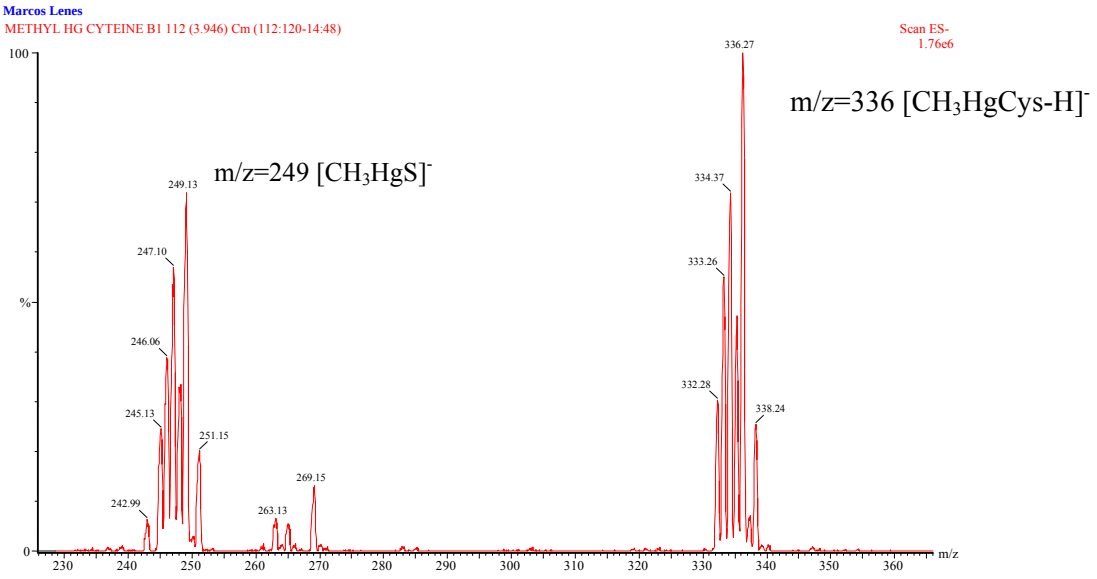

Figure 2.4a – CH_3HgCys (m/z=336) and its fragment CH_3HgS (m/z=249) analyzed in the negative mode (cone voltage= -30V)

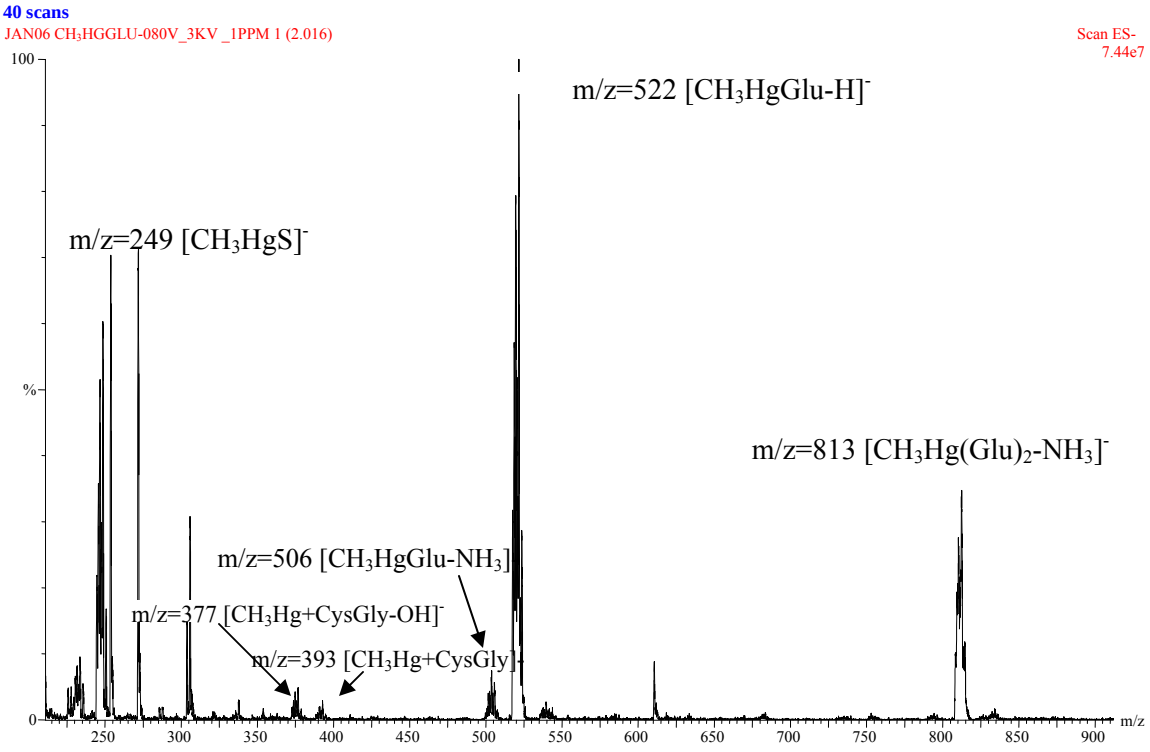

Figure 2.4b – CH_3HgGlu (m/z=522) and its fragments CH_3HgS (m/z=249), CH_3Hg+CysGly-OH (m/z=377), CH_3Hg+CysGly (m/z=393), CH_3HgGlu-NH_2 (m/z=508), and a cluster $CH_3Hg(Glu)_2$ (m/z=813) analyzed in the negative mode (cone voltage= -80V)

2.5.1 CH_3HgCys and its Fragmentation Pattern

Figure 2.5 shows ESI-MS spectra of the synthesized CH_3HgCys and its fragmentation pattern using the negative-ion mode at varying cone voltages. At a low cone voltage of 15 V, the deprotonated parent CH_3HgCys ion ($[CH_3HgCys-H]^-$; *m/z* = 336 for ^{202}Hg) dominated the spectrum, with a minor fragment peak at *m/z*= 249 corresponding to $[CH_3HgS]^-$ and a cluster peak at *m/z*=674 $[CH_3Hg(Cys)_2-2H]^-$. Increasing the cone voltage resulted in a decrease in the intensity of the parent peak and an increase in the $[CH_3HgS]^-$ peak. When the cone voltage was further increased to ≥45

V, a new fragment peak appeared at *m/z* = 234 which we believe was $[Hg^{I}S]^{-}$. As Hg(II) is redox sensitive, the gas phase reduction of Hg(II) to Hg(I) is possible during the ESI process at high cone voltages (Henderson and McIndoe, 2005). Indeed, gas phase reduction of other easily reduced metal ions such as Cu(II) at high cone voltages has been widely observed in the presence of various ligands including amino acids (Henderson and McIndoe, 2005; Vaisar et al., 1996). No other Hg-containing fragments were evident.

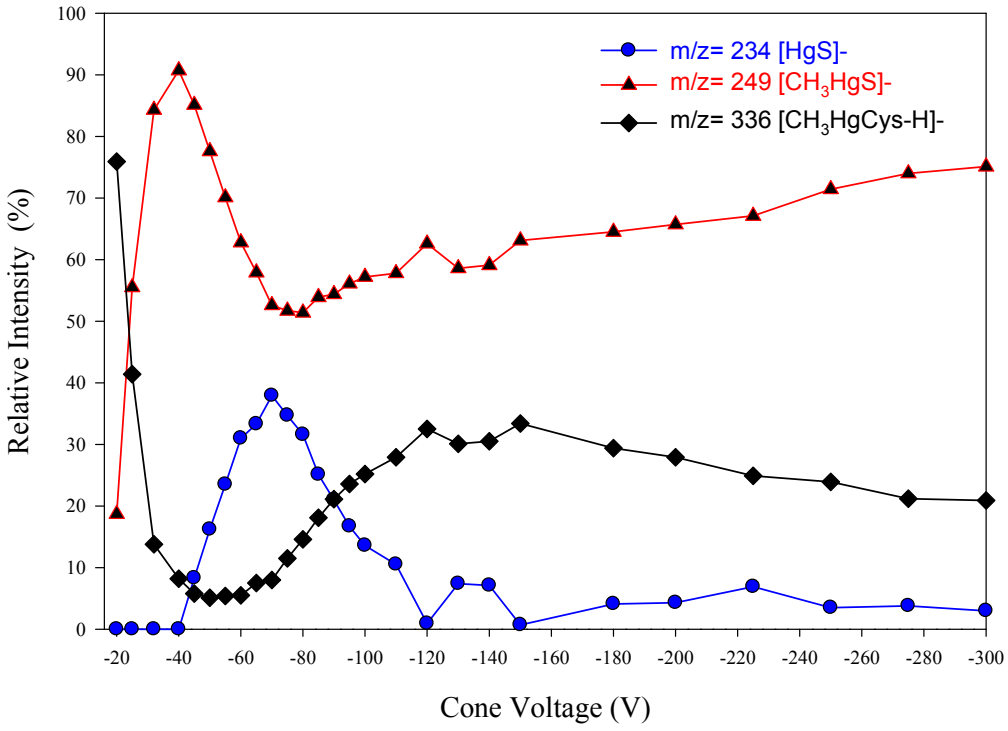

Figure 2.5 - CH_3HgCys and its fragmentation pattern using the negative-ion mode at varying cone voltages

The fragmentation pattern of CH_3HgCys at varying cone voltages was also demonstrated under the positive-ion mode (Fig. 2.6). The predominant peak was at *m/z* = 338 which corresponds to $[(CH_3HgCys+H]^{+}$ at low cone voltage (≤ +20V), with a minor

fragment peaks at *m/z* = 234 $[CH_3HgOH]^+$, *m/z* = 321 $[CH_3HgCys\text{-}NH_3]^+$, and also two clusters corresponding to *m/z* = 360 $[CH_3HgCys]^+ \cdot Na$ and *m/z* = 552 $[(CH_3Hg)_2Cys\text{-}2H]^+$. The fragments at *m/z* = 234 $[CH_3HgOH]^+$ and *m/z*= 321 $[CH_3HgCys\text{-}NH_3]^+$ had the highest intensity at a cone voltage of +20V and decreased with increasing cone voltage. On the other hand upon increasing the cone voltage the $[CH_3HgOH]^+$ and $[CH_3HgCys\text{-}NH_3]^+$ fragments were further fragmented, giving rise to the m/z=217 $[CH_3Hg]^+$ which peaked at a cone voltage of +60V (Fig. 2.6). At the same time, the cluster m/z= 382 $[CH_3HgCys]^+ \cdot 2Na$ increased (Na^+ is a common ions among others in ESI-MS systems). Hg^{2+} (m/z=202) was produced at high cone voltages only (greater than +100V), contributing to about 6% of the intensity at these higher voltages.

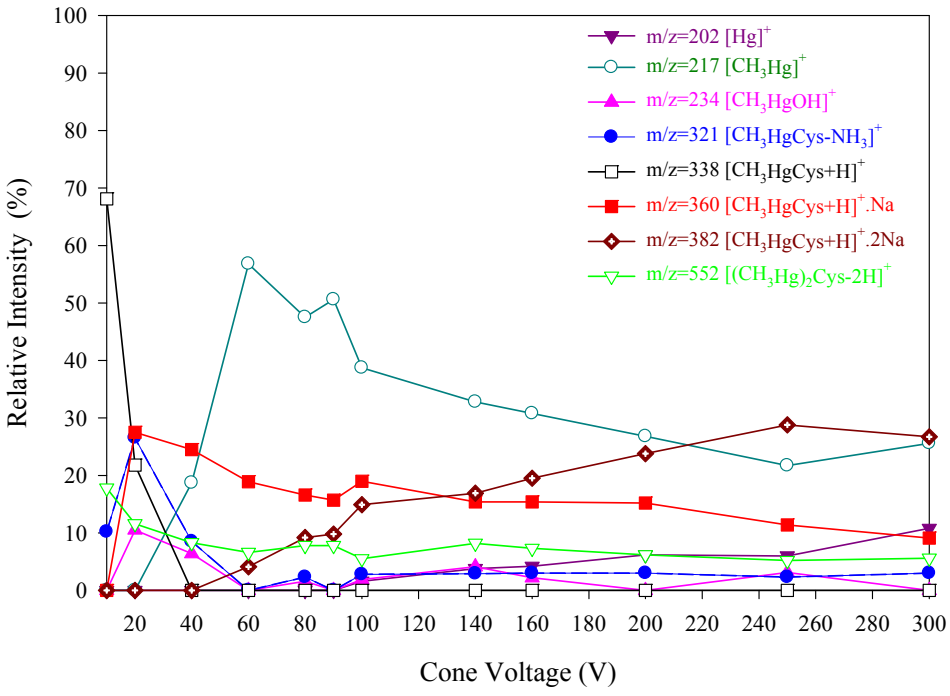

Figure 2.6 - CH_3HgCys and its fragmentation pattern using the positive-ion mode at varying cone voltages

The presence of the parent CH_3HgCys and its fragments under both positive and negative ion modes suggests that the synthesized CH_3HgCys was with a 1:1 stoichiometric ratio between MeHg and CSH. In other words, Hg in the CH_3HgCys has a coordination number of 2: one bonded to the carbon atom of the methyl group and the other to the sulphur atom of CSH (see Fig. 2.3). Given that the amino group in CSH may also bind with Hg and that Hg could have a coordination number up to 4 (Hoffmeyer et al., 2006), CH_3HgCys complexes with other stoichiometric ratios are possible under different molar ratios of MeHg and CSH, such as $(CH_3Hg)_2Cys$ (where one MeHg binds to S and one to the carboxylate group), $CH_3Hg(Cys)_2$, and $CH_3Hg(Cys)_3$ (Canty et al., 1994; Hoffmeyer et al., 2006), but were not observed in this study.

The presence of $[CH_3HgS]^-$ and $[Hg^IS]^-$ fragments and the absence of CH_3Hg^+ fragment in the mass spectra indicate that the Hg-S bonding is stronger than the Hg-C bond. This suggests that demethylation of MeHg compounds to inorganic Hg is possible in the presence of a sulfide ligand which will be further demonstrated in Chapter 5.

Based on these results, the fragmentation pathway of CH_3HgCys is depicted in Scheme 2.1.

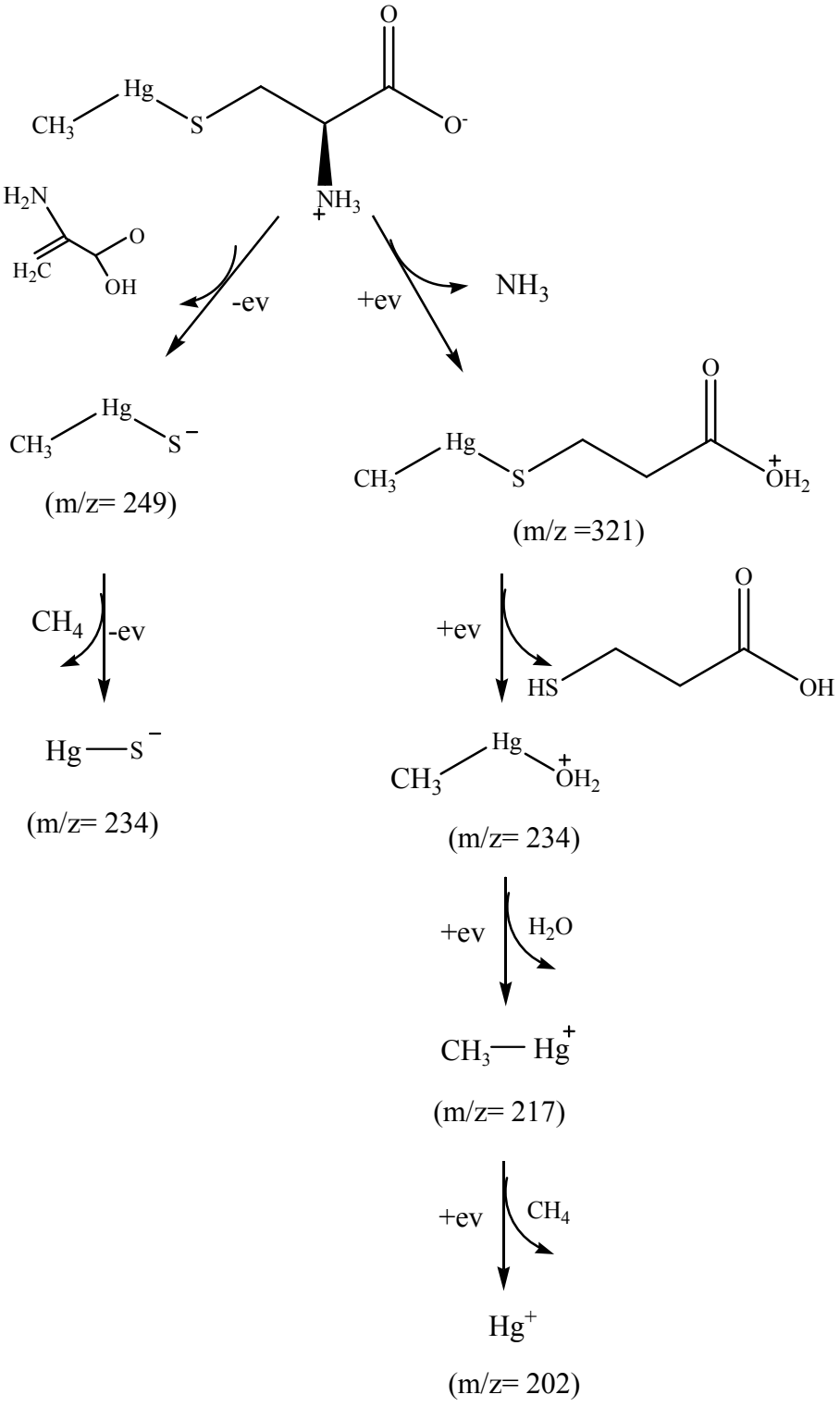

Scheme 2.1 – CH_3HgCys fragmentation pathway

2.5.2 CH_3HgGlu and its Fragmentation Pattern

Figure 2.7 shows ESI-MS spectra of the synthesized CH_3HgGlu and its fragmentation pattern under the negative-ion scan mode at varying cone voltages. Across the entire range of the cone voltages tested, the deprotonated parent CH_3HgGlu ion ($[CH_3HgGlu\text{-}H]^-$; *m/z* = 522 for ^{202}Hg) dominated the spectrum, with minor fragment peaks *m/z*= 249 corresponding to $[CH_3HgS]^-$ and *m/z*= 234 which, similar to the case of CH_3HgCys in the negative mode, was assigned to $[Hg^IS]^-$, and a cluster *m/z*=813 $[CH_3Hg(Glu)_2\text{-}NH_3]^-$. The fragment $[HgS]^-$ was found between cone voltage -80V and -120V only, and the fragment $[CH_3HgS]^-$ was visible starting at -50V, stabilizing at -90V with a smooth decrease until it disappeared at -200V; the two showed similar profiles but $[HgS]^-$ had a lower intensity. The cluster $[CH_3Hg(Glu)_2\text{-}NH_3]^-$ had a continuous increment of intensity starting at -30V. Other fragments (*m/z*= 377, 393, and 506) and clusters (*m/z*= 835 and 1043) showed low variation of intensity over the cone voltage range, counting for ~10% of the intensity.

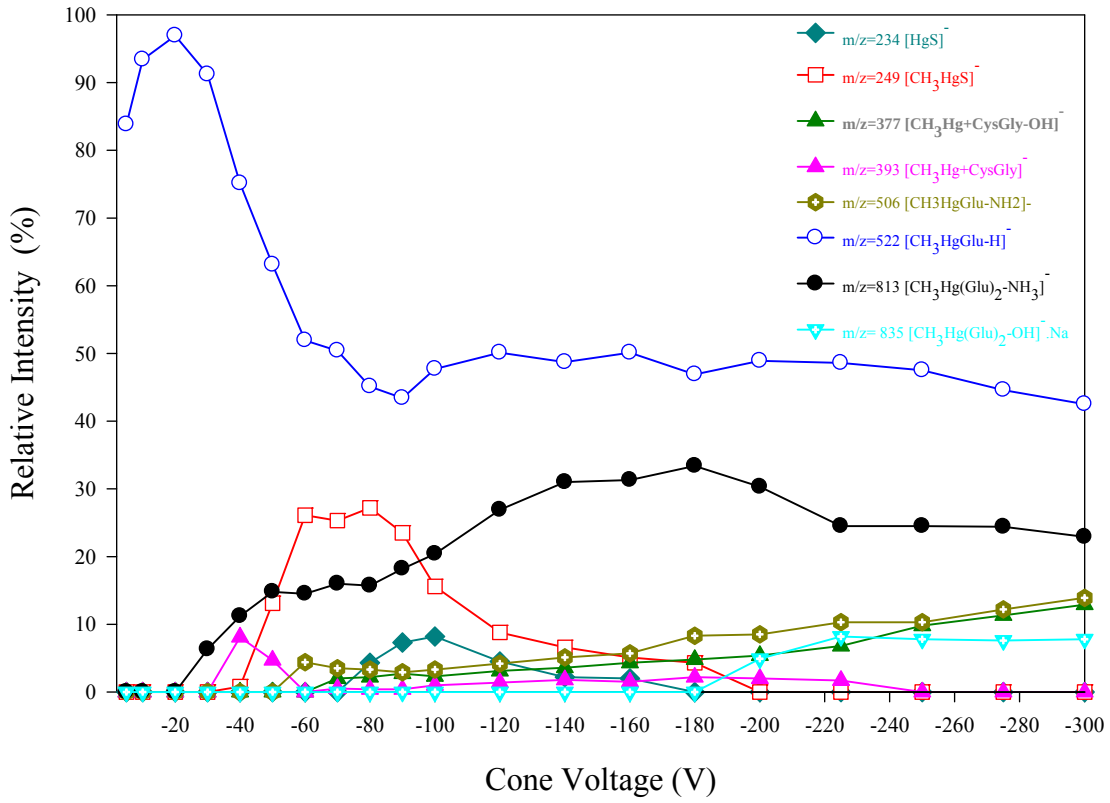

Figure 2.7 - CH_3HgGlu and its fragmentation pattern using the negative-ion mode with varying cone voltages

The fragmentation pattern of CH_3HgGlu was also successfully monitored in the positive-ion mode with varying cone voltages. The spectra were, however, more complicated due to a higher number of fragments. At low cone voltage (≤ +40V), the protonated parent ion $[CH_3HgGlu+H]^+$ (*m/z*=524) accounted for ~50% of the intensity, with ~25% from the cluster $[CH_3HgGlu+H]^+ \cdot Na$ (*m/z*=546) and 12% from $[(CH_3Hg)_2Glu+H]^+$ (*m/z*=738) (Fig. 2.8), such result aggress with Rubino et al. (2006) study (Rubino et al., 2006). The fragment $[CH_3Hg+CysGly\text{-}NH_2]^+$ (m/z=378) can be attributed to a loss of the γ-glutamyl group which dominated between (+30V) to (+50V).

At the higher voltage range (≥ +50V) the fragment $[CH_3Hg]^+$ (m/z=217) became more abundant.

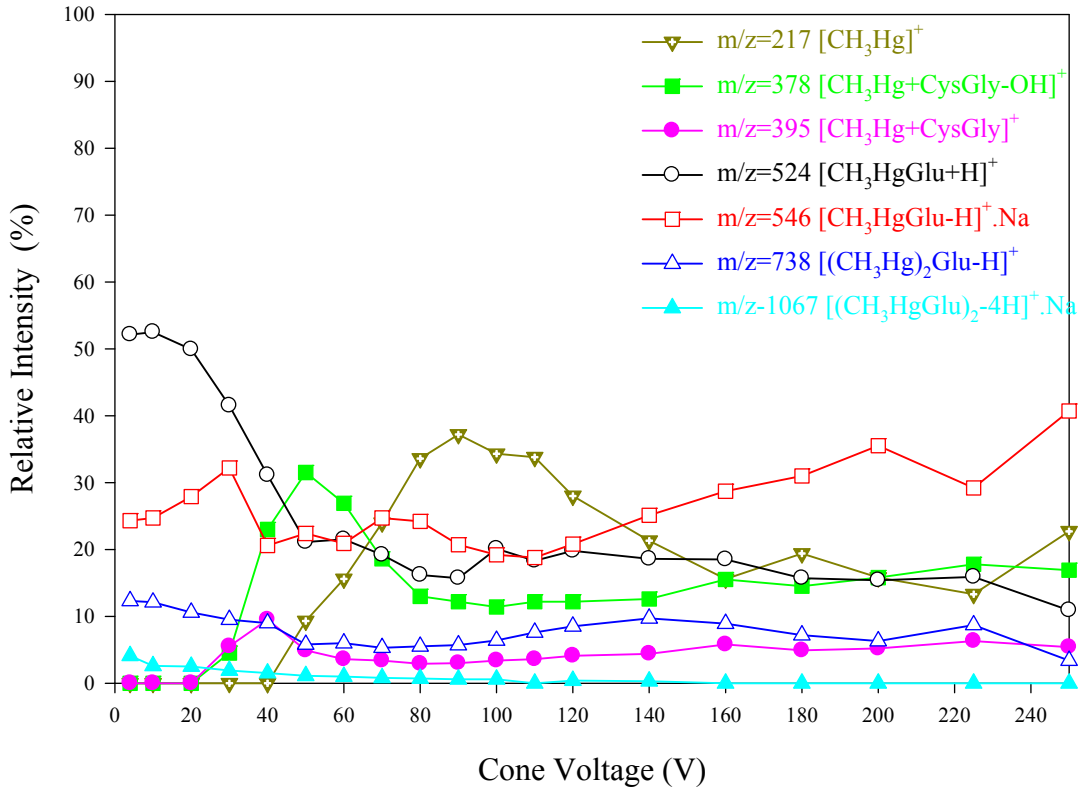

Figure 2.8 - CH_3HgGlu and its fragmentation pattern using the positive-ion mode at varying cone voltages

Scheme 2.2 depicts the fragmentation patterns of CH_3HgGlu based on the above results.

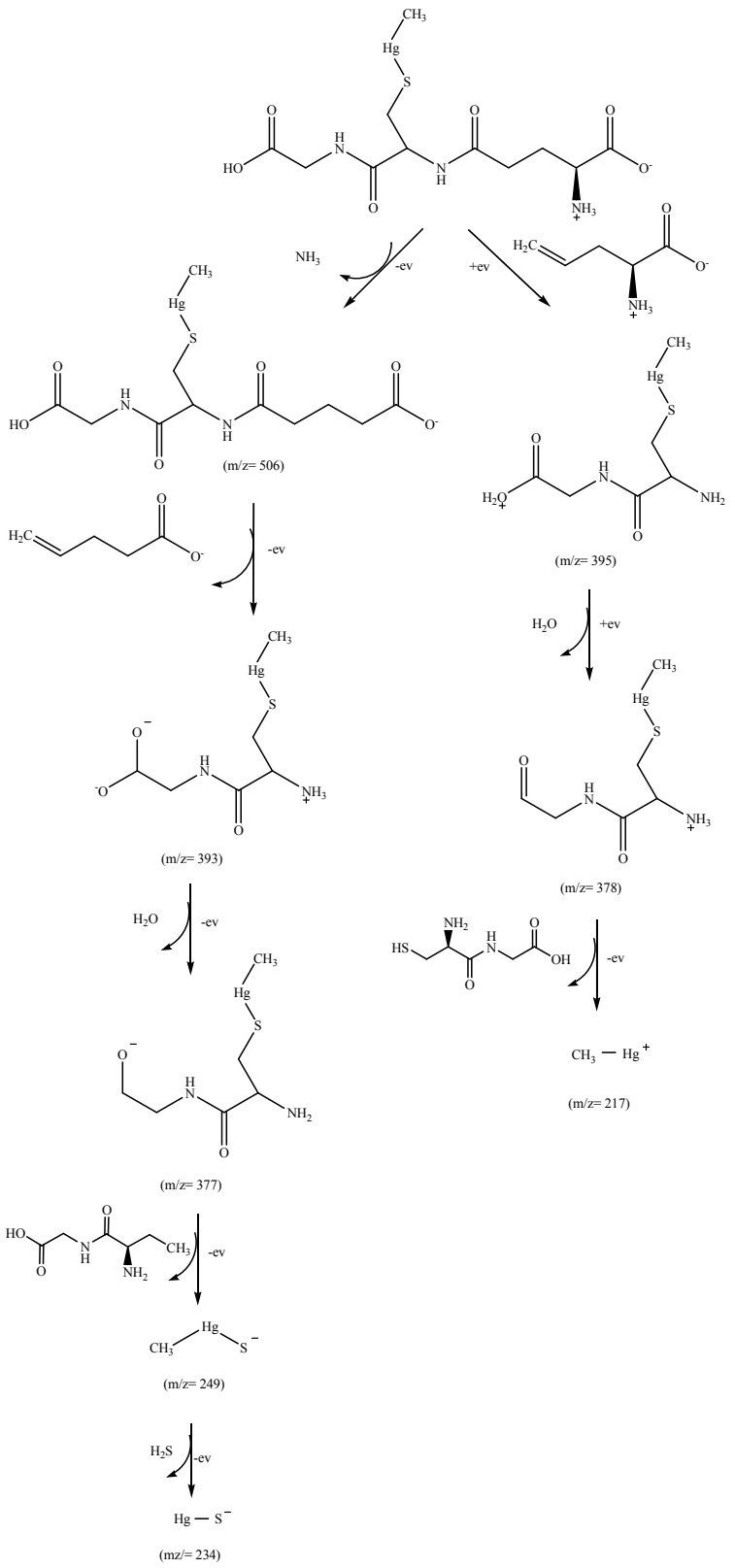

Scheme 2.2 – CH_3HgGlu fragmentation pathway.

2.6 Conclusion

CH_3HgCys and CH_3HgGlu were synthesized and the purity and structures were confirmed by elemental analysis (CH_3HgCys only), ^1H NMR, X-ray crystallography (CH_3HgCys only), and ESI-MS. ^1H NMR spectra of CH_3HgCys and CH_3HgGlu are on higher fields in comparison with CH_3HgCl, and both MeHg-thiols have similar central resonance lines (δ=0.62 ppm, and δ=64 ppm, respectively). The molecular structure of CH_3HgCys was refined by X-ray crystallography showing the locations of all hydrogen atoms and a slightly different molecular geometry of the carboxylate group and more linear C-Hg-S bond angle from what reported in the literature (Taylor et al., 1975). Both compounds were successfully analyzed on ESI-MS under both negative and positive scanning modes and their fragmentation patterns were established. Among the notable features are the possible demethylation of both CH_3HgCys and CH_3HgGlu and reduction of Hg(II) to Hg(I) during the ESI-MS analysis.

Chapter 3. Development and Optimization of a HPLC-ICPMS Method for the Determination of MeHg Speciation in Aqueous Solution

This chapter describes the development and optimization of a new analytical method for the determination of MeHg speciation in aqueous solution. As discussed in Chapter 1, no such method was available in the literature, which had hindered the understanding of the chemistry and toxicology of MeHg in general and MeHg-thiol complexes in specific. The new method was based on the separation by HPLC followed by the determination by ICP-MS. While the method could be tailored for various MeHg species, the key species of interest in this study were CH_3HgCys, CH_3HgGlu, CH_3HgX, and HgX (X = H_2O, OH^-, or Cl^-).

3.1 Methodological Consideration

As mentioned in Chapter 1, various separation techniques have been used for the analysis of total MeHg, including GC, HPLC, and CE (see Table 1.4). HPLC was chosen as the candidate separation technique for determining MeHg speciation because of its versatility for separating polar species such as CH_3HgCys and CH_3HgGlu. HPLC can handle a variety of analytical columns (e.g., C18, ion exchange, chiral, size exclusion), allowing for optimization for various MeHg species. .

ICP-MS was chosen as the Hg-specific detector due to its straight-forward interfacing with HPLC; HPLC effluent can be directly introduced to the ICP nebulizer

and spray chamber. The capability of ICP-MS of determining various Hg isotopes provides further advantage in analyte identification.

To achieve the highest sensitivity and to avoid cross-contamination, all the analytical work was carried out at metal-free Class 100-1000 clean rooms of the Ultra-Clean Trace Elements Laboratory (UCTEL), University of Manitoba.

3.2 Instrumentation

The chromatographic system consisted of an Agilent 1200 HPLC pump with an attached sample injection valve equipped with adjustable loop (5 - 100μL) and polyetheretherketone (PEEK) tubing to connect the injection valve and the column. Analytical columns tested included Luna C18(2) (50 mm×3.0 mm×5 μm, Phenomenex), XDB-C8 (150 mm×4.6 mm×5 μm, Zorbax Eclipse – Agilent), PRP-X200 (150 mm×4.6 mm×10 μm, Hamilton), and SXC (150 mm×4.6 mm×5 μm, Phenomenex). Matching guard column was also used.

An ELAN DRC-II ICP-MS (Perkin Elmer) was used as the Hg specific detector. The effluent from the HPLC column was connected via PEEK tubing to a perfluroalkoxy (PFA) 400 μL self-aspirating micro-nebulizer (Elemental Scientific Inc., Omaha, USA) and a quartz cyclonic spray chamber (Perkin Elmer). A quartz micro injector (0.8 mm I.D.; Perkin Elmer) was used to prevent high organic solvent load from entering the plasma which could destabilize the plasma. The signal intensity of Hg was monitored at m/z=202. Data processing was done by the software Chromera V1.2 (Perkin Elmer). The plasma power, nebulizer gas flow rate, lens voltage, and auto-lens voltage were optimized daily for the analysis.

3.3 Standard Solutions

The standard solutions of CH_3HgCys and CH_3HgGlu (50 μM) were prepared by dissolving respective compound, synthesized following the procedure described in Chapter 2, in ultrapure water. The standard solution of CH_3HgOH (50 μM) was prepared from dilution of 1 M CH_3HgOH (Alfa Easer, 1M). The standard solution of CH_3HgCl (50 μM) was prepared by dissolving CH_3HgCl (Alfa Easer, 98%) in water/ethanol (volume ratio 1:1). The standard solution of Hg(II) was prepared from dilution of 50 μM $HgNO_3$ (Spex Certiprep, Claritas PPT grade).

The calibration standards were prepared daily from a 0.5 μM working solution. The stock solutions and calibration standards were kept in amber flasks at room temperature (22 °C) in order to prevent photoreaction.

3.4 Optimization of the Method

In order to achieve the best performance, various HPLC-ICPMS operating parameters were tested and optimized. These parameters are discussed below.

3.4.1 Analytical Columns

The ion exchange columns (PRP-X200 and SCX) produced peaks with nonsymmetrical shapes, probably due to the strong binding between the column packing and the MeHg species. The XDB-C8 column showed poor resolutions for the MeHg species. The separation with the Zorbax–Eclipse column required lower amount of the organic solvent which resulted in lower intensities for CH_3HgX and HgX (X= Cl^- or OH^-).

Among all the columns tested, Luna C18(2) yielded the best separation and sensitivity, and thus all the subsequent methodological development was based on this column by reversed phase HPLC.

3.4.2 Mobile Phase

A mixture of methanol (CH_3OH) and acetonitrile (ACN) was added to the aqueous mobile phase to assist in the elution of the Hg species from the column; the addition of ACN also reduced the peak broadening of the CH_3HgX species. The composition and pH of the mobile phase had a significant impact on the separation and elution order of the MeHg and Hg species, particularly for CH_3HgGlu. For instance, when the mobile phase had a CH_3OH+ACN concentration <5%, CH_3HgGlu was the last to be eluted. An increase of the concentration of CH_3OH+ACN to 6-8% shortened the retention time of CH_3HgGlu and resulted in CH_3HgGlu being eluted after CH_3HgCys and before CH_3HgX and HgX.

Similar effects were observed on the pH of the mobile phase. At pH < 3, the retention time followed the order of $CH_3HgCys < CH_3HgX < CH_3HgGlu <$ HgX (see Fig. 3.1). When pH > 5, the order changed to $CH_3HgCys < CH_3HgGlu < CH_3HgX <$ HgX (see Fig. 3.4). It was observed that pH has a greater effect on the retention time of CH_3HgGlu, decreasing its retention time as pH increases. The pH effect might be attributed to the acid–base properties of the GSH, which has two carboxyl groups, which have pKa values of 2.09 and 3.12 (see Table 1.3 in Chapter 1). The optimal pH for the greatest resolution of CH_3HgCys, CH_3HgGlu, CH_3HgX and HgX was pH 5.

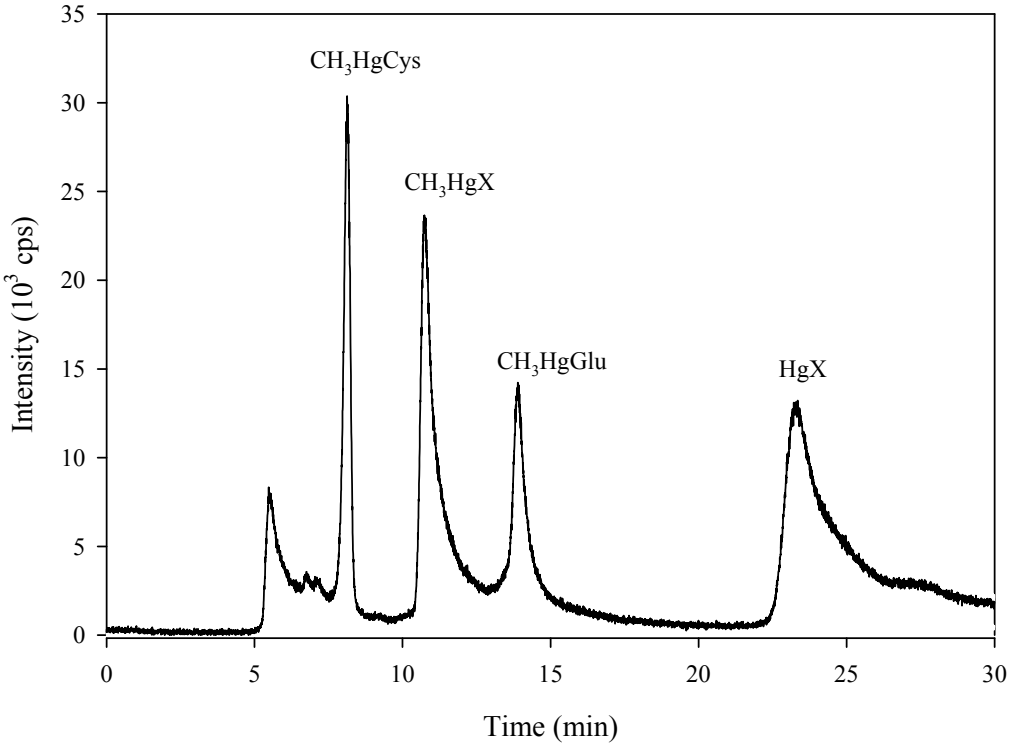

Figure 3.1 - Typical HPLC chromatogram of various MeHg compounds and inorganic Hg (500 mM) with mobile phase containing 8 mM MSA at pH 3.0

Separation of Hg compounds using reversed-phase HPLC usually requires the addition of a chelating or ion-pair reagent with thiol groups (Bramanti et al., 2005; Harrington, 2000; Ho and Uden, 1994; Wan et al., 1997) as an organic modifier in order to improve separation and to avoid adsorption of Hg compounds to the stationary phase (Bramanti et al., 2005). Chemicals such as 2-mercaptoethanol (ME) and CSH are commonly added in the mobile phase due to the high affinity between Hg and the thiol group (Chiou et al., 2001; Harrington and Catterick, 1997; Harrington et al., 1998; Percy et al., 2007; Vallant et al., 2007). Addition of CSH was ruled out in this method, as CH_3HgCys is one of the key species under investigation. ME has a strong affinity to

CH_3Hg^+ (log K = 16.14; (Arnold and Canty, 1983)), inhibiting the chromatographic separation among MeHg complexes. Instead, in this method methanesulfonic acid (MSA) was used as the organic modifier due to its mild affinity for MeHg complexes. MSA ranging from 1-20 mM was investigated in order to obtain the best separation among the compounds of interest. For instance at pH 5 when [MSA] > 10 mM, MSA gives a good height peak for MeHgX and HgX but when a calibration curve of four Hg compounds was done, it was noticed a linearity problem for CH_3HgGlu at lower concentrations, likely due to concentration of the organic modifier. When the [MSA] was between 6 – 8 mM, no interference was observed but all the MeHg compounds were eluted at retention times close to each other. Decreasing [MSA] to less than 5 mM resulted in better separation among the MeHg. The concentration of 2mM MSA was chosen as the best condition for the separation amongst CH_3HgCys, CH_3HgGlu, and CH_3HgX. Although MSA did not affect the retention time of HgX, the peak height increased with higher [MSA].

The effect of ionic strength (due to salts introduced from the pH buffers or other sources) of the mobile phase was also investigated (Fig. 3.2a and b). The salts tested included NH_4Ac (HPLC grade), KH_2PO_4 (99.8%), $(NH_4)H_2PO_4$ (99.999%) obtained from Fisher Scientific and NaCl (99.5%, Sigma). NaCl was found to significantly decrease the ICP-MS signal even at low concentrations, probably due to its negative effect on the plasma ionization (Castillo et al., 2006; Rodushkin et al., 1998). NH_4Ac was chosen as the pH buffer due to its lower interference on the ICP-MS signal amount the buffer salts tested, common usage in HPLC methods (Carro and Mejuto, 2000; Castillo et al., 2006)

and due to its compatibility when interfacing with other equipment (e.g., ESI-MS) (Thiele et al., 2008).

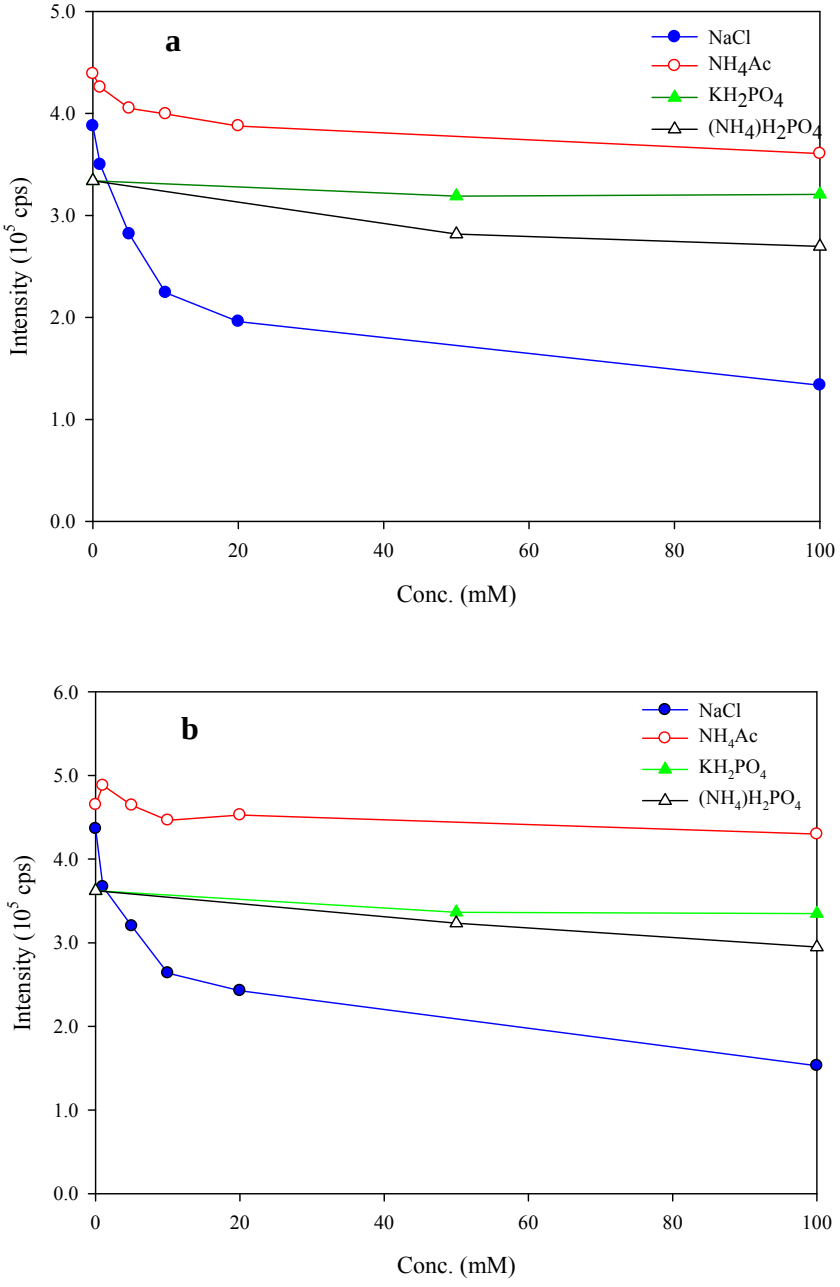

Figure 3.2 – Influence of salts in the mobile phase on the ICP-MS determination of **a)** CH_3HgCys and **b)** CH_3HgGlu.

Since the elution order of the MeHg and Hg species did not comply with the order of the polarity, the separation within the column was driven not only by dissolution process as adsorption to the column may also occur. The latter was particularly the case for CH_3HgX and HgX; the two species that were eluted last. To minimize any memory effect, a gold (Au) solution (Claritas PPT grade) from Spex Certiprep was added to the mobile phase (Chen et al., 2000) at a final concentration of 500 nM. The addition of gold has been shown to inhibit interactions of Hg species with the surface of the system (Chen et al., 2000). A gold solution with concentration ranging from 50 to 2500 nM was tested in this study, and 500 nM was chosen as the optimal Au concentration, as higher Au concentration would result in incomplete separation of the MeHg species.

3.4.3 Other Parameters

The intensity of the Hg species on the ICP-MS was influenced by the flow rate of the HPLC mobile phase. Low flow rate around 0.3 mL min^{-1} produced the highest intensity with both the PFA micro-nebulizer and the regular quartz nebulizer. An increase in the flow rate to 1 mL min^{-1} (with the regular quartz nebulizer) showed a decrease in intensity by ~ 30 % (see Fig. A3 in Appendices). This is likely due to the diminution on the ionization power of the plasma by the high amount of organic olvent vapor (Wan et al., 1997).

The ICP plasma power was also optimized; Hg has a relatively high ionization potential (9.5 eV) (Harbour, 1971), and at cool plasma suffers from matrix suppression effects because most elements cannot be ionized completely in a low-temperature plasma

(Kishi et al., 2004). Increasing the radio frequency (RF) power from 1100 W to 1400W resulted in a ~20% increase of Hg signal (see Fig. A4 in Appendices).

3.5 HPLC - Labile MeHg Species

It should be noted that even though the solids of CH_3HgCys, CH_3HgGlu, and CH_3HgCl were of very high purity, once they are dissolved in aqueous solution a variety of reactions occur resulting in the presence of many different MeHg species. MeHg species that can establish rapid thermodynamic equilibria with other species will not be effectively separated by HPLC as the separation of one species would shift the equilibria among the species. Only species or species groups that do not exhibit such rapid re-supply in the column can be separated and analyzed reliably. These "HPLC-labile" species are also dependent on the HPLC operating parameters (e.g., column type, mobile phase, temperature).

As shown in Fig. 3.4, for 4 major peaks were evident in a typical chromatogram in the mixed standard solution, suggesting that there was no shift in equilibrium within the column. By comparing the retention times with those of the individual standards, four groups of "HPLC-labile" Hg species, namely CH_3HgCys, CH_3HgGlu, CH_3HgX (X = small inorganic ligands such as H_2O, OH^- or Cl^-), and inorganic Hg(II) complexes HgX, where:

$$[CH_3HgCys] = [CH_3Hg\text{-}S\text{-}Cys^-] + [CH_3Hg\text{-}S\text{-}CysH]$$

$$[CH_3HgGlu] = [CH_3Hg\text{-}S\text{-}Glu^{2-}] + [CH_3Hg\text{-}S\text{-}GluH^-] + [CH_3Hg\text{-}S\text{-}GluH_2]$$

$$[CH_3HgX] = [CH_3Hg(H_2O)_x^+] + [CH_3HgOH] + 2[(CH_3Hg)_2OH^+] + [CH_3HgCl]$$

$$[HgX] = [Hg(H_2O)_x^{2+}] + \sum[Hg(OH)_m^{2-m}] + \sum[HgCl_n^{2-n}]$$

The separation and quantitation of these 4 groups of the species is possible due to the strong binding intensities between MeHg and the S-atom in CSH or GSH. As shown in Fig. 3.3, a standard solution of mixed CH_3HgCys and CH_3HgGlu maintained the same retention time and peak area of that of CH_3HgCys and CH_3HgGlu in the respective single standard solution, suggesting that there was no shift in equilibrium within the column.

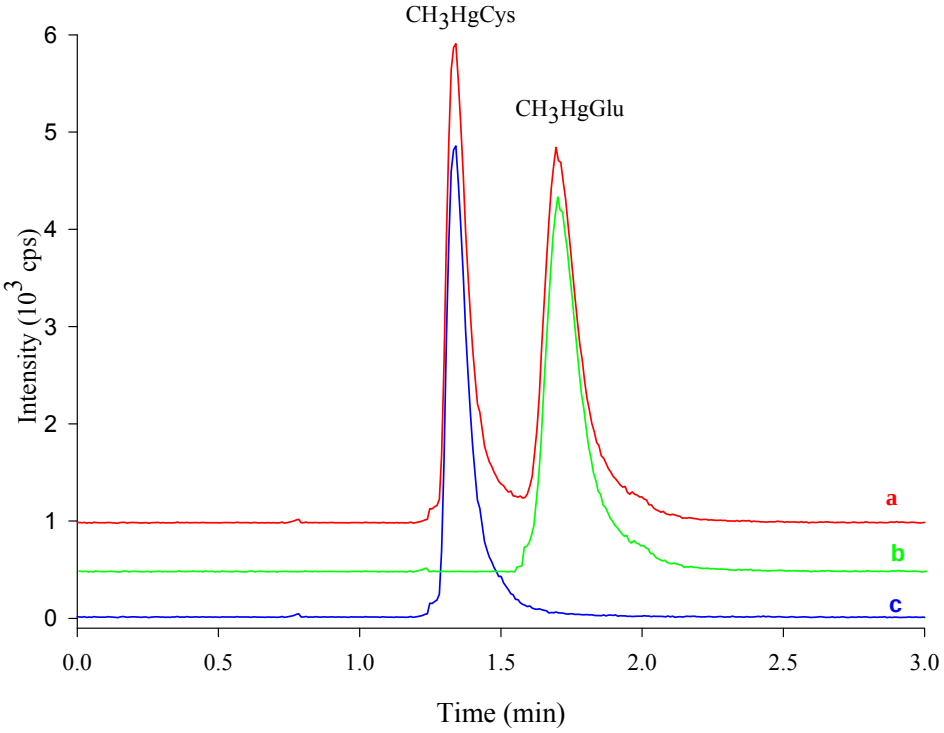

Figure 3.3 - Chromatograms of **a)** a mixed standard solution with 500 nM CH_3HgCys and 500 nM CH_3HgGlu; **b)** a 500 nM CH_3HgGlu solution, and **c)**, a 500 nM CH_3HgCys solution

The species within each group can not be quantified separately, presumably due to the rapid equilibria among them. This was confirmed by the same retention time of the MeHg standards prepared from the CH_3HgOH and CH_3HgCl stock solutions.

3.6 Optimized HPLC-ICPMS Method for MeHg Speciation in Aqueous Solution

Based on the above results, a new HPLC-ICPMS method was developed and the following conditions were deemed optimal for the separation and analysis of MeHg species, particularly for CH_3HgCys and CH_3HgGlu.

- HPLC: Stationary phase: Luna C_{18} (2); Mobile phase: 7.5% CH_3OH / 2.5% ACN / 90% H_2O (v/v) with 2 mM MSA and 510 nM of Au at pH 5. Flow rate: 0.3 mL min^{-1}.
- ICPMS: Plasma power at 1400 W, with a micro-nebulizer at a nebulizer flow rate of 0.6 L min^{-1}

Fig. 3.4 illustrates typical chromatograms obtained under these conditions. The analysis of CH_3HgCys, CH_3HgGlu, CH_3HgX, and inorganic HgX was completed within 6 min with the following retention times: CH_3HgCys at 1.3 min, CH_3HgGlu at 1.7 min, CH_3HgX at 2.2 min, and inorganic HgX at 4.9 min. The r^2 of the calibration curve was 0.999 for CH_3HgCys, CH_3HgGlu, and CH_3HgX, and 0.992 for HgX. The method detection limits, calculated based on the standard deviation of the analysis of 10 replicates of a 5 nM mixed standard and on the 99% confidence level, were as follows: CH_3HgCys, 1.1 nM; CH_3HgGlu, 1.1 nM; CH_3HgX, 1.4 nM; and inorganic HgX, 2.2 nM.

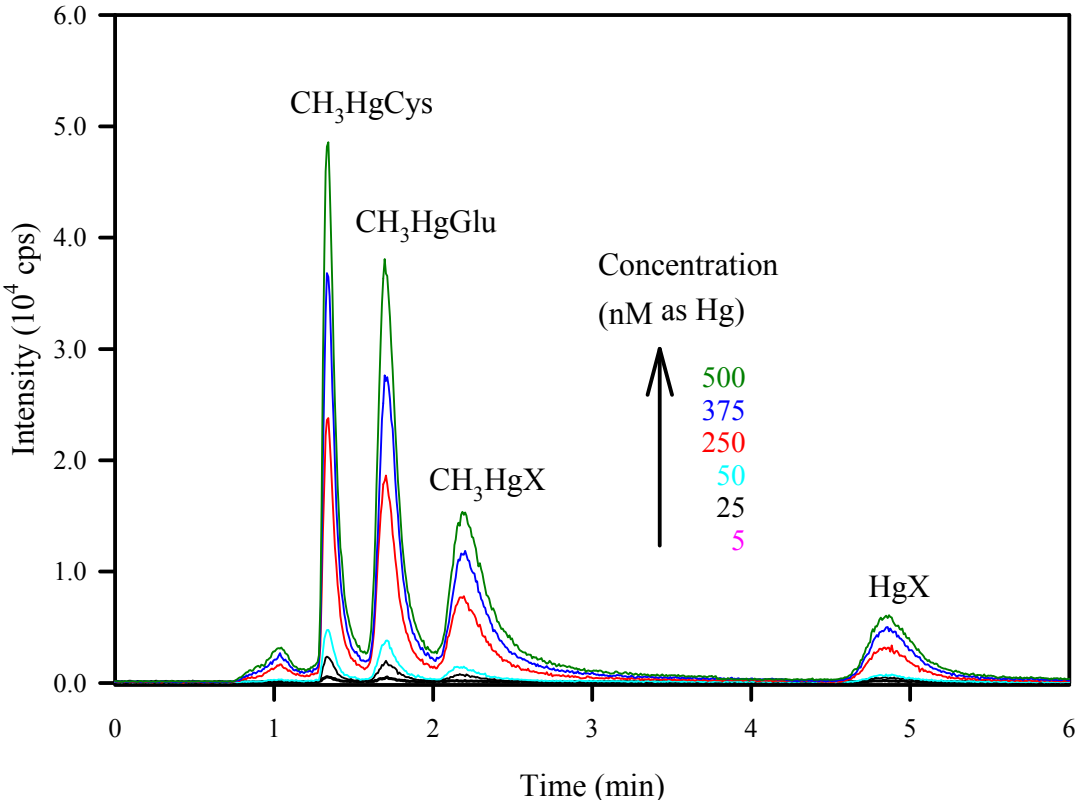

Figure 3.4 - Typical chromatograms of calibration standards of various MeHg compounds and inorganic Hg

3.7 Conclusion

A HPLC-ICPMS method for the speciation of MeHg compounds (CH_3HgCys, CH_3HgGlu, CH_3HgX, and HgX) in aqueous solution was developed successfully using a C_{18} analytical column with detection limits at sub-micromolar levels. The separation of the various species within the column was driven by partitioning and adsorption, and the mobile phase (composition, pH) can be further optimized based on the species of interest.

Chapter 4. Methylmercury Speciation in Fish by HPLC-ICPMS Following Enzymatic Hydrolysis

As mentioned in Chapter 1, the presence of CH_3HgCys in biological systems has long been suspected but never been analytically proven. With the new method as described in Chapter 3, we report the first analytical evidence of the presence and dominance of CH_3HgCys in fish muscle. The MeHg species were first extracted from the dogfish (*Squalus acanthius*) muscle standard reference material (DORM-2) by enzymatic hydrolysis, and then analyzed by the HPLC-ICPMS method described in Chapter 3.

4.1 Enzymatic Hydrolysis of the Fish Muscle Sample

While the new MeHg speciation method developed in Chapter 3 can be readily applied for aqueous samples (see also Chapter 5), a proper extraction procedure needs to be developed when analyzing the MeHg speciation in biological samples. The extraction method should be capable of extracting all the MeHg from the solid biological material while maintaining the *in vivo* speciation information. While no such extraction procedure is reported for MeHg speciation analysis, enzymatic hydrolysis has been shown to be most effective for the extraction of biological samples for the speciation analysis of other elements such as selenium (Chen et al., 2000; Leon et al., 2000) and arsenic (Casiot et al., 1999). Based on these literature studies, three enzymes were tested in this study for the extraction of MeHg species from fish muscles: trypsin, protease type XIV, and pepsin; all were obtained from Sigma (>99.99%). The fish muscle sample used was the dogfish muscle certified reference material DORM-2 (NRCC (National Research Council

Canada), 1993). We chose DORM-2 because of its relatively high MeHg concentration (22.3±0.02 μM for MeHg and 23.15± 1.29 μM for total Hg).

In brief, about 0.1 g of the homogenized, dried DORM-2 was weighed into a 15-mL polypropylene centrifuge tube, to which 10 mL of a mixed solution containing a pH buffer and a specific enzyme (e.g., 0.05 M ammonium acetate at pH 7.5 and 0.01 g of enzyme were added). The centrifuge tube was pretreated with a 4 M HCl (Fisher Scientific) solution for 24 hr followed by being thoroughly rinsed with ultrapure water. The extraction was carried out at 37 °C inside an Isotemp oven (Fisher Scientific) on a tube rotator with rotisserie (VWR) at 20 rpm for 24 hr. For the extraction with 0.01 g pepsin, the pH was adjusted to 2.2 with 0.1 M HCl and the extraction time was set to 12 h. The extraction was performed in the dark to prevent any possible photoreaction during the extraction. The extractant was centrifuged (International Equipment Co) for 30 min, and the supernatant was decanted and filtered through a 0.2 μm membrane (GHP, Pall) and diluted 10 fold with ultra pure water. The dilution was necessary to minimize matrix interference. A small quantity of white precipitate was observed after centrifugation, which is probably due to the fat tissue (about 5 percent (NRCC (National Research Council Canada), 1993)) in DORM-2. The diluted sample was adjusted to pH = 5 with 4 M acetic acid, kept in the dark for several hours, and analyzed for MeHg speciation on the same day.

The MeHg speciation analysis of the extracted solution was performanced using by the HPLC-ICPMS method as described in Chapter 3. The optimized operating conditions are summarized in Table 4.1. The identification of the MeHg species in the chromatograms was done by ESI-MS on an Agilent 6140 A QQQ-MS after the

separation by the same HPLC (Fig. 4.2b). The operating conditions are summarized in Table 4.2.

Table 4.1 - Optimal conditions for MeHg-thiol speciation by HPLC-ICPMS

HPLC (Agilent Model 1200)	ICP-MS (Perkin Elmer, DRC II)
Mobile Phase (isocratic):	Plasma power: 1400 W
MeOH: 7.5 %;	Nebulizer: PFA 400 µL self-aspirating
ACN: 2.5%	micro-nebulizer
2 mM MSA in H_2O: 90 %	Nebulizer gas flow rate: ~ 0.6 L min^{-1}
with 500 nM of Au at pH 5	(optimized daily)
Stationary Phase:	Torch injector: 0.8 mm I.D.
Luna C18(2)	Analytical mode: Standard (non-DRC)
Flow rate:	Internal Standard: Iridium
0.3 mL min^{-1}	

Table 4.2 - Optimal conditions for MeHg-thiol identification by ESI-MS

Capillary (V)	3500
Fragmentor (V)	+70
Drying gas (ºC)	350
Nebulizer pressure (psi)	35
Run mode	Scan
N_2 drying gas flow (L min^{-1})	11

The extraction of a mixed CH_3HgCys and CH_3HgGlu standard solution with protease type XIV resulted in one single, broad peak close to the retention time of CH_3HgCys, suggesting that protease type XIV cleaves CH_3HgGlu to form CH_3HgCys and is thus not appropriate for MeHg speciation analysis. Pepsin preserved the peaks of CH_3HgCys, CH_3HgGlu, and CH_3HgX but was apparently unable to break down the protein peptide bonds of large molecules, which decreased the intensity on ICP-MS and the recovery, perhaps due to their adsorption onto the LC analytical column. Column cleaning up is needed after each run, which is time consuming. Similar problems were reported previously (Yathavakilla and Caruso, 2007). In contrary, enzymatic hydrolysis with trypsin not only preserved all the MeHg compounds (Fig. 4.1), but also did not require the clean up procedure after the analysis.

Therefore, trypsin was used in this study for the extraction of MeHg species from the dogfish muscle sample DORM-2 (Fig. 4.2a). The total Hg in DORM-2 extracted by trypsin hydrolysis, as analyzed by CVAFS, was 19.95±0.04 μM (d.w; n=3), which corresponded to an extraction efficiency of 84±19 % when compared with the certified total Hg value of 23.15 μM (NRCC (National Research Council Canada), 1993).

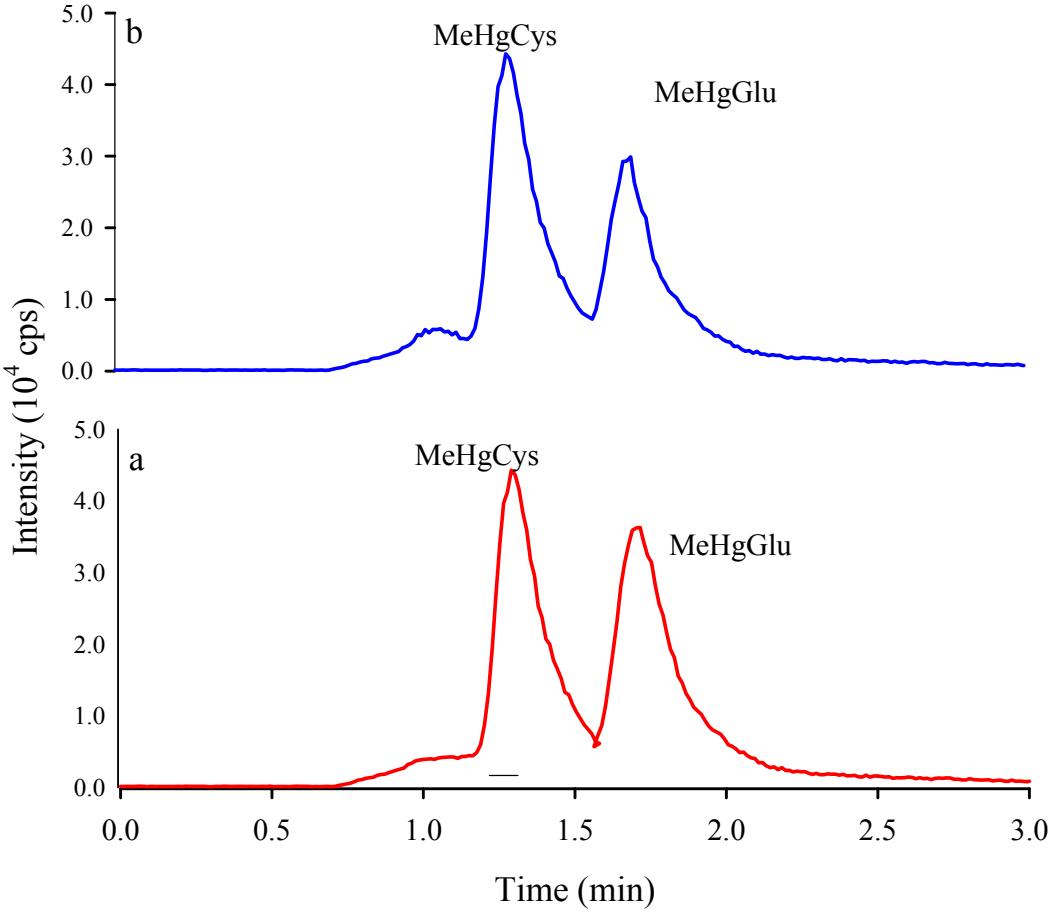

Figure 4.1 - Chromatograms of a mixed standard solution of 500 mM of CH_3HgCys and CH_3HgGlu **a)** before and **b)** after trypsin hydrolysis

4.2 Presence and Dominance of CH_3HgCys in Fish Muscle

As shown in Fig. 4.2a, a sharp and dominant peak of CH_3HgCys was present in the dogfish muscle sample. The peak was further confirmed to be CH_3HgCys by ESI-MS analysis (Fig. 4.2b), with isotopic patterns characteristic to CH_3HgCys at around m/z=338 $[CH_3HgCys+H]^+$. Neither measurable peaks could be identified on the chromatogram for CH_3HgGlu, CH_3HgX, nor for HgX due to its very small concentration in DORM-2. Based on the peak areas and the calibration curves, the CH_3HgCys

concentration was calculated to be 19.50±0.03 μM as Hg (d.w; n=6), which agreed reasonably well with the certified value of 22.3±0.02 μM as Hg. (NRCC (National Research Council Canada), 1993)

To verify whether there was any matrix interference, a standard addition experiment was carried out by spiking a mixture of CH_3HgCys and CH_3HgGlu standards into the extractant (after a 10x dilution). The recovery was 89% for CH_3HgCys and 58% for CH_3HgGlu (Fig. 4.2c), suggesting small matrix interference for the determination of CH_3HgCys but some considerable interference for CH_3HgGlu.

By using XANES, Harris et al. (2003) demonstrated that MeHg speciation in the swordfish muscle is dominated by CH_3Hg-S compounds. To our knowledge Fig. 4.2a is the first analytical evidence showing the presence and dominance of a specific CH_3Hg-S compound, namely CH_3HgCys, in fish muscle. As CH_3HgCys can readily be transported across the BBB (Aschner et al., 1994; Bridges and Zalups, 2006; Simmons-Willis et al., 2002), this raises critical questions about the health of the fish and its predators including humans. The lack of a CH_3HgGlu peak is also interesting, suggesting the detoxification process of MeHg does not occur in the muscle tissue.

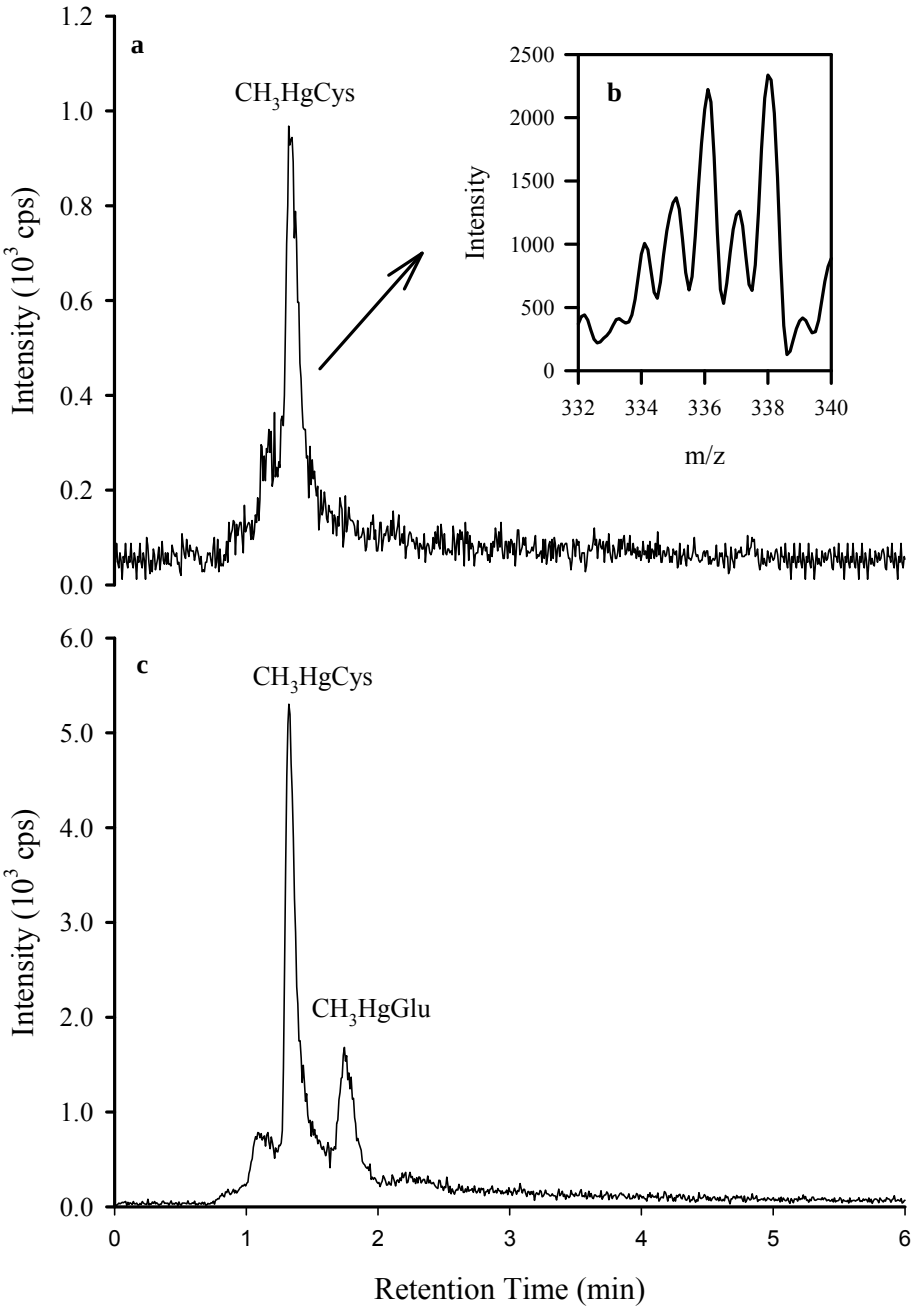

Figure 4.2 - a) Chromatogram of the dogfish muscle (DORM-2) after being extracted by the enzymatic hydrolysis with trypsin (after 10x dilution); **b)** ESI-MS spectrum confirming the CH_3HgCys peak in **a**; **c)** Same as **a** but the extractant was spiked with 30 nM of CH_3HgCys and 19 nM of CH_3HgGlu standard solution

4.3 Molecular Weight Distribution of Methylmercury in the Fish Muscle Extractant

It should be noted, however, that the CH_3HgCys in fish muscle reported here is not necessarily the "free" CH_3HgCys complex. Since many proteins contain CSH moieties, any MeHg-bound CSH moieties that are released from the proteins during the enzymatic hydrolysis would be eluted at the same retention time as the free CH_3HgCys. Therefore, the CH_3HgCys determined in fish muscle included both the "free" CH_3HgCys and the CH_3HgCys moieties in trypsin hydrolysable proteins. Therefore, size exclusion chromatography (SEC) was used to determine which molecular size mercury was associated in the fish muscle extract.

The extracted DORM-2 as described in Section 4.1 was first solubilized with 0.5% sodium dodecyl sulfate (SDS – Fisher Scientific) at 37 °C for 3 hr. Five milliliters of the solubilized product was then injected onto a calibrated 3.0×97 cm Sephadex G-75 (Sigma) column and eluted at 4 °C with 10 mM Tris-HCl (Sigma) buffer (pH 7.5) containing 10 mM glycerol (J.T. Baker). The protein determination in each fraction was done by UV absorption at 280 nm on a Spectronic 3000 Array (Milton Roy). Calibration of the column was performed using a mixture of standard proteins with different molecular weights (albumin: 66 kDa, carbonic anhydase: 29 kDa, myoglobin: 17.6 kDa) which were obtained from Sigma. The Hg determination in the total extractant and each molecular weight fraction was done by cold vapor atomic fluorescence spectroscopy (CVAFS; Tekran).

As shown in Fig. 4.3, about 57% of the total Hg was found in the high molecular weight region (~66 kDa) and 21% was associated with molecules with even higher

molecular weight. A smaller fraction was associated with smaller molecular weights: 8% at ~29 kDa and 6% at ~17Kda. Since Hg in the fish muscle is dominated by CH_3HgCys (Fig. 4.2), this molecular weight distribution pattern also reflects the association of CH_3HgCys. Of particular interest is the molecular weight fraction near 17 kDa, which includes cysteine-rich metallothioneins (MTs) that are known to bind both physiological (e.g., Zn, Cu, Se) and xenobiotic (e.g., Cd, Hg, Ag) metal ions (Garcia et al., 2006).

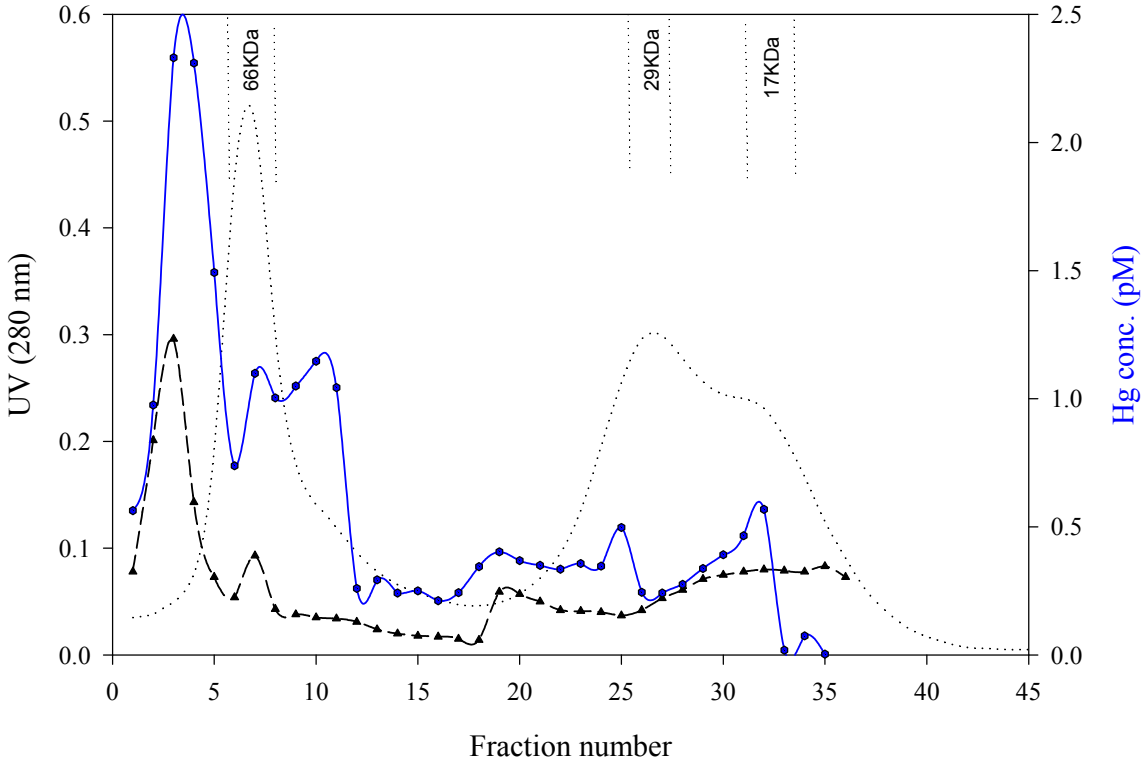

Figure 4.3 - Elution profile of UV absorbance (280 nm) and total Hg in solubilized DORM-2 extractant after SEC. The dotted line shows the UV absorbance of the three molecular weight markers

4.4 Conclusion

Enzymatic hydrolysis with trypsin followed by HPLC-ICPMS analysis provides a promising analytical method for the determination of MeHg speciation in biological samples. The dominance of CH_3HgCys in fish muscle is of particular interest in the context of human exposure to MeHg, though further studies are warranted to probe the mobility and reactivity of free CH_3HgCys and CH_3HgCys associated with large proteins, as well as the metabolic pathways and metallomics of MeHg in general.

Chapter 5. Kinetic Stability and Decomposition Products of Methylmercury Cysteinate and Glutathionate

As mentioned in Chapter 1, while extensive studies have been carried out on the formation of MeHg in the environment, few studies have reported the kinetic stability of MeHg *in vivo* or *in vitro*. The existing studies are almost exclusively focused on photolytic or microbial demethylation of MeHg in the form of CH_3HgCl and/or CH_3HgOH (Ahmed and Stoeppler, 1986; Ahmed and Stoeppler, 1987; Fitzgerald et al., 2007; Hammerschmidt and Filtzgerald, 2006; Sellers et al., 1996; Yu and Yan, 2003). In Chapter 4, we demonstrated the dominance of CH_3HgCys in fish muscle. CH_3HgCys and CH_3HgGlu were also suggested to be dominant in sediment porewaters. Here we report the first kinetic study of CH_3HgCys and CH_3HgGlu in aqueous solutions under a variety of conditions.

5.1 Kinetic Stability Study

The stability study was conducted in 125-mL borosilicate glass bottles (with low alkali content; Wheaton Science Products) with Teflon lined caps under constant shaking (100 rpm) in a metal-free, Class 100 laminar-flow workstation (Microzone, Ottawa, ON) at room temperature (20 ± 2 ^{o}C). The bottles were pretreated with a 4M HCl (Fisher Scientific) solution for 24 hr followed by being thoroughly rinsed with ultrapure water, and tested for acceptable background Hg levels (≤ 1.0 pM) prior to use.

The environmental parameters tested included light, pH, and ionic strength. The pH was adjusted and buffered with 4 M NH_4Ac (HPLC grade, Fisher Scientific) and 7 M NH_4OH (ACS reagent, Sigma). The ionic strength was adjusted by 5 M $NaNO_3$ (99.0%, Sigma). For the test of light, the bottles were either completely wrapped with aluminum foil ("darkness") or exposed to a 36 W white fluorescence light ("light") inside a laminar-flow workstation. All the experiments were done in triplicate. In each bottle, 100 mL of a solution containing 50 nM of CH_3HgCys or CH_3HgGlu were prepared at the specific pH and ionic strength. 0.5 mL of the solution was sampled from each bottle at various time intervals for analysis of MeHg speciation.

The samples collected at various time intervals were analyzed for MeHg speciation by HPLC-ICPMS as detailed in Chapter 3. In brief, the separation was carried out isocratically on an Agilent LC1200 on a Luna C18(2) column (Phenomenex). The mobile phase was composed of 7.5% methanol, 2.5% acetonetrile, and 90% H_2O (v/v), 2 mM MSA (pH 5.0) containing 510 nM of Au with a flow rate of 1 mL min^{-1}. The Hg analysis was done by ICP-MS on Elan DRC II (Perkin Elmer) under the standard mode. Data processing was done by the software Chromera (Perkin Elmer). The analysis of total Hg (Hg_T) was done in a similar manner with the exception that the LC analytical column was bypassed.

5.1.1 Influence of Light

The light vs darkness experiment was done at pH 5.5-6.0 in otherwise ultra-pure water ($I < 0.001$ M) for up to 1 month (Fig. 5.1). The concentrations of CH_3HgCys and CH_3HgGlu at various time intervals are shown in Fig. 5.1. Over the first 10 days period,

there was no observed difference in concentration between the light and dark environments. Statistically, the stability of CH_3HgCys with or without light in the first 10 days ($p = 0.603$; two-paired t test; SigmaPlot) (Fig. 5.1a,c). *On day 11,* CH_3HgCys under the light environment showed a decrease in concentration, which continued until it, was undetected by Day 26. Accompanying the sharp decrease in CH_3HgCys near the end of the experiment was a corresponding decrease in pH (from 5.5 to 3.5-4.0) despite the solution being buffed with NH_4OH and NH_4Ac. A slight decrease in CH_3HgCys was also observed under darkness after 600 hrs, but the extent was much less than that in the presence of light. No significant difference was found in the stability of CH_3HgGlu for the entire duration ($p = 0.506$; two-paired t test; SigmaPlot) (Fig. 5.1b,d) with or without light. Both compound concentrations decreased after Day 20.

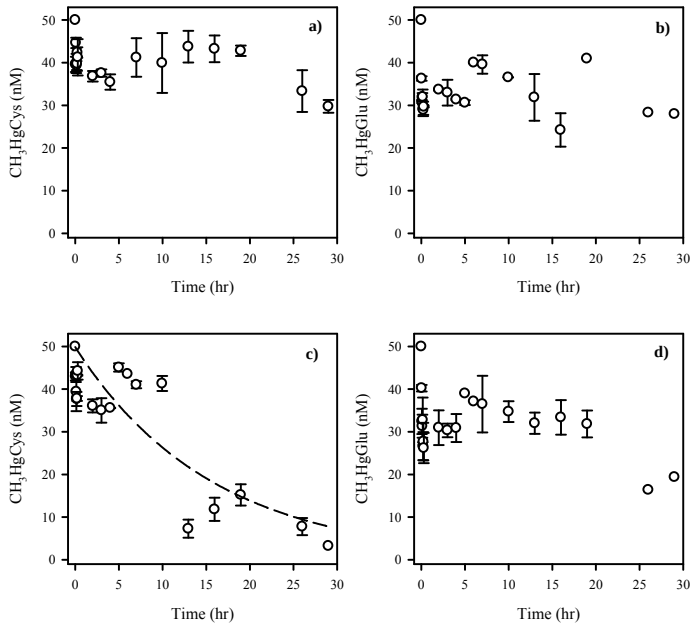

Figure 5.1 - Stability of CH_3HgCys (**a, c**) and CH_3HgGlu (**b, d**) under dark (**a, b**) and with white fluorescence light (**c, d**). pH = 5.5; T = 22 ^oC. The dashed line represent the modeled result based on a first order reaction

5.1.2 Influence of Ionic Strength

The ionic strength study was carried out at pH 7.5 at I = 0.01 M, 0.10 M, and 0.5 M, respectively, in the presence of light. As shown in Fig. 5.2, the stability of both CH_3HgCys and CH_3HgGlu is very sensitive to ionic strength; both were much less stable at higher ionic strength. At I = 0.5 M, CH_3HgCys decreased to lower than the detection limit after 2 days, whereas CH_3HgGlu became undetectable after 11 days. At the same ionic strength, CH_3HgGlu is more stable than CH_3HgCys.

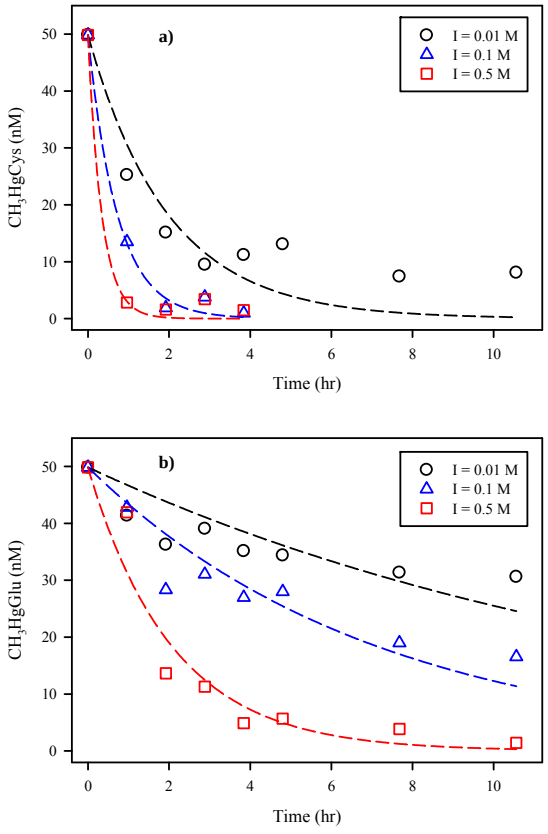

Figure 5.2 - Stability of CH_3HgCys (**a**) and CH_3HgGlu (**b**) at different ionic strengths in the presence of white light. pH = 7.5, T = 22 ^{o}C. Concentrations were the averages of triplicate measurements. The dashed lines represent the modeled results based on a first order reaction

5.1.3 Influence of pH

Figure 5.3 shows the stability of CH_3HgCys and CH_3HgGlu at two different pH values in the presence of light. Both compounds were more stable at pH 5.5. Increasing pH to 7.5 resulted in a rapid decomposition of CH_3HgCys, and to a lesser extent of CH_3HgGlu. It should be noted, however, that the two experiments were done at different ionic strengths. The pH 5.5 experiment was done at I = <0.001 M (same as Fig. 5.1), whereas the pH 7.5 experiment was done at I = 0.01 M.

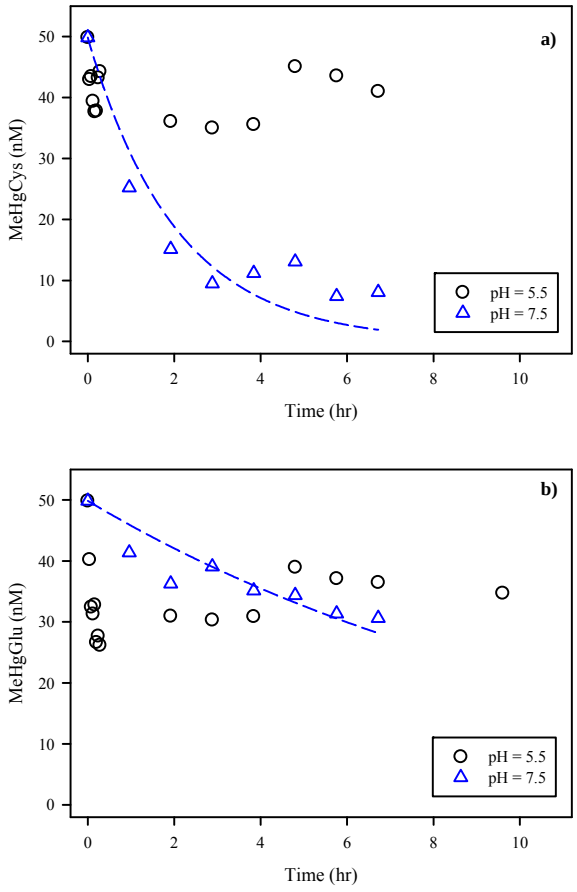

Figure 5.3 - Stability of CH_3HgCys (**a**) and CH_3HgGlu (**b**) at pH 5.5 (I < 0.001M) and pH 7.5 (I = 0.01 M) in the presence of white light. T = 22 ^{o}C. Concentrations were the averages of triplicate measurements. The dashed lines represent the modeled results based on a first order reaction for pH 7.5

5.2 Degradation Kinetics

The degradation of CH_3HgCys or CH_3HgGlu in the presence of light can be generally fitted with a first-order reaction kinetics:

$$CH_3HgSR + h\nu \rightarrow \text{decomposition products} \qquad \text{(Eq. 5.1)}$$

$$\frac{d[CH_3HgSR]}{dt} = -k[CH_3HgSR]$$

where –SR represents CSH or GSH, and k is the decomposition rate constant. The rate constants and half-lives under various experimental conditions are listed in Table 5.1, and the fitting of the data is shown as the modeled lines in Fig. 5.1-5.3. The coefficient of determination (R^2) of the model fitting is also shown in Table 5.1. The rate constant depends on ionic strength, ranging from 5.6×10^{-5} to 3.2×10^{-4} s^{-1} for CH_3HgCys and 7.4×10^{-6} to 5.4×10^{-5} s^{-1} for CH_3HgGlu for the ionic strength range studied (0.01 – 0.5 M) when pH = 7.5. At the same ionic strength, CH_3HgGlu is more stable than CH_3HgCys. Both compounds degrade rapidly when I = 0.5 M, with a half life of 5.9 hr for CH_3HgCys and 35.9 hr for CH_3HgGlu. The small decomposition rate constant of CH_3HgCys at I < 0.001 M (7.4×10^{-6} s^{-1}) explains the lack of decomposition of CH_3HgCl in the presence of CSH in distilled water (Rowland et al., 1977).

Among all the parameters studies, ionic strength has the most significant effect on the decomposition rate constant. Although pH seemed to have an effect (Fig. 5.3), much of it was likely due to different ionic strengths used in the two studies. As shown in Fig. 5.2 and Table 5.1, the decomposition rate constant for both CH_3HgCys and CH_3HgGlu increases significantly with increasing ionic strength, so does the goodness of the first-order model fitting. This is rather surprising, as the stability of free (i.e., not bound to

MeHg) CSH or GSH in aqueous solution, though poorly studied, appears to be not dependent on ionic strength (Aruga et al., 1980).

Table 5.1 - First-order degradation rate constants and half-lives of CH_3HgCys and CH_3HgGlu in the presence of white light (T = 22 ºC)

	pH	I (M)	Rate constant (s^{-1})	Half-life (h)	R^2
CH_3HgCys	5.5	<0.001	7.42×10^{-6}	260	0.67
	7.5	0.01	5.64×10^{-5}	34.1	0.83
	7.5	0.1	1.53×10^{-4}	12.6	0.99
	7.5	0.5	3.25×10^{-4}	5.9	0.99
CH_3HgGlu	5.5	<0.001	N.D.	N.D.	
	7.5	0.01	7.44×10^{-6}	259	0.47
	7.5	0.1	1.56×10^{-5}	124	0.84
	7.5	0.5	5.36×10^{-5}	35.9	0.93

5.3 Decomposition Products and Pathways

The recent development of a MeHg speciation method by HPLC-ICPMS (see Chapter 3) allowed us to further identify the decomposition products of CH_3HgCys and CH_3HgGlu. Both CH_3HgX (X = an inorganic ligand) and HgX are produced from the decomposition of CH_3HgCys and CH_3HgGlu. An unknown species U1, with a retention time between that of CH_3HgCys and CH_3HgX, is also evident in the decomposition of CH_3HgCys (Fig. 5.4a), particularly at lower ionic strength (see appendix 6, Fig. A5a).

Hg(0), if produced, is not present at any significant concentration as the Hg_T concentration stayed constant throughout the experiment

Given the strong binding affinity between the sulfhydryl group and MeHg, the detachment of the MeHg group from MeHg-thiols is most likely via the desulfurization of the corresponding thiols. Based on this and on the peaks from the chromatograms (Fig. 5.4a,b), we propose the following degradation pathways for CH_3HgCys and CH_3HgGlu (Scheme 5.1).

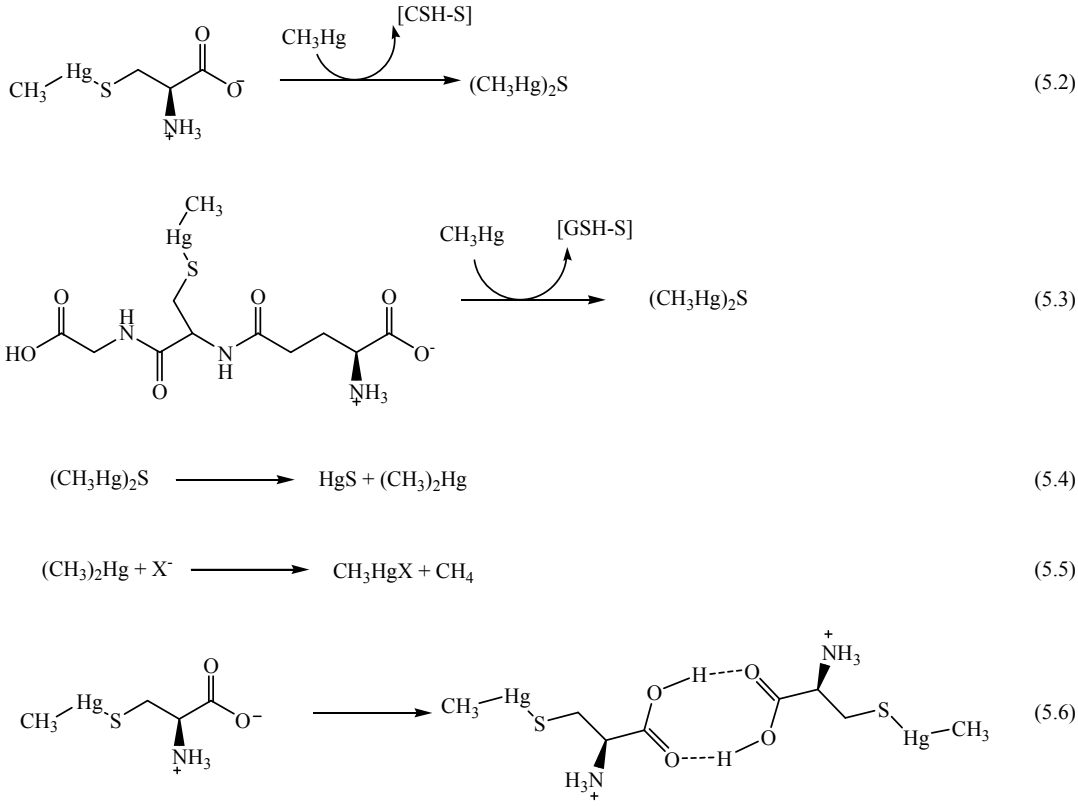

Scheme 5.1 - Proposed degradation pathways of CH_3HgCys and CH_3HgGlu. For simplicity, the reactions only show the main reactants and products, and are not balanced.

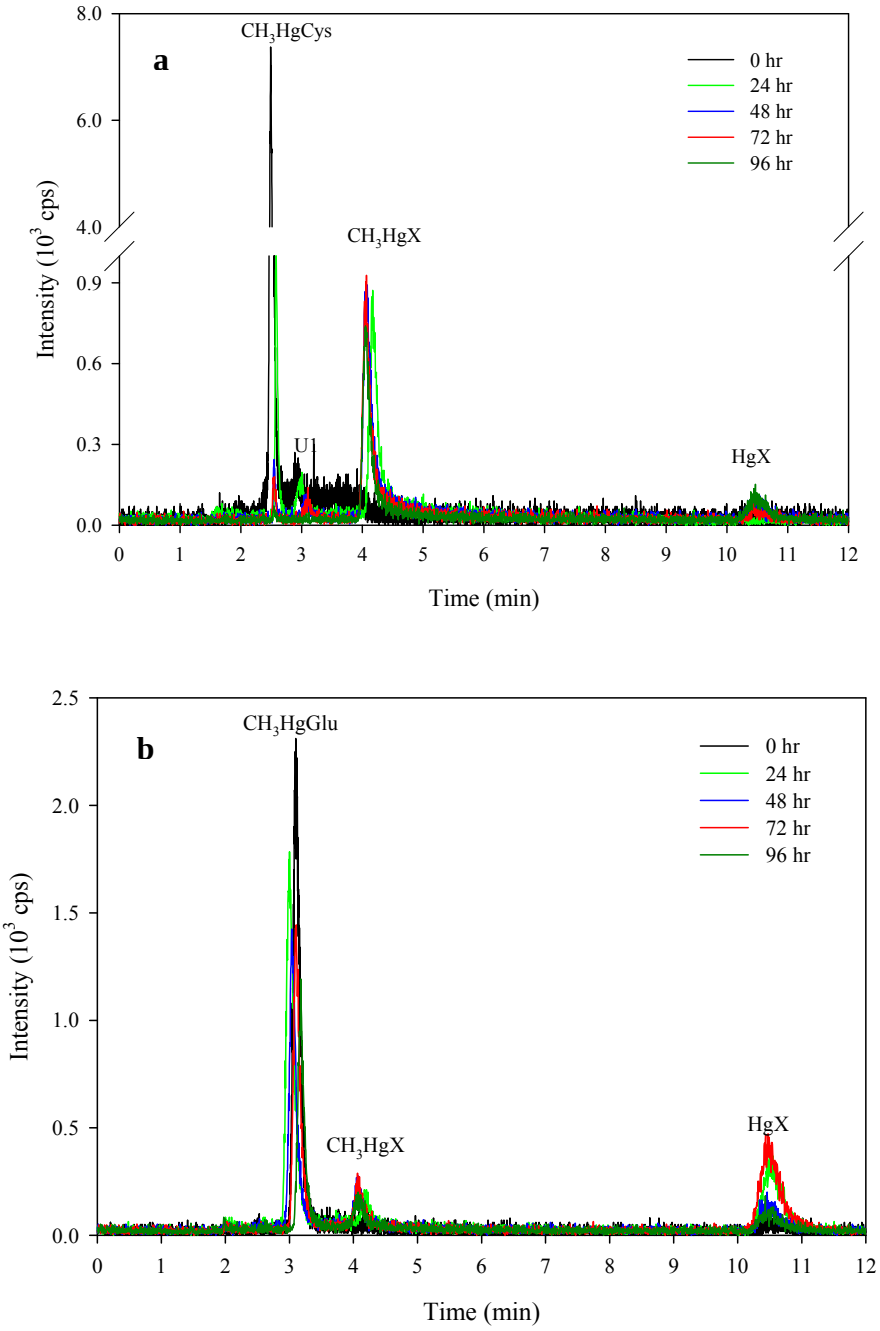

Figure 5.4 - Chromatograms of the CH_3HgCys (**a**) and CH_3HgGlu (**b**) solution after various times of exposure to white light (pH = 7.5, I = 0.1 M, T = 22 ^oC)

Reactions (5.2) and (5.3) are proposed based on the desulfurization of CSH and GSH (Awano et al., 2005; Rubino et al., 2006). The formation of $(CH_3Hg)_2S$ from

CH_3HgCys in Reaction (5.2) was first reported by (Craig and Bartlett, 1978), and given the CSH residue in GSH we propose $(CH_3Hg)_2S$ is also formed from the desulfurization of CH_3HgGlu (Reaction 5.3). $(CH_3Hg)_2S$ is not stable and decomposes to HgS and $(CH_3)_2Hg$ (Reaction 5.4) (Craig and Bartlett, 1978). The gaseous $(CH_3)_2Hg$ can further degrade to CH_4 and CH_3HgX (X^- is a ligand, e.g., OH^-, HS^-; Reaction 5.5) (Craig and Bartlett, 1978) which gives the corresponding peak in the chromatograms (Fig. 5.5). Since the total Hg concentration in the solutions was constant throughout the experiment, the gaseous $(CH_3)_2Hg$ is likely present only as an intermediate.

Attempts at identifying U1 by ESI-MS were not successful due to the low total MeHg concentration (50 nM) used in the experimental solution. Its formation from CH_3HgCys was, however, favored at lower ionic strength; at ionic strength of <0.001 M U1 became the dominant species in the CH_3HgCys solution after 20 days (data not shown). Based on this strong dependence on low ionic strength, we tentatively propose that U1 could be due to the formation of a CH_3HgCys dimer or polymer $(CH_3HgCys)_n$ at lower ionic strength. This molecular association could occur via hydrogen bonding between the carboxyl groups of two or more CH_3HgCys molecules (Reaction 5.6). The formation of polycysteine $(Cys)_n$ ($n \geq 2$) has been well documented in the literature (Sakakibara and Tani, 1956; Wade et al., 1956). The most striking feature from Fig. 5.4 is the formation of inorganic HgX from the decomposition of both CH_3HgCys and CH_3HgGlu. While demethylation of MeHg occurs both photochemically and microbiologically, MeHg is known to resist chemical demethylation (Fitzgerald et al., 2007) and the only known chemical demethylation pathway is via Reaction (5.4) (Craig and Bartlett, 1978). If the resulting HgS(s) is precipitated out from the solution, it would

decrease the Hg_T concentration in the solution and would not likely produce a HPLC-ICPMS peak as shown in Fig. 5.4. The observations that the Hg_T concentration remained constant and that there was a HgX peak in the chromatograms suggest that if HgS were the demethylation product it would have stayed in solution. This is indeed possible, as thiols such as CSH and GSH could act as a stabilizing agent preventing the HgS and HgSe nanoparticles from aggregation into precipitates (Gailer et al., 2000; Khan and Wang, 2009b). Formation of HgSe from the decomposition of MeHg-selenoamino acid complexes has recently been reported (Khan and Wang, 2009a).

The effect of ionic strength is very likely via Reactions (5.2 and (5.3), where occur the desulphurization by the presence of $NaNO_3$, chemical used to adjust the ionic strength. Sodium is one of the major elements found in seawater. The ionic strength apparently plays a major role on decomposition on CH_3HgCys and CH_3HgGlu, being a catalyst of desulfurization by reaction with alkali metals, according to a β-elimination mechanism (Nicolet, 1931; Walter et al., 2006).

5.4 Conclusion

This study confirms the earlier finding that CH_3HgCys resists to chemical decomposition in distilled water. However, rapid decomposition occurs for both CH_3HgCys and CH_3HgGlu with increasing ionic strength. Therefore, markedly different stabilities of CH_3HgCys and CH_3HgGlu are expected in freshwater, seawater, and biological systems. In freshwater where I is typically less than 0.01 M, the half lives of CH_3HgCys and CH_3HgGlu are expected to be in the order of several days and several months, respectively. In contrast, CH_3HgCys and CH_3HgGlu are not stable in seawater

where I = 0.7 M; the half-lives are in the order of hours and days, respectively. Intermediate half lives are expected for CH_3HgCys (12 hr) and CH_3HgGlu (120 hr) at the physiological pH (7.4) and ionic strength (0.16 M). As CH_3HgCys is thought to be the main MeHg species responsible for the neurotoxicity of MeHg, its decomposition is expected to decrease the toxicity of MeHg. A better understanding of the kinetic stability of CH_3HgCys and CH_3HgGlu will thus shed new light on the metabolic processes of MeHg and its detoxification strategies. Further studies are, however, warranted to probe the mechanism for the strong dependence on ionic strength, as well as the identity of the unknown species U1.

Chapter 6. Conclusions

6.1 Objectives Achieved

As described in Chapter 1, the objectives of this research project were to 1) synthesize and characterize CH_3HgCys and CH_3HgGlu compounds; 2) develop an analytical method to speciate CH_3HgCys and CH_3HgGlu complexes; 3) apply this new method to speciate MeHg complexes in biological tissues; and, 4) study the kinetic stability of CH_3HgCys and CH_3HgGlu under various conditions.

As described in Chapter 2, CH_3HgCys and CH_3HgGlu were synthesized and the purity and structures were confirmed by elemental analysis, ^1H NMR, X-ray crystallography (CH_3HgCys only), and ESI-MS. The structural analysis demonstrated the 1:1 stoichiometric ratio between MeHg and the respective thiol (CSH and GSH). The molecular structure of CH_3HgCys was re-established demonstrating the location of all hydrogen atoms; an angle of C-Hg-S was also found more linear than previous reported by Taylor et al. (1975). ESI-MS study demonstrated how the fragmentation pathway might happen up to the demethylation of both CH_3HgCys and CH_3HgGlu.

With the availability of these two compounds, a new HPLC-ICPMS analytical technique was successfully developed which was capable of speciating CH_3HgCys and CH_3HgGlu, as well as CH_3HgX and HgX ($X=OH^-$, Cl^-), in aqueous solutions (Chapters 3, and 5) and in a fish muscle sample (Chapter 4). The speciation of the proposed species plus CH_3HgX and HgX was achieved due to the use an organic modifier with mild affinity with Hg with detection limit at sub-micromolar level.

To apply the MeHg speciation method for biological samples, a new enzymatic hydrolysis method was developed. The techniques were then applied for determining MeHg speciation in a fish muscle sample which provided the first analytical evidence for the presence and dominance of CH_3HgCys in biological samples. The success of the trypsin application to extract MeHg bound to amino acid shows the importance of a mild digestion for effective speciation of MeHg-thiols in biological tissues. The SEC technique provided further insight into the molecular weight distribution of free and bound CH_3HgCys in the fish muscle sample.

The kinetic stability of CH_3HgCys and CH_3HgGlu as reported in Chapter 5, demonstrated a significant effect of ionic strength on the kinetic stability of MeHg-thiol complexes. For CH_3HgCys only, at the lower ionic strengths tested, 0.001 M and 0.10 M, an intermediate species was observed, whereas the higher ionic strength showed no intermediate. Of the two lower ionic strengths, a greater presence was observed at the 0.001 M. MeHgX and HgX species were the decomposed species detected for CH_3HgCys and CH_3HgGlu at $I > 0.10$ M, suggesting that both CH_3HgCys and CH_3HgGlu are unstable in sea water with probable half lives of hours and days, respectively. In contrast, in freshwater, where I is typically less than 0.01 M, the half lives of both CH_3HgCys and CH_3HgGlu are in the order of several days and several months, respectively. Both decomposed species (MeHgX and HgX) detected on kinetic stability study agree very well with what was demonstrated by ESI-MS through their fragmentation pathways for both CH_3HgCys and CH_3HgGlu. CH_3HgGlu demonstrated to have higher level of demethylation than CH_3HgCys, what is in accordance with the literature, suggesting that GSH acts as detoxifier for MeHg.

6.2 Novelty and Significance of the Findings

The most novel and significant result from this thesis research is the development of the first quantitative analytical technique for determining MeHg speciation in aqueous solutions and in biological samples. This makes it possible to move beyond "total MeHg" toward a molecular understanding of the cycling and toxicity of MeHg. This work is expected to contribute significantly in the study of metallomics of Hg and MeHg.

The dominance of CH_3HgCys in fish muscle is of particular interest in the context of human exposure and uptake of MeHg. Due to its structural similarity with methionine, CH_3HgCys has been shown to be transported across BBB by the LAT1 transporter resulting in neurotoxicity (see Chapter 1). The finding that MeHg in the fish muscle is predominately in the form of MeHgCys suggests that almost all the MeHg in the fish muscle could be potentially neuro-available to predators including humans, though speciation change is possible during metabolic processes. Although extensive studies have been carried out on the toxicity of Hg and MeHg, molecular understanding has been very limited. The method developed in this thesis opens up the opportunity to start to unveil molecular-level mechanisms of toxicity. As mentioned in Chapter 1, CSH and GSH are the two most abundant sulfhydryl amino acids and they likely hold the key to the metallomics of MeHg.

The rapid decomposition of both MeHg-thiols at high ionic strengths observed during the kinetic stability studies (Chapter 5), particularly for CH_3HgCys, leads us to consider how CH_3HgCys and CH_3HgGlu would behave inside biological systems. This sparks interest in the study of *in vivo* kinetic stability of mercury-thiol compounds in

body fluids. As neurotoxicity of Hg has been attributed to CH_3HgCys, a better understanding of the kinetic stability of CH_3HgCys and CH_3HgGlu will shed new light on the metabolic processes of MeHg and its detoxification strategies.

6.3 Lessons Learned

One of the first things I learnt from this thesis research was that "lessons" learned from most organometallic compounds do not apply to MeHg. Since I was the first to develop analytical techniques for MeHg speciation, the only literature I could access was for other "similar" organometallic compounds. They all turned out to be poor surrogates. For example, several extraction and analytical methods have been published on selenium complexes with amino acids (Amoako et al., 2007; Biera et al., 2008; Bird et al., 1997; Encinar et al., 2003; Encinar et al., 2004; Larsen et al., 2001; Leon et al., 2000); I tested them in the lab extensively and all of them failed for MeHg.

The inability of obtaining CH_3HgGlu in a crystal form left a gap on its structural characterization. However, the powder form I obtained is one step further from the syrup form obtained by an earlier study (Neville and Drakenberg, 1974), and has been successfully used as a standard material for the subsequent studies. It remains unknown whether CH_3HgGlu could be purified in a crystal form.

Another lesson learnt was in the study of the kinetic stability of MeHg-thiol complexes. The darkness vs. light experiment was done at very low ionic strength which turned out not to be the best condition for the study of the kinetic study, as both compounds were quiet stable at low ionic strength.

My original plan was to further integrate HPLC with ICP-MS and ESI-MS. However, due to the extensive effort on the HPLC-ICPMS method and due to the insufficient detection limit of ESI-MS in this study, the coupling of HPLC-ICPMS/ESI-MS remains to be developed further.

6.4 Future Perspectives

One of the major challenges in the study of cycling, speciation, and toxicity of MeHg has been the lack of sensitive analytical techniques to measure specific MeHg compounds. The development of the first MeHg speciation method from this thesis work has closed this gap and is expected to open many new opportunities for the study of environmental chemistry and metallomics of Hg and MeHg, including, but not limited to:

1) Further improvement in detection limits to allow for direct measurement of MeHg speciation in natural waters, (total MeHg is found around 0.5 pM in aqueous system) and interfacing with ESI-MS for simultaneous isotopic and molecular speciation. This further improvement would lead us to clarify which MeHg species would be formed in the environment where mercury methylation occurs;
2) Further integration with ESI-MS for simultaneous isotopic and molecular identification and determination of MeHg in biological samples;
3) MeHg dynamics in aquatic ecosystems: using the method to investigate the MeHg speciation in different trophic levels of the aquatic ecosystems (e.g., phytoplankton, zooplankton, fish, and mammals). Such study would provide

unprecedented information on the uptake, biomagnification and toxicity of MeHg in aquatic ecosystem;

4) Study the MeHg speciation in other matrices such as plants and aliments (e.g., rice). The latter is of particular importance as they could be an overlooked exposure pathway of MeHg to humans;
5) Update the toxicological modeling studies. Toxicological thresholds of MeHg so far have been based exclusively on MeHgCl and MeHgOH. Given their *in vitro* and *in vivo* occurrence and toxicological relevance, MeHg-thiols are perhaps better suited as toxicological surrogates for MeHg;
6) Metallomics of MeHg, particularly the metabolic pathways and detoxification of MeHg in biological systems. The knowledge of how mercury is transported within an organism and the specific chemical forms present within a specific tissue would shed new light on molecular understanding of and solution for MeHg toxicity;
7) Interaction of MeHg with selenoamino acids: The method could be potentially extended for the analysis of MeHg complexes with selenoamino acids as well, which would provide a powerful analytical tool for the study of Hg-Se antagonism, and in the development of Se-based detoxification strategies for Hg and MeHg poisoning.

REFERENCES

Ahmed R, Stoeppler M. Decomposition and stability studies of methylmercury in water using cold vapour atomic absorption spectrometry. Analyst 1986; 111: 1371-1374.

Ahmed R, Stoeppler M. Storage and stability of mercury and methylmercury in sea water. Anal. Chim. Acta 1987; 192: 109-113.

Allibone J, Fatemian E, Walker PJ. Determination of mercury in potable water by ICP-MS using gold as a stabilising agent. J. Anal. At. Spectrom. 1999; 14: 235–239.

Amoako PO, Kahakachchi CL, Dodova EN, Uden PC, F. TJ. Speciation, quantification and stability of selenomethionine, S-(methylseleno)cysteine and selenomethionine Se-oxide in yeast-based nutritional supplements. J. Anal. At. Spectrom. 2007; 22: 938–946.

Arnold AP, Canty AJ. Methylmercury (II) sulfhydryl interactions. Potentiometric determination of the formation constants for complexation of methylmercury (II) by sulfydryl containing amino acids and related molecules, including glutathione. Can. J. Chem. 1983; 61: 1428-1434.

Arnold AP, Canty AJ, Moors PW, Deacon GB. Chelation therapy for methylmercury(II) poisoning. Synthesis and determination of solubility properties of MeHg(II) complexes of thiol and dithiol antidotes. J. Inorg. Biochem. 1983; 19: 319-327.

Arnold AP, Canty AJ, Reid RS, Rabenstein DL. Nuclear magnetic resonance and potentiometric studies of the complexation of methylmercury(II) by dithiols. Can. J. Chem. 1985; 63: 2430-2436.

Aruga M, Awazu S, Hanano M. Kinetic studies on decomposition of glutathione. II. Anaerobic decomposition in aqueous solution. Chem. Pharm. Bull. 1980; 28: 514-520.

Aschner M, Aschner JL. Mercury neurotoxicity: Mechanism of blood-brain barrier transport. Neurosci. Biobehav. Rev. 1990; 14: 169-176.

Aschner M, Mullaney KJ, Wagoner D, Lash LH, Kimelberg HK. Intracellular glutathione (GSH) levels modulate mercuric chloride (MC)- and methylmercuric chloride (MeHgCl)-induced amino acid release from neonatal rat primary astrocytes cultures. Brain Res. 1994; 664: 133-140.

Awano N, Wada M, Mori H, Nakamori S, Takag H. Identification and functional Analysis of escherichia coli cysteine desulfhydrases. Appl. Environ. Microbiol. 2005; 71: 4149–4152.

Baeyens W, M. Leermakers, Papina T, Saprykin A, Brion N, Noyen J, De Gieter M, Elskens M, Goeyens L. Bioconcentration and biomagnification of mercury and methylmercury in North Sea and Scheldt estuary Fish. Arch. Environ. Contam. Toxicol. 2003; 45: 498-508.

Bannai S, Tateishi N. Role of membrane transport in metabolism and function of glutathione in mammals. J. Membrane Biol. 1986; 89: 1-8.

Bergquist BA, Blum JD. Mass-dependent and -independent fractionation of Hg isotopes by photoreduction in aquatic systems. Science 2007; 318: 417-420.

Biera K, Vacchina V, Szpunar J, Bertin G, Ryszard L. Simultaneous derivatization of selenocysteine and selenomethionine in animal blood prior to their specific

determination by 2D size-exclusion ion-pairing reversed-phase HPLC-ICP MS. J. Anal. At. Spectrom. 2008; 23: 508–513.

Bird SM, Uden PC, Tyson JF, Block E, Denoyer E. Speciation of selenoamino acids and organoselenium compounds in seleniumenriched yeast using high-performance liquid chromatography–inductively coupled plasma mass spectrometry. J. Anal. At. Spectrom. 1997; 12: 785–788.

Blanco RM, Villanueva MT, Uria JES, Sanz-Medel A. Field sampling, preconcentration and determination of mercury species in river waters. Anal. Chim. Acta 2000; 419: 137–144.

Bloom N. Determination of picogram levels of methylmercury by aqueous phase ethylation, followed by cryogenic gas chromatography with cold vapor atomic fluorescence detection. Can. J. Fish. Aquat. Sci. 1989; 46: 1131-40.

Bloom NS, Horvat M, Watras CJ. Results of the international aqueous mercury speciation intercomparison exercise. Water Air Soil Pollut. 1995; 80: 1257-1268.

Boszke L. High-performance liquid chromatography as a valuable tool for determination of mercury species in environmental samples. A review. Chem. Anal. 2005; 50: 489-505.

Botana JC, Rodriguez RR, Diaz AMC, Ferreira RAL, Torrijos RC, Pereiro IR. Fast and simultaneous determination of tin and mercury species using SPME, multicapillary gas chromatography and MIP-AES detection. J. Anal. At. Spectrom. 2002; 17: 904–907.

Bramanti E, Cristina Lomonte, Onor M, Zamboni R, D'Ulivo A, Raspi G. Mercury speciation by liquid chromatography coupled with on-line chemical vapour

generation and atomic fluorescence spectrometric detection (LC–CVGAFS). Talanta 2005; 66: 762–768.

Bridges CC, Zalups RK. Molecular mimicry as a mechanism for the uptake of cysteine S-conjugates of methylmercury and inorganic mercury. Chem. Res. Toxicol. 2006; 19: 1117-1118.

Brown R, Gray DJ, Tye D. Hydride generation ICP-MS (HG-ICP-MS) for the ultra low level determination of mercury in biota. Water Air Soil Pollut. 1995; 80: 1237-1245.

Cai Y, Jaffe R, Alli A, Jones RD. Determination of organomercury compounds in aqueous samples by capillary gas chromatography-atomic fluorescence spectrometry following solid-phase extraction. Anal. Chim. Acta 1996; 334: 251-259.

Cai Y, Monsalud S, Furton KG. Determination of methyl- and ethylmercury compounds using gas chromatography atomic fluorescence spectrometry following aqueous derivatization with sodium tetraphenylborate. Chromatographia 2000; 52: 82-86.

Canle M, Ramos DR, Santaballa JA. A DFT study on the microscopic ionization of cysteine in water Chem. Phys.Lett. 2006; 417: 28–33.

Canty AJ, Colton R, D'Agostino A, Traeger JC. Positive and negative ion electrospray mass spectrometry studies of some amino acids and glutathione, and their interactions with alkali metal ions and methylmercury. Inorg. Chim. Acta 1994; 223: 103-107.

Cappon CJ, Smith JC. A simple and rapid procedure for the gas-chromatographic determination of methylmercury in biological samples. Bull. Environ. Contam. Toxicol. 1978; 19: 600-607.

Carro AM, Mejuto MC. Application of chromatographic and electrophoretic methodology to the speciation of organomercury compounds in food analysis - Review. J. Chromatogr., A 2000; 882: 283–307.

Casiot C, Szpunar J, Łobinski R, Potin-Gautier M. Sample preparation and HPLC separation approaches to speciation analysis of selenium in yeast by ICP-MS. J. Anal. At. Spectrom. 1999; 14: 645–650.

Castillo A, Roig-Navarro AF, Pozo OJ. Method optimization for the determination of four mercury species by micro-liquid chromatography–inductively coupled plasma mass spectrometry coupling in environmental water samples. Anal. Chim. Acta 2006; 577: 18–25.

Cela-Torrijos R, Miguens-Rodriguez M, Carro-Diaz AM, Lorenzo-Ferreira A. Optimization of supercritical fluid extraction-gas chromatography of methylmercury in marine samples. J. Chromatogr., A 1996; 750: 191-199.

Chemaly SM. The link between vitamin B_{12} and methylmercury: a review. S. Afr. J. Sci. 2002; 98: 568-572.

Chen W, Wee P, Brindle ID. Elimination of the memory effects of gold, mercury and silver in inductively coupled plasma atomic emission spectroscopy. J. Anal. At. Spectrom. 2000; 15: 409-413.

Chen Y-W, Tong J, D'Ulivo A, Belzile N. Determination of mercury by continuous flow cold vapor atomic fluorescence spectrometry using micromolar concentration of sodium tetrahydroborate as reductant solution. Analyst 2002; 127: 1541–1546.

Chiou C-S, Jiang S-J, Danadura KSK. Determination of mercury compounds in fish by microwave-assisted extraction and liquid chromatography-vapor generation-inductively coupled plasma mass spectrometry. Spectrochim. Acta, Part B 2001; 56: 1133-1142.

Christmann DR, Ingle JD. Problems with sub-p.p.b. mercury determinations: preservation of standards and prevention of water mist interferences Anal. Chim. Acta 1976; 86: 53-62.

Christopher SJ, Long SE, Rearick MS, Fassett JD. Development of isotope dilution cold vapor inductively coupled plasma mass spectrometry and its application to the certification of mercury in NIST Standard Reference Materials. Anal. Chem. 2001; 73: 2190-2199.

Clarkson TW. Mercury: Major issues in environmental health. Environ. Health Perspect. 1992; 100: 31-38.

Clarkson TW. Molecular and ionic mimicry of toxic metals. Annu. Rev. Pharmacol. Toxicol. 1993; 33: 545-71.

Clement GE, Hartz TP. Determination of the microscopic ionization constants of cysteine. J. Chem. Educ. 1971; 48: 395-397.

Compeau G, Bartha R. Effects of sea salt anions on the formation and stability of methylmercury. Bull. Environ. Contam. Toxicol. 1983; 31: 486-493.

Compeau G, Bartha R. Methylation and demethylation of mercury under controlled redox, pH, and salinity conditions. Appl. Environ. Microbiol. 1984; 48: 1203-120.

Compeau G, Bartha R. Effect of salinity on mercury-methylating activity of sulfate-reducing bacteria in estuarine sediments. Appl. Environ. Microbiol. 1987; 53: 261-265.

Compeau GC, Bartha R. Sulfate-reducing bacteria: principal methylators of mercury in anoxic estuarine sediment. Appl. Environ. Microbiol. 1985; 50: 498-502.

Craig P. Organometallic compounds in the environment: John Wiley & Wiley, 2003.

Craig PJ, Bartlett PD. The role of hydrogen sulphide in environmental transport of mercury. Nature 1978; 275: 635-637.

Craig PJ, Moreton PA. The role of speciation in mercury methylation in sediments and water. Environ. Pollut. B 1985; 10: 141-158.

Craig PJ, Morton SF. Kinetics and mechanism of the reaction between methylcobalamin and mercuric chloride. J. Organomet. Chem. 1978; 145: 79-89.

Davis WC, Christopher SJ, Pugh RS, Donard OFX, Krupp EA, Point D, Horvat M, Gibièar D, Kljakovic-Gaspic Z, Porter BJ, Schantz MM. Certification of methylmercury content in two fresh-frozen reference materials: SRM 1947 Lake Michigan fish tissue and SRM 1974b organics in mussel tissue (*Mytilus edulis*). Anal. Bioanal. Chem. 2007; 387: 2335–2341.

Devai I, Delaune RD, Patrick Jr. WH, Gambrell RP. Changes in methylmercury concentration during storage: effect of temperature. Org. Geochem. 2001; 32: 755–758.

Dringen R, Gutterer JM, Hirrlinger J. Glutathione metabolism in brain metabolic interaction between astrocytes and neurons in the defense against reactive oxygen species - MINI REVIEW. Eur. J. Biochem. 2000; 267: 4912-4916.

Dyrssen D, Wedborg M. The sulfur-mercury (II) system in natural waters. Water Air Soil Pollut. 1991; 56: 507-519.

Ebdon L, Foulkes ME, Le Rouxa S, Muñoz-Olivas R. Cold vapour atomic fluorescence spectrometry and gas chromatography-pyrolysis-atomic fluorescence spectrometry for routine determination of total and organometallic mercury in food samples. Analyst 2002; 127: 1108–1114.

Ekstrom EB, Morel FMM, Benoit JM. Mercury methylation independent of the acetyl-coenzyme: a pathway in sulfate-reducing bacteria. Appl. Environ. Microbiol. 2003; 69: 5414–5422.

Encinar JR, Ruzik R, Buchmann W, Tortajada J, Lobinski R, Szpunar J. Detection of selenocompounds in a tryptic digest of yeast selenoprotein by MALDI time-of-flight MS prior to their structural analysis by electrospray ionization triple quadrupole MS. Analyst 2003; 128: 220–224.

Encinar JR, Schaumloffel D, Ogra Y, Lobinski R. Determination of selenomethionine and selenocysteine in human serum using speciated isotope dilution-capillary HPLC-inductively coupled plasma collision cell mass spectrometry. Anal. Chem. 2004; 76: 6635-6642.

EPA Method 1631. Mercury in water by oxidation, purge and trap, and cold vapor atomic fluorescence spectrometry. 2002.

Evans RD, Hintelmann H, Dillon PJ. Measurement of high precision isotope ratios for mercury from coals using transient signals. J. Anal. At. Spectrom. 2001; 16: 1064–1069.

Fatemian E, Allibone J, Walker PJ. Use of gold as a routine and long term preservative for mercury in potable water, as determined by ICP-MS. Analyst 1999; 124: 1233–1236.

Finney LA, O'Halloran TV. Transition Metal Speciation in the Cell: Insights from the Chemistry of Metal Ion Receptors. Sciemce 2003; 300: 931-936.

Fischer R, Rapsomanikis S, Andreae MO. Determination of methylmercury in fish samples using GC/AA and sodium tetraethylborate derivatization. Anal. Chem. 1993; 65: 763-766.

Fitzgerald WF, Lamborg CH, Hammerschmidt CR. Marine biogeochemical cycling of mercury. Chem. Rev. 2007; 107: 641-662.

Foltin M, Megová S, Procházková T, Steklác M. Speciation of mercury by ion chromatography with post-column derivatization J. Radioanal. Nucl. Chem. 1996; 208: 295-307.

Forsyth DS, Casey V, Dabeka RW, McKenzie A. Methylmercury levels in predatory fish species marketed in Canada. Food Addit. Contam. 2004; 21: 849–856.

Foucher D, Hintelmann H. High-precision measurement of mercury isotope ratios in sediments using cold-vapor generation multi-collector inductively coupled plasma mass spectrometry. Anal Bioanal Chem 2006; 384: 1470–1478.

Gachhui R, Pahan K, Ray S, Chaudhuri J, Mandal A. Cell free glutathione synthesizing activity of mercury resistant bacteria. Bull. Environ. Contam. Toxicol. 1991; 46: 336-342.

Gailer J, George GN, Pickering IJ, Madden S, Prince RC, Yu EY, Denton MB, Younis HS, Aposhian HV. Structure basis of the antagonism between inorganic mercury and selenium in mammals. Chem. Res. Toxicol. 2000; 13: 1135-1142.

Garcia JS, Magalhaes CSd, Arruda, Marco Aurelio Zezzi. Trends in metal-binding and metalloprotein analysis. Talanta 2006; 69: 1-15.

Gardfeldt K, Munthe J, Stromberg D, Lindqvist O. A kinetic study on the abiotic methylation of divalent mercury in the aqueous phase. Sci. Tot. Environ. 2003; 304: 127-136.

Gaspar A, Pager C. Capillary electrophoretic determination of mercury compounds in different matrices. . Chromatographia 2002; 56: S115-S120.

Geier G, Erni I. Kinetics and mechanisms of methylmercury complex formation Chimia 1973; 27: 635-637.

Gibièar D, Logar M, Horvat N, Marn-Pernat A, Ponikvar R, Horvat M. Simultaneous determination of trace levels of ethylmercury and methylmercury in biological samples and vaccines using sodium tetra(*n*-propyl)borate as derivatizing agent. Anal Bioanal Chem 2007; 388: 329–340.

Gilmour CC, Henry EA, Mitchell R. Sulfate stimulation of mercury methylation in freshwater sediments. Environ. Sci. Technol. 1992; 26: 2281-2287.

Gilmour CC, Riedel GS. Measurement of Hg methylation in sediments using high specific-activity ^{203}Hg and ambient incubation. Water Air Soil Pollut. 1995; 80: 747-756.

Hammerschmidt CR, Filtzgerald W. Photodecomposition of Methylmercury in an Arctic Alaskan Lake. Environ. Sci & Technol. 2006; 40: 1212-1216.

Harada M. Minamata disease: Methylmercury poisoning in Japan caused by environmental pollution. Crit. Rev. Toxicol 1995; 25: 1-24.

Haraguchi H. Metallomics as integrated biometal science. J. Anal. At. Spectrom. 2004; 19: 5-14.

Harbour PJ. The detection and ionization potential of mercury clusters. J. Phys. B: Atom. Molec. Phys. 1971; 4: 528-530.

Harrington CF. The speciation of mercury and organomercury compounds by using high-performance liquid chromatography. Trends Anal. Chem. 2000; 19: 167-179.

Harrington CF, Catterick T. Problems encountered during the development of a method for the speciation of mercury and methylmercury by high-performance liquid chromatography coupled to Inductively coupled plasma mass spectrometry. J. Anal. At. Spectrom. 1997; 12: 1053-1056.

Harrington CF, Romeril J, Catterick T. The speciation of mercury and organomercury compounds by high performance liquid chromatography/atmospheric pressure ionization mass spectrometry. Rapid Commun. Mass Spectrom. 1998; 12: 911-916.

Harris HH, Pickering IJ, George GN. The chemical from of mercury in fish. Science 2003; 201: 1203.

Hasegawa T, Asano M, Takatani K, Matsuura H, Umemura T, Haraguchi H. Speciation of mercury in salmon egg cell cytoplasm in relation with metallomics research. Talanta 2005; 68: 465–469.

Hashemi-Moghaddam H, Saber-Tehrani M. Sensitive mercury speciation by reversed-phase column high performance liquid chromatography with UV-visible detection after solid phase extraction using 6-mercaptopurine and dithizone. J. AOAC Intern. 2008; 91: 1453-1458.

Henderson W, McIndoe JS. Mass spectrometry of inorganic and organometallic compounds. Chichester: Wiley 2005.

Heumann KG. Isotope-dilution ICP–MS for trace element determination and speciation: from a reference method to a routine method? Anal Bioanal Chem 2004; 378.

Hintelmann H, Ebinghaus R, Wilken RD. Accumulation of mercury (II) and methylmercury by microbial biofilms. Wat. Res. 1993; 27: 237-242.

Hintelmann H, Evans RD. Application of stable isotopes in environmental tracer studies – Measurement of monomethylmercury (CH_3Hg^+) by isotope dilution ICP-MS and detection of species transformation. Fresenius J Anal Chem 1997; 358: 378–385.

Hintelmann H, Nguyen HT. Extraction of methylmercury from tissue and plant samples by acid leaching. Anal Bioanal Chem 2005; 381: 360-365.

Hintelmann H, Simmons DA. Determination of aqueous methylmercury species using electrospray mass spectrometry. Can. J. Anal. Sc. Spectrosc. 2003; 48: 244-249.

Hintelmann H, Welboum M, Evans RD. Measurement of complexation of methylmercury(II) compounds by freshwater humic substances. Environ. Sci. Technol. 1997; 31: 489-495.

Ho Y-S, Uden PC. Determination of inorganic Hg(II) and organic mercury compounds by ion-pair high-performance liquid chromatography. J. Chromatogr., A 1994; 688: 107-116.

Hoffmeyer RE, Singh SP, Doonan CJ, Ross ARS, Hughes RJ, Pickering IJ, George GN. Molecular mimicry in mercury toxicology. Chem. Res. Toxicol. 2006; 19: 753-759.

Horvat M, Bloom NS, Liang L. Comparison of distillation with other current isolation methods for the determination of methyl mercury compounds in low level environmental samples. Part I. Sediments Anal. Chim. Acta 1993; 281: 135-152.

Imura N, Sukegawa E, Pan S-K, Nagao K, Kim J-Y, Kwan T, Ukita T. Chemical methylation of inorganic mercury with methylcobalamin, a vitamin B_{12} analog. Science 1971; 172: 1248-1249

Inoko M. Studies on the photochemical decomposition of organomercurials—methylmercury (II) chloride Environ. Pollut. B 1981; 2: 3-10

Karlsson T, Skyllber U. Bonding of ppb levels of methyl mercury to reduced sulfur groups in soil organic matter. Environ. Sci. Technol. 2003; 37: 4912-4918.

Keper LE, Ballatori N, Clarkson TW. Methylmercury transport across the blood-brain barrier by an amino acid carrier. Am. Physiol. Soc. 1992: R761-765.

Khan M, Wang F. Reversible Dissolution of Glutathione-Mediated HgSexS1-x Nanoparticles and Possible Significance in Hg-Se Antagonism. Chem. Res. in Toxicol. 2009a; 22: 1827-1832.

Khan MAK, Wang F. Reversible dissolution of glutathione-mediated $HgSe_xS_{1-x}$ nanoparticles and possible significance in Hg-Se antagonism. Chem. Res. Toxicol. 2009b: DOI: 10.1021/tx900234a.

Kishi Y, Kawabata K, Shi H, Thomas R. Reduction of carbon-based interferences in organic compound analysis by dynamic reaction cell ICP-MS. www.spectroscopyonline.com, Duluth, MN, 2004.

Krishna MVB, Castro J, Brewer TM, Marcus RK. Online mercury speciation through liquid chromatography with particle beam/electron ionization mass spectrometry detection. J. Anal. At. Spectrom. 2007; 22: 283–291.

Krupp EM, Milne BF, Mestrot A, Meharg AA, Feldmann J. Investigation into mercury bound to biothiols: structural identification using ESI–ion-trap MS and introduction of a method for their HPLC separation with simultaneous detection by ICP-MS and ESI-MS. Anal. Bioanal. Chem. 2008; 390: 1753–1764.

Kubán P, Houserová P, Kubán P, Hauser PC, Kubán V. Mercury speciation by CE: a review. Electrophoresis 2007; 1: 58-68.

Lanses P, Meuleman C, Baeyens W. Long-term stability of methylmercury standard solutions in distilled, dionized water. Anal. Chim. Acta 1990; 229: 281-285.

Larsen EH, Hansen M, Fan T, Martin V. Speciation of selenoamino acids, selenonium ions and inorganic selenium by ion exchange HPLC with mass spectrometric

detection and its application to yeast and algae. J. Anal. At. Spectrom. 2001; 16: 1403–1408.

Lee Y-H, Hultberg H, Andersson I. Catalytic effect of various metal ions on the methylation of mercury in the presence of humic substances. Water Air Soil Pollut. 1985; 25: 391-400.

Leermakers M, Baeyens W, Quevauviller P, Horvat M. Mercury in environmental samples: Speciation, artifacts and validation. Trends Anal. Chem. 2005; 24: 383-393.

Leermakers M, Lansens P, Baeyens W. Storage and stability of inorganic and methylmercury solutions. Fresenius J Anal Chem 1990; 336: 655- 662.

Leon CAP, Sutton K, Caruso J, Uden PC. Chiral speciation of selenoamino acids and selenium enriched samples using HPLC coupled to ICP-MS. J. Anal. At. Spectrom 2000; 15: 1103-1107.

Li F, Wang D-D, Yan X-P, Lin J-M, Su R-G. Development of a new hybrid technique for rapid speciation analysis by directly interfacing a microfluidic chip-based capillary electrophoresis system to atomic fluorescence spectrometry. Electrophoresis 2005a; 26: 2261–2268.

Li Y, Jiang Y, Yan X-P. On-line hyphenation of capillary electrophoresis with flame-heated furnace atomic absorption spectrometry for trace mercury speciation. Electrophoresis 2005b; 26: 661–667.

Lo JM, Wai CM. Mercury loss from water during storage: Mechanisms and prevention. Anal. Chem. 1975; 47: 1869-1870.

Logar M, Horvat M, Akagi H, Pihlar B. Simultaneous determination of inorganic mercury and methylmercury compounds in natural waters. Anal. Bioanal. Chem. 2002; 374: 1015–1021.

Logar M, Horvat M, Falnoga I, Stibilj V. A methodological study of mercury speciation using Dogfish liver CRM (DOLT-2). Fresenius J. Anal. Chem. 2000; 366: 453–460.

Martin-Doimeadios RCR, Krupp E, Amouroux D, Donard OFX. Application of isotopically labeled methylmercury for isotope dilution analysis of biological samples using gas chromatography/ICPMS. Anal. Chem. 2002; 74: 2505-2512.

Morton J, Carolan VA, Gardiner PHE. The speciation of inorganic and methylmercury in human hair by high-performance liquid chromatography coupled with inductively coupled plasma mass spectrometry. J. Anal. At. Spectrom. 2002; 17: 377–381.

Nagase H, Ose Y, Sato T, Ishikawa T. Mercury methylation by compounds in humic material. Sci. Total Environ. 1984; 32: 147-158.

Neville GA, Drakenberg T. Mercuric mercury and methylmercury complexes of glutathione. Acta Chem. Scand. 1974; B28: 473-477.

Nicolet BH. The mechanism of sulfur lability in cysteine and its derivatives. I Some thio ethers readily split by alkali. J. Am. Chem. Soc. 1931; 53: 3066-3072.

NRC (National Research Council). Toxicological effects of methylmercury. Washington: National Research Council, 2000.

NRCC (National Research Council Canada). DORM-2: Dogfish Muscle Certified Reference Material for Trace Metals. In: Canada: NRC, editor, Ottawa, 1993.

Olson BH, Cooper RC. Comparison of aerobic and anaerobic methylation of mercury chloride by San Francisco Bay sediments. Water Res. 1976; 10: 113-116.

Olson KR. Loss of carbon-14 and mercury-203 labeled methylmercury from various solutions. Anal. Chem. 1977; 49: 23-26.

Ortiz AIC, Albarran YM, Rica CC. Evaluation of different sample pre-treatment and extraction procedures for mercury speciation in fish samples. J. Anal. At. Spectrom. 2002; 17: 1595–1601.

Pager C, Gaspar A. Possibilities of determination of mercury compounds using capillary zone electrophoresis. Microchem. J. 2002; 73: 53–58.

Park CJ, Do H. Determination of inorganic and total mercury in marine biological samples by cold vapor generation inductively coupled plasma mass spectrometry after tetramethylammonium hydroxide digestion. J. Anal. At. Spectrom. 2008; 23: 997–1002.

Parkinson D-R, Inge B, Christ I, Pawliszyn J. Full automation of derivatization—solid-phase microextraction–gas chromatography–mass spectrometry with a dual-arm system for the determination of organometallic compounds in aqueous samples. J. Chromatogr., A 2004; 1025: 77–84.

Percy AJ, Korbas M, George GN, Gailer J. Reversed-phase HPLC separation of Hg^{2+} and CH_3Hg^+ driven by their different coordination chemistry towards thiols. J. Chromatogr., A 2007; 1156: 331–339.

Qvarnstrom J, Frech W. Mercury species transformations during sample pre-treatment of biological tissues studied by HPLC-ICP-MS. J. Anal. At. Spectrom. 2002; 17: 1486-1491.

Rabenstein DL. Microscopic ionization constants of glutathione and methylmercury-complexed glutathione. J. Am. Chem. Soc. 1973; 95: 2797-2803.

Rabenstein DL. The chemistry of methylmercury toxicology. J. Chem. Educ. 1978; 55: 292-296.

Rabenstein DL, Evans CA. The mobility of methylmercury in biological systems. Bioinorg. Chem. 1978; 8: 107-114.

Rabenstein DL, Fairhurst MT. The binding of methylmercury by sulfhydryl-containing amino acids and by glutathione. J. Am. Chem. Soc. 1975; 97: 2086-2092.

Rabenstein DL, Isab AA, Reid RS. A proton nuclear magnetic resonance study of the binding of methylmercury in human erythrocytes. Biochim. Biophys. Acta 1982; 696: 53-64.

Rabenstein DL, Reid RS. Ligand-exchange kinetics of methylmercury(II)-thiol complexes. Inorg. Chem. 1984; 23: 1246-1250.

Rai R, Maher W, Kirkowa F. Measurement of inorganic and methylmercury in fish tissues by enzymatic hydrolysis and HPLC-ICP-MS. J. Anal. At. Spectrom. 2002; 12: 1560–1563.

Ramalhosa E, Segade SR, Pereira E, Vale C, Duarte A. Microwave-assisted extraction for methylmercury determination in sediments by high performance liquid chromatography-cold vapour atomic fluorescence spectrometry. J. Anal. At. Spectrom. 2001; 16: 643–647.

Raycheba JMT, Geier G. Methylmercuration of carbon-donor ligands. A kinetic preference for methylmercury(II) transfer over proton transfer. Inorg. Chem. 1979; 18: 2486-2491.

Reid RS, Rabenstein DL. Formation constants for the complexation of methylmercury by sulfhydryl-containing amino acids and related molecules. Can. J. Chem. 1981; 59: 1505-1514.

Rio-Segade S, Bendicho C. On-line high-performance liquid-chromatographic separation and cold vapor atomic absorption spectrometric determination of methylmercury and inorganic mercury. Talanta 1999; 48: 477–484.

Rodushkin I, Ruth T, Klockare D. Non-spectral interferences caused by a saline water matrix in quadrupole and high resolution inductively coupled plasma mass spectrometry. J. Anal. At. Spectrom. 1998; 13: 159–166.

Rowland IR, Davies MJ, Grasso P. Volatilisation of methylmercuric chloride by hydrogen sulphide. Nature 1977; 265: 718 - 719.

Rubino FM, Pitton M, Brambilla G, Colombi A. A study of the glutathione metaboloma peptides by energy-resolved mass spectrometry as a tool to investigate into the interference of toxic heavy metals with their metabolic processes. J. Mass Spectrom. 2006; 41: 1578–1593.

Sakakibara S, Tani H. Synthesis of polycysteine. Bull. Chem. Soc. Jpn. 1956; 29: 85-88

Sanchez-Urıa JE, Sanz-Medel A. Inorganic and methylmercury speciation in environmental samples - Review. Talanta 1998; 47: 509–524.

Sarzanini C, Sacchero G, Aceto M, Abollino O, Mentasti E. Simultaneous deternination of methyl-, ethyl-, phenyl- and inorganic mercury by cold vapour atomic absorption spectrometry with on-line chromatographic separation. J. Chromatogr. A 1992; 626: 151-157.

Schuster E. The behavior of mercury in the soil with special emphasis on complexation and adsorption processes - A review of the literature. Water Air Soil Pollut. 1991; 56: 667-680.

Schwarzenbach G, Schellenberg M. Die komplexchemie desmethylquecksilber-kations. Helv. Chim. Acta 1965; 1: 28-47.

Sellers P, Kelly CA, Rudd JWM, MacHutchon AR. Photodegradation of methylmercury in lakes. Nature 1996; 380: 694-697.

Shabani AMH, Dadfarnia S, Nasirizadeh N. Speciation analysis of mercury in water samples by cold vapor atomic absorption spectrometry after preconcentration with dithizone immobilized on microcrystalline naphthalene. Anal Bioanal Chem 2004; 378: 1388–1391.

Shade CW, Hudson RJM. Determination of MeHg in environmental sample matrices using Hg-thiourea complex ion chromatography with on-line cold vapor generation and atomic fluorescence spectrometric detection. Environ. Sci. Technol.. 2005; 39: 4974-4982.

Shanker G, Aschner M. Identification and characterization of uptake systems for cystine and cysteine in cultured astrocytes and neurons: Evidence for methylmercury-targeted disruption of astrocyte transport. J. Neurosci. Res. 2001; 66: 998-102.

Silva da Rocha M, Soldado AB, Blanco-Gonzalez E, Sanz-Medel A. Speciation of mercury by capillary electrophoresis-inductively coupled plasma mass spectrometry. Biomed. Chromatogr. 2000a; 14.

Silva da Rocha M, Soldado AB, Blanco-Gonzalez E, Sanz-Medel A. Speciation of mercury compounds by capillary electrophoresis coupled on-line with quadrupole

and double-focusing inductively coupled plasma mass spectrometry. J. Anal. At. Spectrom. 2000b; 15: 513-518.

Silva da Rocha M, Soldado AB, Blanco E, Sanz-Medel A. Speciation of mercury using capillary electrophoresis coupled to volatile species generation-inductively coupled plasma mass spectrometry. J. Anal. At. Spectrom. 2001; 16: 951–956.

Simmons-Willis TA, Koh AS, Clarkson TW, Ballatori N. Transport of a neurotoxicant by molecular mimicry : the methylmercury–L-cysteine complex is a substrate for human L-type large neutral amino acid transporter (LAT) 1 and LAT2. Biochem. J. 2002; 367: 239-246.

Smith RG. Determination of mercury in environmental samples by isotope dilution/ ICPMS. Anal. Chem. 1993; 65: 2485-2488.

Spek AL. PLATON, A Multipurpose Crystallographic Tool. . Utrecht: Utrecht University, Utrecht, The Netherlands, 2005.

Stets EG, Hines ME, Kiene RP. Thiol methylation potential in anoxic, low-pH wetland sediments and its relationship with dimethylsulfide production and organic carbon cycling. FEMS Microbiol. Ecol. 2004; 47: 1-11.

Stumm W, Morgan JJ. Aquatic chemistry: Chemical equilibria and rates in natural waters. New York: Wiley & Sons, 1996.

Szpunar J. Metallomics: a new frontier in analytical chemistry. Anal Bioanal Chem 2004; 378: 54–56.

Taylor NJ, Wong YS, Chieh PC, Carty AJ. Syntheses, X-ray crystal structure, and vibrational spectra of $_{L}$-cysteine (methyl)mercury(II) monohydrate. Dalton Trans. 1975: 438-442.

Thiele B, Füllner K, Stein N, Oldiges M, Kuhn AJ, Hofmann D. Analysis of amino acids without derivatization in barley extracts by LC-MS-MS. Anal Bioanal Chem 2008; 391: 2663–2672.

Tossell JA. Theoretical study of the photodecomposition of methyl Hg complexes. J. Phys. Chem. A 1998; 102: 3587-3591.

Vaisar T, Gatlin CL, Turecek F. Oxidation of peptide-copper complexes by alkali metal cations in the gas phase. J. Am. Chem. Soc. 1996; 118: 5314-5315.

Vallant B, Kadnar R, Goessler W. Development of a new HPLC method for the determination of inorganic and methylmercury in biological samples with ICP-MS detection. J. Anal. At. Spectrom. 2007; 22: 322–325.

Velez Z, Hubbard PC, Hardege JD, Barata EN, Canário AVM. The contribution of amino acids to the odour of a prey species in the Senegalese sole (*Solea senegalensis*). Aquaculture 2007; 265: 336–342.

Wade R, Winitz M, Greenstein JP. Studies on polycysteine peptides and proteins. III. Configurations of the peptides of $_{L}$-cystine obtained by oxidation of $_{L}$-cysteinyl-$_{L}$-cysteine. J. Am. Chem. Soc. 1956; 78: 373–377.

Wagemann R, Trebacz E, Boila G, Lockhart WL. Methylmercury and total mercury in tissues of arctic marine mammals. Sci. Tot. Environ. 1998; 218: 19-31.

Walter P, Welcomme E, Hallegot P, Zaluzec NJ, Deeb C, Castaing J, Veyssiere P, Breniaux R, Leveque J-L, Tsoucaris G. Early use of PbS nanotechnology for an ancient hair dyeing formula. Nano Lett. 2006; 6: 2215-2219.

Wan C-C, Chen C-S, Jiang S-J. Determination of mercury compounds in water samples by liquid chromatography–inductively coupled plasma mass spectrometry with an in situ nebulizer/vapor generator. J. Anal. At. Spectrom. 1997; 12: 683–687.

Watras CJ, Back RC, Halvorsen S, Hudson RJM, Morrison KA, Wente SP. Bioaccumulation of mercury in pelagic freshwater food webs. Sci. Total Environ. 1998; 219: 183-208.

Watras CJ, Morrison KA, Kent A, Price N, Regnell O, Eckley C, Hintelmann H, Hubacher T. Sources of methylmercury to a wetland-dominated lake in Northern Wisconsin. Environ. Sci. Technol. 2005; 39: 4747-4758.

Weber JH. Review of possible paths for abiotic methylation of mercury(II) in the aquatic environment. Chemosphere 1993; 26: 2063-2077.

Westoo G. Determination of methylmercury compounds in foodstuffs I. Methylmercury compounds in fish, identification and determination. Acta Chem. Scand. 1966; 20: 2131-2137.

Westoo G. Determination of methylmercury compounds in foodstuffs II. Determination of methylmercury in fish, egg, meat, and liver. Acta Chem. Scand. 1967; 21: 1790-1800.

Wilken RD, Falter R. Determination of methylmercury by the species-specific isotope addition method using a newly developed HPLC-ICPMS coupling technique with ultrasonic nebulization. Appl. Organomet. Chem. 1998; 12: 551-557.

Wilson AJC. International tables for X-ray crystallography Vol C. Dordrecht, Netherlands: Kluwer, 1992.

Yathavakilla, S. K. V. , Caruso JA. A study of Se-Hg antagonism in Glycine max (soybean) roots by size exclusion and reversed phase HPLC–ICPMS. Anal. Bioanal. Chem. 2007; 389: 715–723.

Yu L-P, Yan X-P. Factors affecting the stability of inorganic and methylmercury during sample storage. Trends Anal. Chem. 2003; 22: 245-253.

Zhang J, Wang F, House JD, Page B. Thiols in wetland interstitial waters and their role in mercury and methylmercury speciation. Limnol. Oceanogr. 2004; 49: 2276-2286.

APPENDICES

Appendix 1.

The following figure shows the selection of various product ions for CH_3HgCys parents ion (m/z=338) under different voltages for positive mode on Agilent 6410 Triple Quad LC-MS.

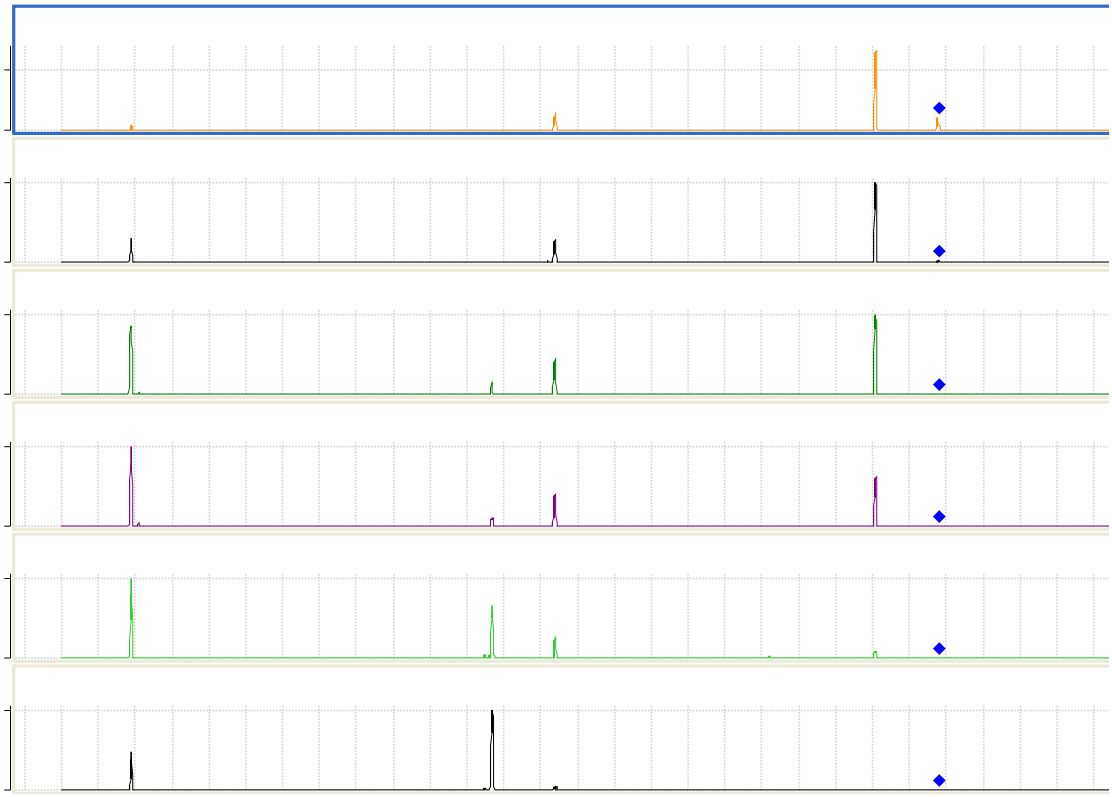

Figure A1 – Product ions setting for CH_3HgCys on positive mode

x10 2 + Product Ion (2.528,

Appendix 2

The following figure shows the selection of various product ions for CH_3HgGlu parents ion (m/z=524) under different voltages for positive mode on Agilent 6410 Triple Quad LC-MS.

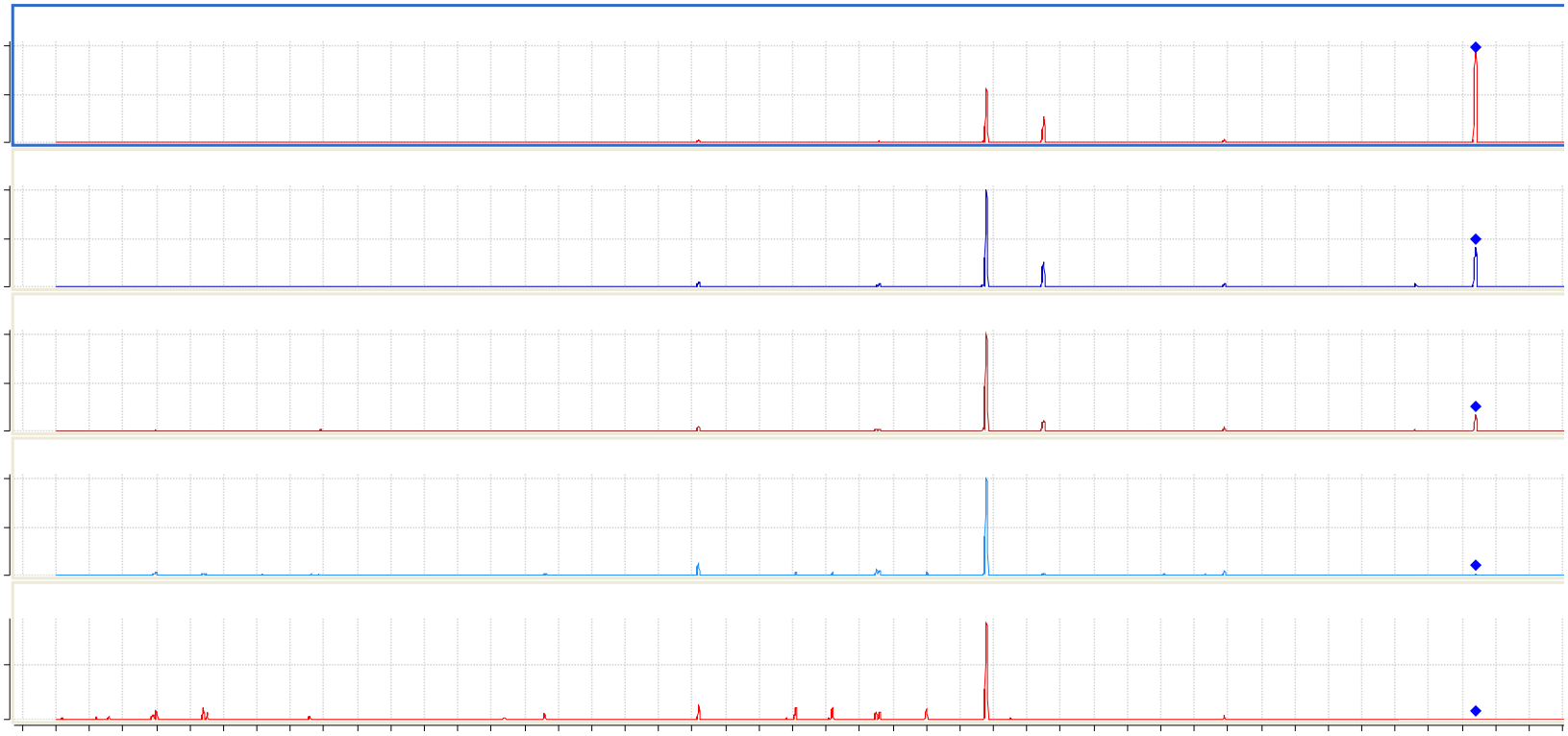

Figure A2 – Product ions setting for CH_3HgGlu on positive mode

x10 2 + Product Ion (2.782, 2.799, 2.815, 2.832 ... min, 6 scans)

Appendix 3

Optimal parameters (transition, fragment voltage, and collision energy voltage) for quantifying CH_3HgCys and CH_3HgGlu under both positive and negative modes using Agilent 6410 Triple Quad LC/MS.

Table A1 – ESI-MS parameters for CH_3HgCys and CH_3HgGlu in both positive and negative modes

CH_3HgCys (+ev)			
Transition		**Fragment (V)**	**Collision Energy (V)**
m/z = 338 - 321	(quantifier)	70	2
m/z = 338 - 317	(qualifier)	70	25
m/z = 338 - 119		70	10
CH_3HgCys (-ev)			
Transition		**Fragment (V)**	**Collision Energy (V)**
m/z = 336 - 249	(quantifier)	60	10
m/z = 338 - 234	(qualifier)	60	20
CH_3HgGlu (+ev)			
Transition		**Fragment (V)**	**Collision Energy (V)**
m/z = 524 - 395	(qualifier)	100	5
m/z = 524 - 378	(quantifier)	100	10
CH_3HgGlu (-ev)			
Transition		**Fragment (V)**	**Collision Energy (V)**
m/z = 522 - 272	(qualifier)	100	10
m/z = 524 - 243	(quantifier)	100	20

Appendix 4

This graph is part of the HPLC-ICPMS method optimization described in Chapter 3. The influence of HPLC flow rate with two types of nebulizers (quartz and PFA) on CH_3HgCys.

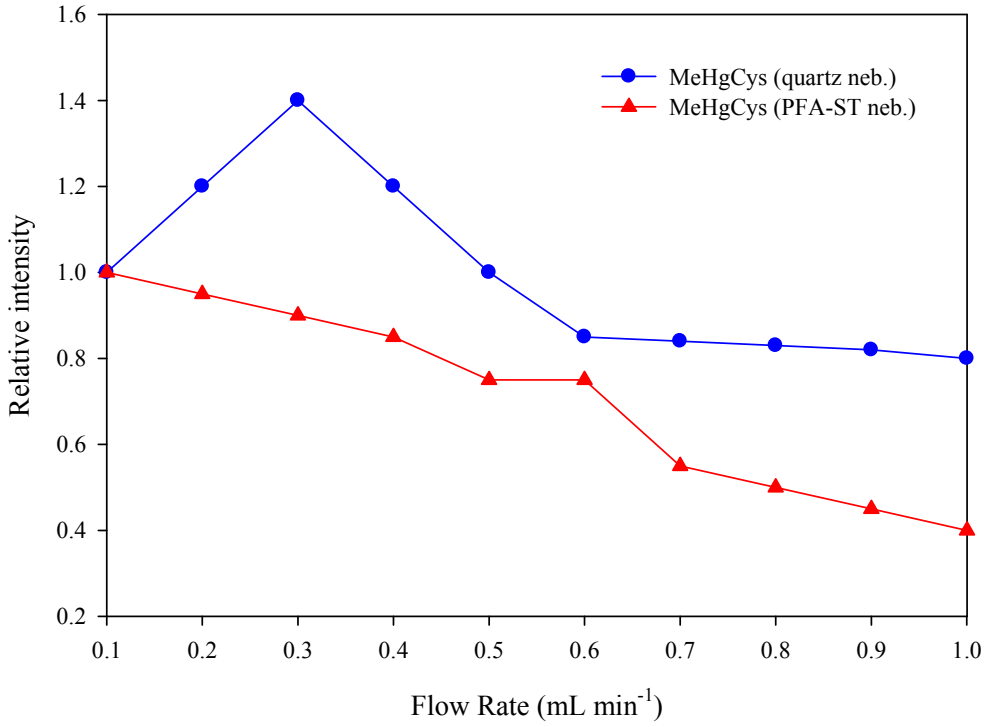

Figure A3 – Normalized signal obtained with different nebulizers for CH_3HgCys analysis by HPLC-ICPMS

Appendix 5.

This graph is part of the HPLC-ICP-MS method optimization as described in Chapter 3, showing how ICP-MS plasma power affects the intensity of Hg species. 1400 W was deemed to be the optimal RF power.

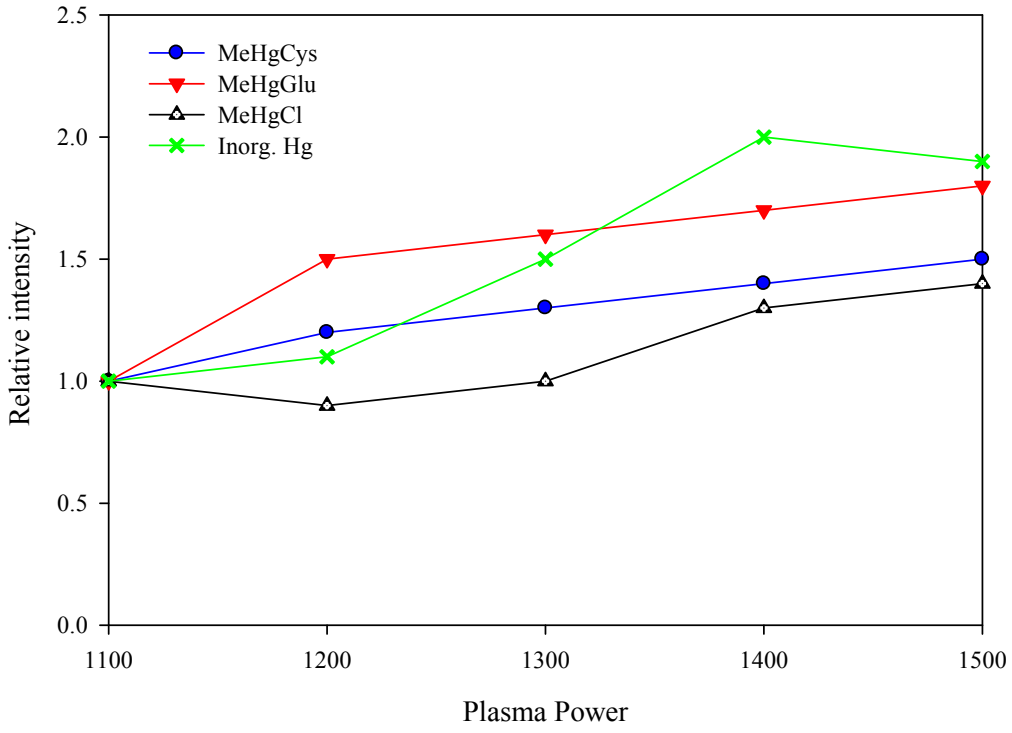

Figure A4 – Normalized signal obtained on influence of RF power on the intensity of Hg species by HPLC-ICPMS

Appendix 6.

Comparison of CH_3HgCys decomposition during a 30-day experiment under light. CH_3HgCys demonstrated a) decomposition to 3 unknown species (U1, U2, and U3) at I= <0.001 M at pH = 5. When the condition is changed to b) higher ionic strength was observed CH_3HgX, HgX, with U1 in much lower level, and U2 and U3 disappeared at I= 0.10 M at pH = 7.5. HgX peak increased over time.

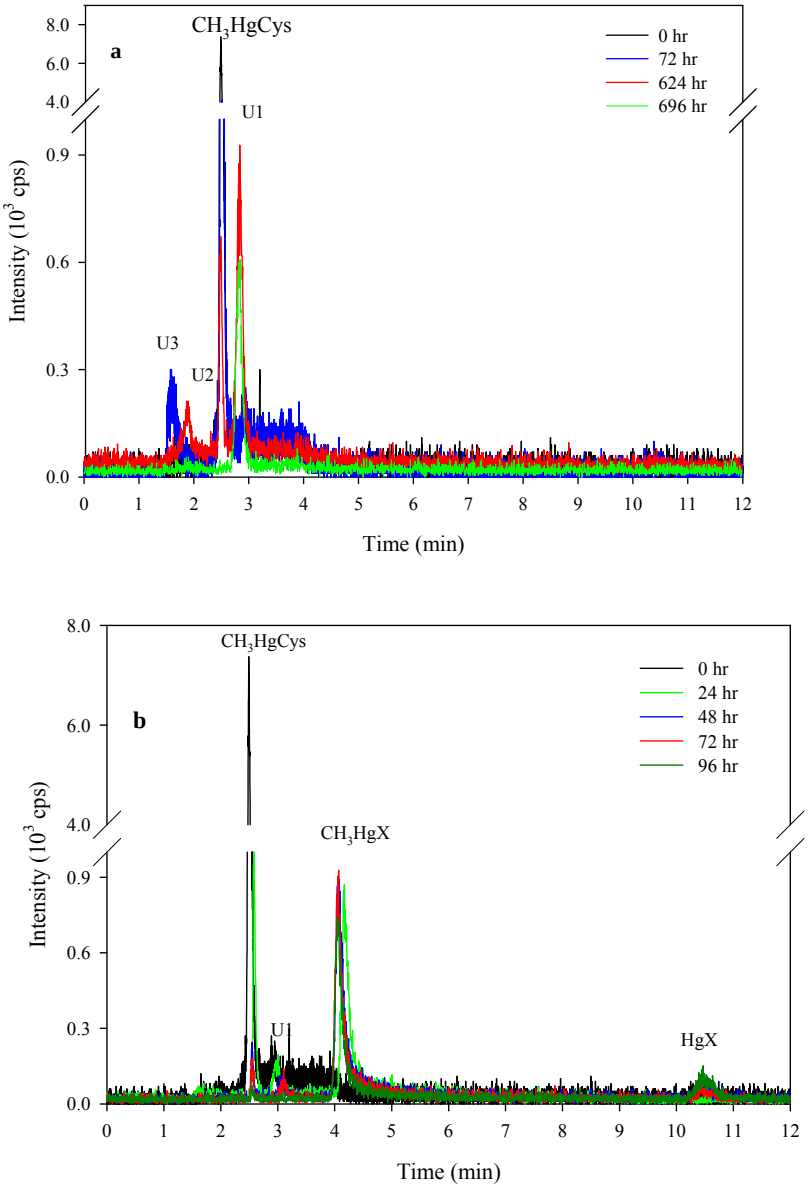

Figure A5 – Chromatograms of the CH_3HgCys solution after various times of exposure to white light. at **a)** pH = 5.5, I = <0.001 M, and **b)** pH = 7.5, I = 0.10 M, T = 22 ^{o}C

Appendix 7.

Comparison of CH_3HgGlu decomposition during a 30-day experiment in light. CH_3HgGlu demonstrated a) decomposition to 1 unknown species (U4), CH_3HgCys, CH_3HgX, and HgX at I= <0.001 M at pH = 5.5. When the condition is changed to b) higher ionic strength only CH_3HgX and HgX were observed. HgX peak increased over time.

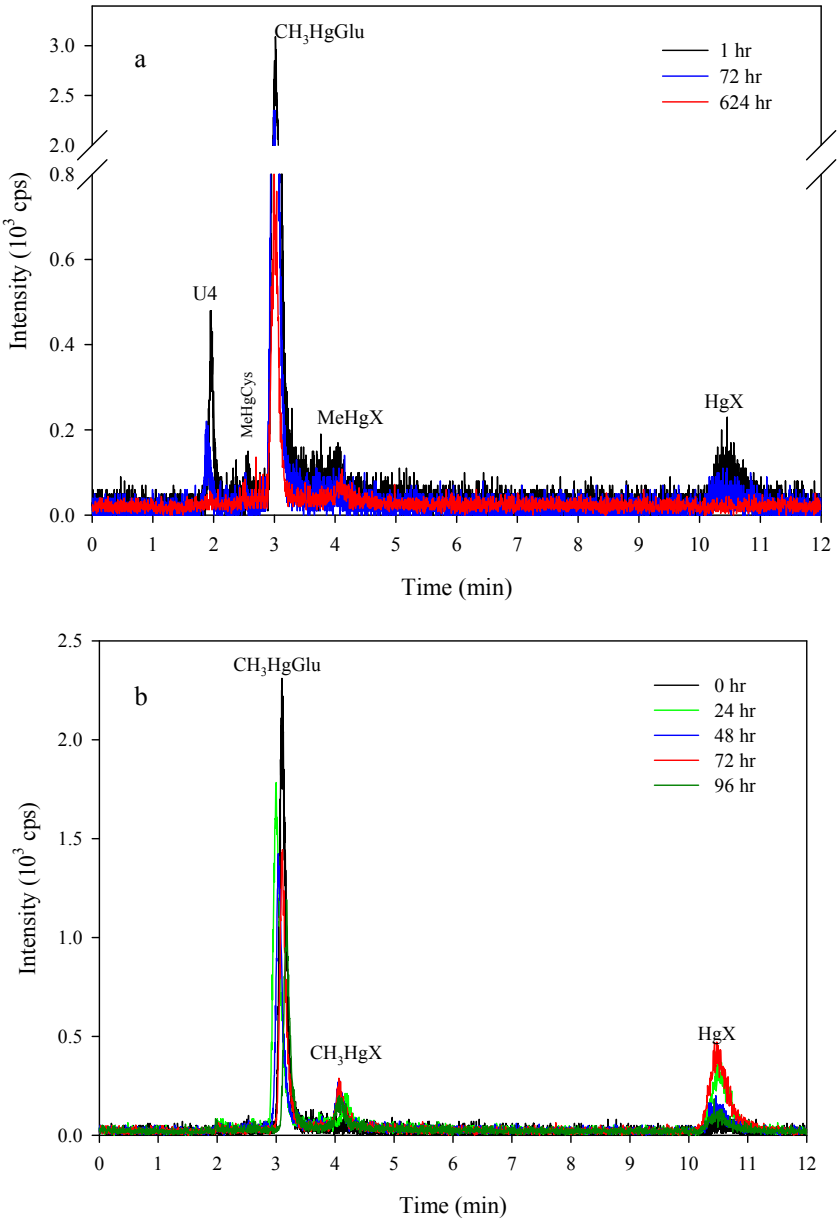

Figure A6 - Chromatogram of the CH_3HgGlu solution after various times of exposure to white light at **a)** pH= 5.5, I= <0.001 M, and **b)** pH= 7.5, I = 0.10 M, T= 22 ^oC